Realisation of Computer Generated Integral Three Dimensional Images

Paul Cartwright

Faculty of Computing Sciences and Engineering

School of Engineering and Manufacture

De Montfort University

A thesis submitted for the degree of Doctor of Philosophy

December, 2000

This is dedicated to:

My friends

My family

ABSTRACT

With the current development trends in display technology towards high-resolution flat panel displays, there has been a renewed interest in three-dimensional imaging technologies. Currently, most of the major international display and electronics companies have investigated one or more methods of producing auto-stereoscopic direct view three-dimensional images.

However, apart from modern production methods and new display media, three-dimensional imaging has hardly changed since the beginning of the century. Most methods utilise two or several two-dimensional views (multi-view image) to form a stereoscopic three-dimensional presentation. This approach produces systems that do not provide the casual view with a natural viewing situation and physical and psychological problems can occur after extended viewing.

Systems that produce optical models and therefore allow natural viewing to occur are beneficial. Holography is an example of this but high quality lasers and vibration free environments are required for production. An alternative approach Integral photography is reported. This utilises non-coherent optical radiation to produce images that exist as full optical models independent of the observer, thus allowing natural viewing to occur.

Chapter 2 introduces the field of Integral imaging it shows the progression of the field from its origin in 1908 to the present day. Also, associated three-dimensional imaging techniques are discussed and their merits analysed.

Chapter 3 shows introduces the fundamental knowledge for general production of images using a computer. This chapter then discusses the development and analysis of several methods to achieve the goal of producing computer generated integral images. The chapter goes on to show methods of extending the technique to produce photo-realistic computer generated integral images.

The next chapter, shows various uses of the information about the structure of integral images when applied to general integral imaging. This covers aliasing effects and resolution dependent upon sampling.

Chapter 5, develops the generation technique with respect to image manipulation. This section covers depth extraction from integral images and image distortion for subsequent projection.

Finally, the projects goals are re-evaluated and conclusions are drawn.

ACKNOWLEDGEMENTS

I would like to extend my thanks for help and support to the members of the Three-Dimensional and Medical Imaging Group, De Montfort University. Especially, Malcolm McCormick, Neil Davies, Wei Wang, Amar Aggoun and Mike Brewin.

Special thanks go to Victoria Morris, Anthony Williams and Richard Wilson.

STATEMENT OF ORIGINALITY

The work contained within this thesis is purely that of the author unless otherwise stated. This work has not been submitted for any examination, qualification or publication.

Paul Cartwright

TABLE OF CONTENTS

TABLE OF FIGURES

1. INTRODUCTION

1.1. Aims

The ultimate aim of this project is to gain the knowledge necessary to produce rendered, photo-realistic computer generated integral images (Lippmann, 1908) and to show proof of the underlying principles. At the start of this project, three-dimensional images of this type (integral images) had only been briefly investigated with respect to artificial synthesis. In addition, established theories (Okoshi, 1976; Burckhardt, 1968[1]) suggested that the amount of information contained in an integral image would preclude any attempt at generating or displaying an image on currently available pixelated devices. Previous research undertaken by Brewin (Brewin and Davies, 1996), suggested that not only was integral imaging possible on a pixelated medium but replay could be effected with a much reduced information content than that predicted or contained in photographic media.

1.2. General Introduction

At present, the visualisation of three-dimensional computer information involves either a two-dimensional projection of the information or, as with stereo based systems, several (≥2) two-dimensional projections to the eye-brain. These methods are primitive when compared with the three-dimensional information gained through everyday viewing of real world objects. This is because these imaging systems mainly include the use of the psychological depth cues (shading, obscuration and texture gradients) and only basic physiological depth cues, in the case of the stereo systems, convergence. Problems arise in the viewing of these images as only two views are seen at any one time.

Integral imaging devised by Lippmann, uses an array of small simple lenses to capture scenes with continuous parallax. These can be replayed as valid three-dimensional optical models (Grebennikov, 1971), existing independently in space, allowing the resulting images to be interrogated with focusing devices. This immediately gives an extra dimension of realism over existing flat perspective projections (standard computer images) whilst also removing the inherent viewing discomfort of current stereoscopic and multi-view display, by allowing natural viewing to take place, where accommodation and convergence simultaneously operate.

The generation of standard two-dimensional computer representations of three-dimensional scenes involves the mathematical projection of the objects in space onto a fixed two-dimensional plane, located at the viewing screen. Generally, one of two common methods is used to achieve this goal. Geometric projection uses the objects spatial position data to map from object space to image space. This technique uses several approximations to achieve fast image generation speeds, including converting the model into faceted shapes.

The alternative technique of ray tracing (Appel, 1968) requires the casting of a large number of rays to produce an image with results approaching photo-realism. For example, to produce an image for standard high-resolution computer output with standard anti-aliasing techniques requires roughly [1024*768*9*8] = 56,623,104 rays to be traced through the scene. Standard computer generated multi-view three-dimensional systems require N such planar views to be created per image, obviously increasing the necessary computation.

To create photo-realistic images large amounts of geometric transformations need to be applied. This procedure creates the problem that enormous amounts of high precision, floating-point arithmetic is required and therefore the procedure is very computer intensive.

This project investigates techniques of producing integral images with the expressed objective of producing photo-realism whilst the extended aim is to keep calculation costs (which relates to computation time) to a minimum and to develop a technique which can be translated into a real-time process.

1.3. Project Background

Currently, several different families of three-dimensional recording/replay systems exist, these systems can be separated into two main groups. Those that require the viewer to wear some sort of device capable of separating the information destined for the left and right eyes (stereoscopic) and those systems which require no such device to be worn, i.e. they can be free viewed (auto-stereoscopic).

The group of displays that require the observer to "wear" an optically selective device date back to the earliest three-dimensional viewing systems. These primitive devices devised by Wheatstone in 1832 are known as "stereoscopes". They operate by displaying two images side by side one for each eye. These views are channelled separately to the corresponding eye by simple optical elements and/or baffled viewing channels. In later developments of stereoscopic displays, viewers are required to wear special image selective glasses, with the channels to each eye being controlled by either a polarising filter (Benton, 1980), red-green filters (as popularised in the cinematic film "Jaws 3D" (Alves, 1983)) or LCD shutters (Kratomi, 1972). These perform similar tasks by selective filtering of the image in space or time and thereby only allowing the correct image to be viewed by the corresponding eye.

Displays that require viewers to wear selective devices (McCollum, 1943) are now deemed as being unrealistic for domestic three-dimensional television (3DTV). However, recent developments in this area, such as virtual reality headsets (Virtuality plc, 1997), still rely on the basic idea of physically presenting separate images to each eye, although the method of channelling the image to the eye is usually slightly more sophisticated than the Victorian systems.

Auto-stereoscopic display systems (free viewing) are more easily acceptable to the casual observer and therefore a great deal of research into this type of display has been undertaken. This type of display can be further subdivided into systems that create the view of an object though reconstruction of the wavefronts emanating from the original using phase information from the interference of a highly coherent source (holography)(Gabor, 1948,1949); those which use a physical sampling optical device to encode the angular information contained in a scene (lenticular/parallax barriers (Moore, Travis, Lang and Castle, 1992; Horou and Minoru, 1992; Nims and Lo, 1974)) or use complex tracking systems to channel the correct information to the viewer (Tetsutani, Omura and Kishino, 1994; Xenotech, 1996).

The latter suffer the disadvantages of requiring a huge amount of processing to accommodate the tracking of the viewer, being too complex to extend to a multi-viewer system and are impossible to extend to an arbitrary number of viewers.

Holographic and multiview auto-stereoscopic systems are much better suited to casual viewing by any number of observers.

Gabor (Gabor, 1948, 1949) reported the basic principles of holography in 1948. He suggested that an object placed in front of a high resolution, radiation sensitive plane illuminated by a coherent source of electro-magnetic radiation would produce an interference pattern on the sheet when developed. This sheet, when re-illuminated by a similar coherent source, would reproduce the original wavefronts as created by the object. Gabors original proposals were relating to electron beams and the production of lenses for electron microscopes. The system devised by Gabor is very limited in practice. The object that is being imaged actually casts a shadow on the recording plate, therefore reducing the interference achieved and thereby reducing the detail in the replay. These application limiting problems were resolved and the system improved through further work by Leith and Upatnieks (Leith and Upatnieks, 1962, 1963, 1964), using a two beam method of holography. This system uses a single coherent beam to illuminate object/scene and another to illuminate the photographic plate (reference beam). Essentially, this is the modern method for the production of holograms.

However, the holography process inherently presents several limitations:

- A source of coherent radiation must be used for recording (i.e. a laser);
- Images are monochrome (true colour images are created through a multi-exposure process using separate red, green and blue laser passes);
- Very high resolution film and specialist dark room facilities are required;
- The subject and equipment must remain absolutely still during exposure (to within the wavelength of light);
- Computer generation of holograms is possible but requires extremely complex mathematical formulas that need to be solved. Electronic holographic displays have been demonstrated (Benton, 1992) but these require Gigabits of information per frame.

Therefore, holographic images are not ideal as a general-purpose display medium. This leaves as an alternative non-coherent imaging.

Non-coherent auto-stereoscopic displays based around parallax barriers, lenticular and micro-lens sheets were developed as an alternative method for channelling the left/right stereo images to the correct eye. By multiplexing a stereo-pair alternately behind the lens sheet, each eye can receive the correct information as long as the viewer is within a specific viewing zone. The viewing zone is typically 15-20°.

Consequently, these stereo systems are unable to accommodate more than one viewer and require some sort of head tracking (Street, 1994) if some sense of reality is to be retained when the viewer is moving. To prevent undesired movement effects and disturbances such as stereo reversal (Schwartz, 1986) the system response needs to be good. Additionally, these type of images suffer universally from the effect of "cardboarding" that is the scene is discretised into planes.

Multi-view systems have the advantage over simple stereo systems in that they can accommodate more than one viewer at a time. However, they suffer the disadvantages of a smaller angle of view and flipping between image fields. They still have a flattening of depth planes but this effect is reduced as the number of views is increased. Stereo (including multi-view) systems also tend to cause severe eye strain (Yamazaki, 1989) after prolonged viewing as the user is required to focus to the screen plane, but converge their eyes to a point in space, producing a very unnatural physiological situation.

Previous to multi-view/stereo imaging, a system known as integral photography had been developed. This is a technique for creating optical models which, like holograms, exist in space as a full optical model independent of the observer. The image is auto-stereoscopic (requiring no worn viewing aids) and exhibits continuous parallax throughout the viewing zone. Unlike holograms integral imaging does not require specialised film or facilities, does not require lasers and exists in full natural colour.

The continuous nature of the images produced with this method eliminates the effect of "cardboarding", a flattening of objects into discrete depth planes present in stereo and multi-view systems (Travis, 1993). This produces an image with a natural solidity, allowing natural viewing (focusing and converging to the same point in space), thus eliminating eye strain.

To date, the three problems that have slowed the development of integral imaging are:

1. The inherent difficulty in manufacturing high quality micro-lens arrays;

2. Orthoscopic integral imaging is a two stage process;

3. Published theory on the topic indicates that integral images will not reconstruct at the resolutions currently attainable in modern electronic display devices (Okoshi, 1976).

However, on examination the analyses are not consistent with each other or experimental evidence recently produced (Brewin, Forman and Davies, 1995). This suggests that the nature of an integral image is not well understood.

In addition, several advancements in the production of integral images have been made in recent years. For example, the three-dimensional imaging group at De Montfort University had; pioneered the optical configuration necessary to record a one stage orthoscopic integral image photographically; developed a method of manufacturing high quality micro-lens arrays using a photo-sensitive material and shown that integral images were inherently tolerant to severe information degradation. The latter factor indicated that it is possible to display images from highly sampled data.

1.4. Objectives

To achieve the overall aim a number of objectives had to be attained. Perhaps the most obvious is to gain a through the understanding of the processes involved in the formation of an integral image.

In addition, the chief goals set are:

- Investigate and determine the nature of the lens decoding elements used.

  Theoretical work and practical experiments are used to produce concise analyses of the optical processes at work, providing useful information for image related work;

- Establish the feasibility of a complete mathematical analysis of integral image generation.

  Current optical approaches (i.e. Ray-tracing) produce discrete descriptions of image formation due to micro-lenses.

- To create simple computer generated images.

  Apart from providing the knowledge that creation of simple integral three-dimensional images is possible, this achievement would allow subjective experimentation to establish the relative importance of each of the optical effects. Therefore, a better understanding of the nature of integral images can be gained;

- Full computer generated images.

  The objective is to create highly detailed photo-realistic computer generated images as proof of principle.

1.5. Overview

The next chapter introduces the history and previous knowledge associated with general three dimensional imaging focusing on the field of integral imaging and its development. The origins of this subject are followed through the progressions ending at the current day.

Chapter three specifically deals with computer generation of images. Starting with standard computer graphics generation methods and then specifically into computer generation of integral images. This later section shows the progression and evolution of the methods investigated and their relative merits. Finally, in this chapter the progression towards photo-realistic images are shown.

The next chapter shows general application of the optical principals involved in the production of integral images. Analysis of the spatial resolutions of integral images are investigated and conclusions drawn.

Chapter five documents other associated work that was associated with the produced integral images.

Finally, conclusions from the previous chapters are brought together and overall conclusions are drawn.

2. DEVELOPMENT OF INTEGRAL IMAGING TECHNOLOGIES

2.1. The Origins of Integral Photography

"Integral photography" was invented and first reported by the French physicist M G Lippmann in 1908 (Lippmann, 1908). It was described as a process in which an array containing a large number of small spherical lenses (termed fly's-eye lens sheet because of their resemblance to an insects compound eye) was used to collect image data from many viewpoints. These lenses were placed in front of and in close contact with a photographic film in such a way that the refracting surface and the film surface are separated by the lenses focal length [figure 2-1].

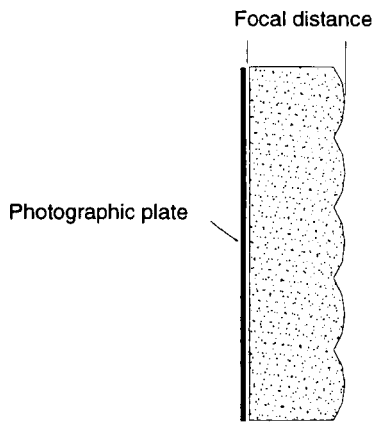

Figure 2-1, Micro-lens arrangement for recording.

The spatially differing positions of these micro-lenses allow the objects in a scene to be recorded from numerous slightly different viewing positions. The scene, recorded in the form of these micro-images, can be reconstructed by replaying the information through a similar array of lenses. This produces a spatial reconstruction of object space displayed in full natural colour. The technique utilises incoherent light radiation for both capture and replay. The process retains most of the benefits of normal photography (single exposure, single camera and non-coherent light source) but additionally records object parallax in all directions. This basic method suffers from the problems that all scenes recorded are captured as a photographic negative and are inverted in depth (pseudoscopic), meaning that near objects in the scene obscure the far scene correctly, but move relative to the viewer as if they were positioned at a distance, giving the eye/brain system conflicting information.

Lippmann devised a two stage optical process to correct these effects, which was later reported by H Ives (Ives, 1931). The method involves the object being captured, then replayed and then recaptured through a similar arrangement of lenses. This process reverses both the spatial and the photographic orientation and when the second integral image is replayed, forms a correctly translated, positive, orthoscopic image identical to the original scene [figure 2-2].

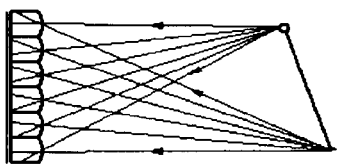

A. Recording an integral photograph

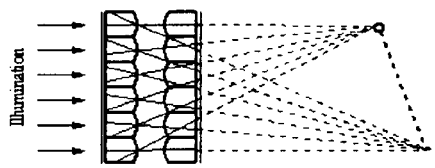

C. Recording second stage integral photograph

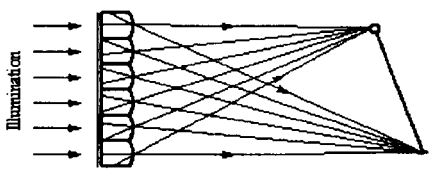

B. Replaying processed pseudoscopic 3D image

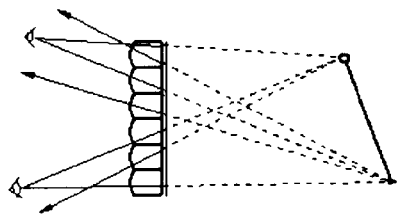

D. Replaying and viewing the orthoscopic image

Figure 2-2, Two stage integral imaging.

Unfortunately, the use of a second stage introduces significant amounts of noise, due to degradation in the sampling caused by aberrations (and possibly diffraction, depending upon the physical size of the lens) in the lenses (both replay and capture) and from moiré interference patterns caused by the similar frequencies of the sampling arrays. These effects are made more apparent as each micro-lens images the whole scene. Therefore the limited resolving power of the micro-lenses is compounded by this process.

One of the earliest tests of Lippmanns theories was performed by Sokolov in 1911 (Sokolov, 1911) (subsequently reported by Valyus (Valyus, 1966)). The early practical tests of integral photography were hindered by the need for a photographic emulsion plate to be covered by microscopically small lens elements. Sokolov overcame this by performing the photography using a multi-chambered integral pinhole plate as the imaging device. Several electric filament bulbs were used as discrete points in the scene and captured using the experimental set-up similar to the one shown [figure 2-3].

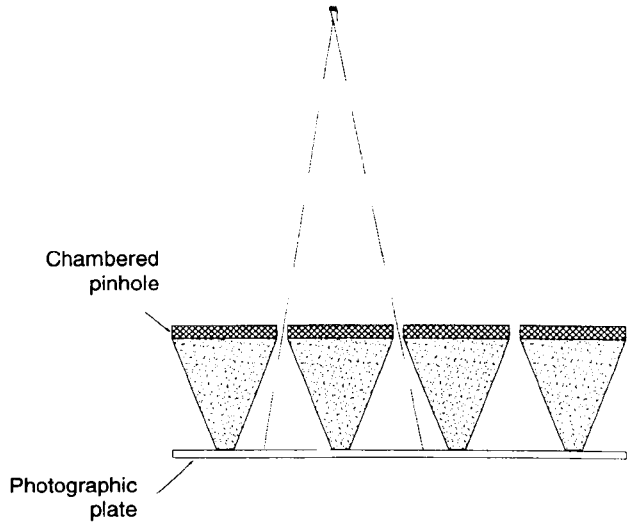

Figure 2-3, Sokolovs pinhole experiment.

Valyus described the sensation of viewing integral images as;

> *...the spectator should get the impression he would obtain by looking at the panorama through an open window. As he approaches the integral optic image he sees, just as if he were approaching the window, that the objects outside approach, the panorama expands, and the perspective and angular subtense alter.*

As an integral image is viewed from a changing viewpoint, the scene limits alter and the objects contained within behave as if they are valid points in the viewers space. This is unlike viewing stereoscopic images where the observer gains the unnerving impression that as their viewpoint changes, the image undergoes alterations in both shape, position and scale.

In later work, Burckhardt (Burckhardt, 1976), discusses a method of producing beaded photographic plates for integral imaging. In this method a photographic emulsion is coated onto a glass substrate which is coated with thousands of densely packed tiny (typically 50μm diameter) glass spherical beads [Figure 2-4]. By using a glass material for the beads with an index of refraction of N=2 the paraxial approximation of the focal surface of the element is the back surface of the bead.

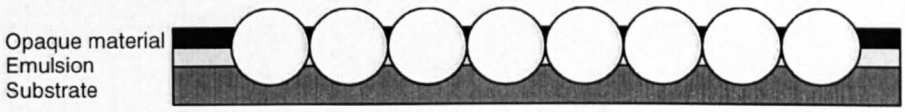

Figure 2-4, Glass beaded plate with inter-lens masking.

An extension to this method was proposed by Burckhardt, in which gaps between the glass beads were filled with an optically opaque substance [figure 2-4]. This was suggested as a method of producing a higher contrast image, preventing unlensed light from reaching the photographic emulsion. This was never attempted due to the practical problems associated with the fabrication of the beaded sheets and the subsequent photographic development.

Burckhardt continued his work in integral imaging and devised several alternative methods, advancements and theories relating to integral imaging. He performed analysis of integral images, with respect to resolution and devised depth of focus rules dependent upon the micro-lens pitch (Burckhardt, 1968(1)).

2.2. Close and Remote Integral Imaging

Essentially, there exists two differing ways of producing an integral image (Ignatev, 1983). Both modes of operation have different physical requirements and produce significantly different forms of images. These cases are known as close imaging and remote imaging.

Remote imaging describes a case when the capture screen and the objects of the scene are separated by a reasonable distance [figure 2-5]. In this case, the majority of the micro-lens images contain information about the position and intensity of every point in the scene. More importantly, in the replayed image every image point is replayed back in front of the micro-lens screen. A second stage spatial inversion of this image produces an orthoscopic image positioned totally behind the lens plane.

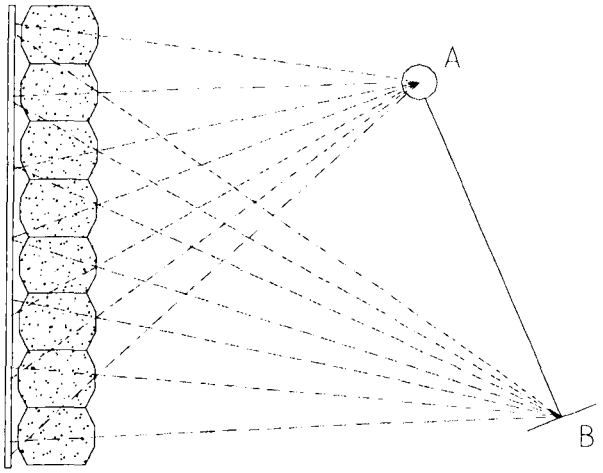

Figure 2-5, Remote imaging.

Close imaging is the case when the objects in the scene straddle the micro-lens recording plane [figure 2-6]. Close imaging can only be achieved when the scene is produced by optical methods (a single lens, a complex array of lenses or by projection of another integral image), as the capture plane is physically located within the imaged scene. The imaged object points in this case are located, unevenly across the whole sheet, but concentrated in areas defined by the projecting aperture size and distance. Hence, the number of lenses that define a point in space is almost entirely dependent upon the points distance from the recording plane.

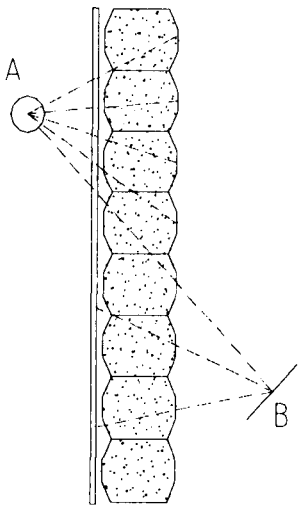

Figure 2-6, Close imaging.

The two-stage Lippmann method of integral imaging uses both modes of operation. Remote imaging is used to capture the first stage image, then either a remote or close imaging second stage can be used to re-capture and re-invert the space, thus recovering the original object. In this way, objects can be captured either to be totally behind the plate or to straddle it. Lippmanns method is limited in its flexibility because as the second stage recording plane is moved away from the position of the first stage replay the images degradation is increased due to the limited resolution capability and optical aberrations of the micro-lenses.

Burckhardts theory, relating depth of acceptable focus against a given lens pitch, gives two different requirements for lens pitch for each of the situations. Close imaging requires small pitch lenses and produces images with a lateral resolution dependent upon the lens pitch. Remote imaging requires a large lens pitch to capture the inherent depth and produces images with a resolution limited by the physical properties of the lens. Small lenses however, introduce diffraction effects that have a detrimental effect on the imaging quality and therefore the resolvable depth.

2.3. Viewing a Reconstructed Integral Image

The sensation of realism achieved when viewing a photographic integral image, is akin to the sensations gained when viewing real objects. This is because the viewers eyes converge and accommodate to the same spatial position, not to the screen plane as in stereo/multi-view systems (Yamazaki, 1989). Points from objects in the integral image form an "optical model" of the original scene (Bogusz, 1989), allowing the image to be viewed naturally or interrogated at a specific depth using a focusing plane. When moving a focusing plane through the scene, the coincident points in the image at that depth are in sharp focus while other points in the image are out of focus.

The optical model is recreated from the simple, angular information from the scene that each micro-lens records as an intensity pattern [figure 2-7 (A)]. When this is illuminated for replay, each micro-lens transmits a directional bundle of rays at the correct angle to reform the original point. Each individual micro-lens replays the angular scene information that was presented to it at recording. The effect of arranging these micro-optical devices onto a plane is that the angular information from any single micro-lens is combined with information from several other adjacent micro-lenses. This distributed angular information allows the recreation of points by ray bundles that appear to emanate from any point in space [figure 2-7 (B)].

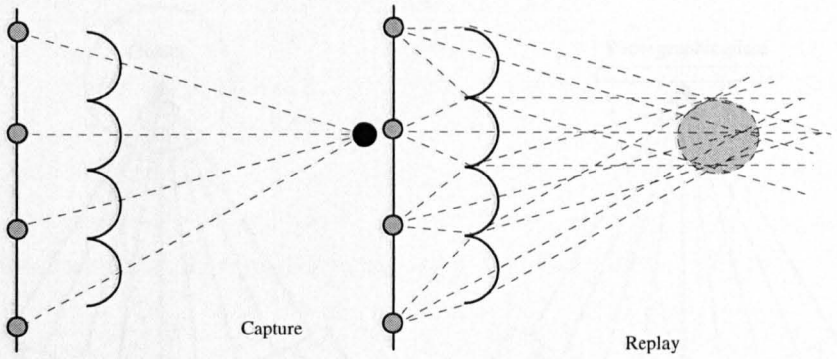

Figure 2-7 , Capture (A) and replay (B) of an integral image point.

Figure 2-7 also shows how the micro-lens pitch governs the physical resolution of replayed points. Points are recreated through the intersection of ray bundles, with the ray bundles having a physical width dependent upon the lens pitch. This results in an image point defined by the area of the intersecting beams that form it. However, in reality these rays are deviated due to geometric aberrations and diffraction in the lens, resulting in an overall spread that is larger than the micro-lens pitch. This effect was demonstrated by Stevens (Stevens, 1998) using a micro-optical element known as a Gabor super-lens (Gabor, 1940). A Gabor super-lens is constructed from an afocal pair of micro-lens arrays. However, the second array of micro-lenses has a different pitch to the first, this creates a global steering effect of the ray bundles, and hence acts like a lens.

Overall, small micro-lenses (≈50μm) are better suited to producing a more defined spatially located point, but due to increased diffraction effects these cannot image over large distances. Large micro-lenses are relatively diffraction free and image over large distances but cannot provide the lateral resolution required. This trade off between depth of focus and resolution, is dealt with by Burckhardt (Burckhardt, 1968[1]). The process in which individual bundles of light are directed towards a point in space illustrates the optical and viewing differences between integral images and stereo/multi-view images. Stereo/multi-view images are formed from several spatially separate two-dimensional images [figure 2-8 (A)]. These planar images are then projected onto a lenticular sheet [figure 2-8 (B)], and it is the angular information of the projectors that the micro-lenses record and replay. A viewer would see a single two-dimensional image located on the photographic plate only when located where a projector was used for the recording. Three-dimensional information is only recovered if the view uses two eyes and subsequent eye/brain processing to fuse the stereo-pair. Convergence and accommodation do not work in unison and this method can lead to eyestrain if the viewer is exposed to these images for too long. To achieved the sensation of continuous parallax in the image, a large number of projectors/cameras are needed, leading to situations where up to 64 cameras have been used to take a single multi-view image.

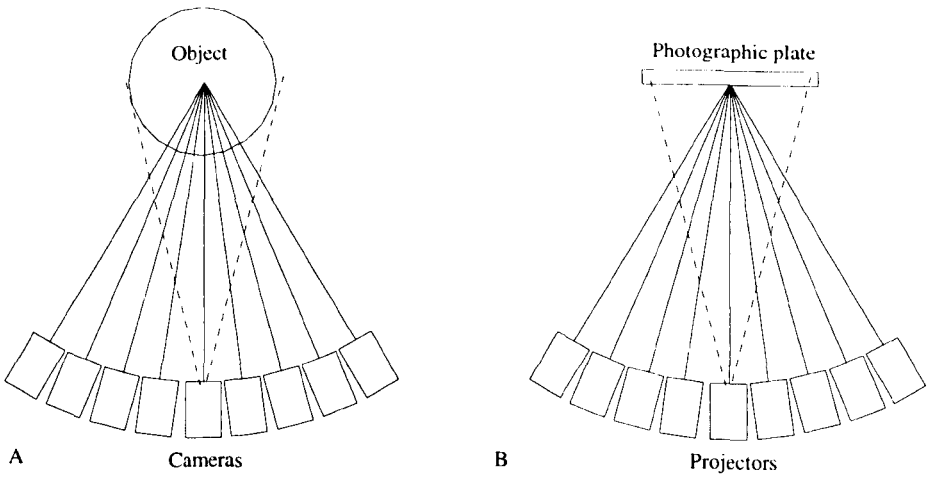

Figure 2-8, Production of a multi-view stereo-image.

In contrast, replay of an integral image occurs over an angular displacement dependent upon the characteristics of the micro-lenses used for replay and capture. Over this angle, the images appear to move as if the view was observing the original scene through a window limited by the extent of the replay screen and the size of the aperture stops used at capture. Within this replay zone, the image is constructed from rays being projected through the same lenses that captured them. Outside this main viewing area, subsidiary viewing zones are formed. These viewing zones are constructed from rays being projected through neighbouring lenses not those through which they were originally recorded. These side-viewing lobes repeat the original angular field of the main lobe and extend the usable viewing zone of the system. In practice, it is preferable to provide a physical limit so that individual micro-lenses images do not interfere with each other. This removes the possibility of capturing a confused image in the transition zone caused by the mixing of images at their limits.

2.4. Transmission Inversion Optics

Several major advancements in integral image have been made in recent years. For example, by the use of novel optical array configurations, it is possible to optically transfer a true, spatial model which exists independent to the observer. This along with new, flexible micro-lens fabrication techniques have enabled the two-stage Lippmann method of creating an orthoscopic integral image to be reduced to a single optical stage; thus making real-time electronic capture of integral images a possibility.

The next sections relate the development of the optical configurations which enable integral images to be produced in real-time.

2.4.1. Single tier auto-collimation optics

By placing two micro-lens sheets back to back and separating their optical surfaces by twice their focal distances, a "transmission auto-collimation screen" is formed [figure 2-9]. Auto-collimation is a process in which incident light is transmitted through the system and emerges from the back surface at the original angle of incidence. This optically enables points in the scene to be translated from in front of the screen to co-locations behind the screen.

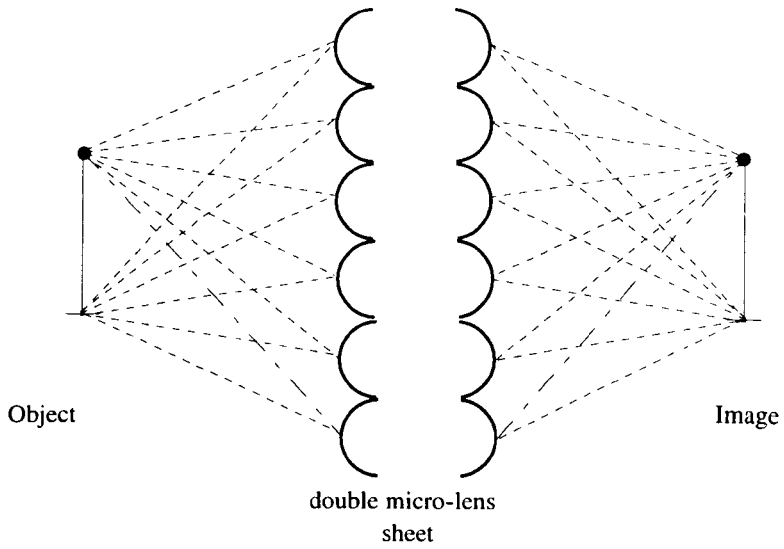

Figure 2-9, Single tier transmission and inversion optics.

Single tier auto-collimation screens have one major disadvantage. The effective depth of field of the transmission screen is limited by the diffraction effects inherent in the small micro-optical structures. The trade-off is between the small pitch desirable for high lateral resolution and a large pitch that is desirable to reduce diffraction and therefore maintain a satisfactory depth of focus.

Problems also occur in afocal lens pair combinations, if incident light is allowed to fall on the screen at an angle such that, at exit, it falls onto a neighbouring lens [figure 2-10]. In this case, instead of light being replayed at an equivalent angle it is replayed into a side lobe.

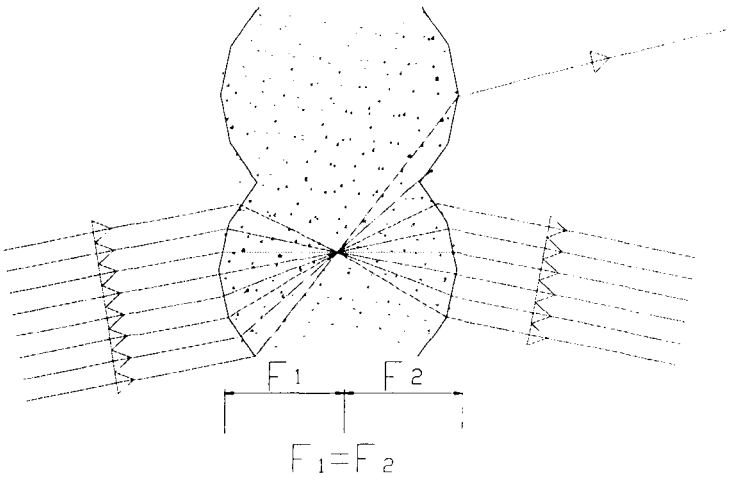

Figure 2-10, Side-lobe reconstruction by an afocal lens pair.

This occurs with an array of afocal, simple lens pairs for any incident angle other than rays entering along the optical axis. This reaches a maximum when all of the rays exit through a neighbouring lens at a ray angle (α) greater than;

$$\alpha = \sin^{-1}\left(N \times \sin\left(\tan^{-1}\left(\frac{pitch}{2 \times focal}\right)\right)\right) \qquad (2\text{-}1)$$

In equation 2-1, pitch is the lens pitch, f is the lens focal length and N is the index of refraction. For example, a lens array having 1.27mm pitch lenses, 3.08mm focal length and an index of refraction of 1.5 allows a maximum incident ray angle of 17.63°.

This implies that the intensity of the image transferred though the main lobe of the double micro-lens screen is reduced due to the marginal rays of off axis points being misplaced. This effect is doubly compounded by including the effects of spherical aberration in the lenses, as the spread of the rays deviates in practice by a greater amount than the simple paraxial rays equation predicts.

However, this vignetting effect can be reduced if micro-field lenses are introduced into the auto-collimating transmission element [figure 2-11].

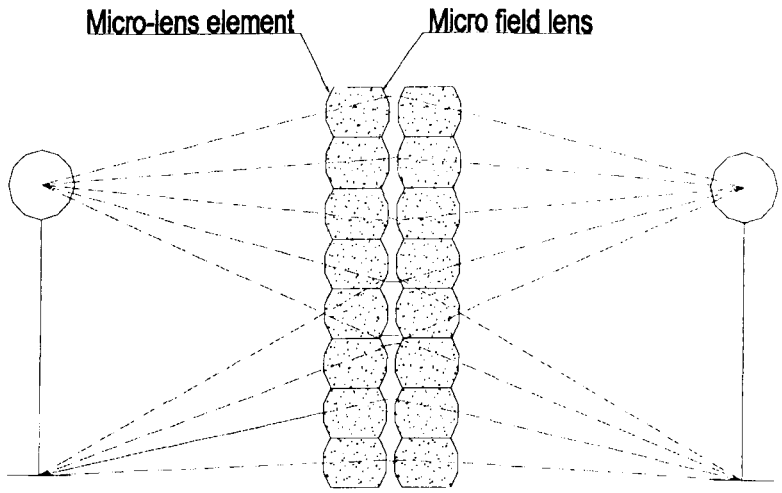

Figure 2-11, Transmission auto-collimation device with micro-field lenses.

This arrangement improves the situation and gives a maximum incident ray angle onto the auto-collimation sheet of 18.849° for the 1.27mm pitch lens.

Imaged scenes created from a single lens also exhibit another property. The geometric location of any point also corresponds to the phase information of the scene. However, any complex optical arrangement, especially the process of auto-collimation, disrupts the wave-fronts in the incident light, resulting in the location of an image point geometrically, but lacking the phase information. Parallel light falling on an auto-collimation screen [figure 2-12], is sampled and the angle of the incident rays wave-fronts adjusted so that a geometric co-location is formed. The temporal orientation of the wave fronts, in this case, is not maintained and is incorrectly propagated through the system. Therefore, phase information within an integral image can only be considered important over very small areas (the width of the sampling micro-lens pitch) and not as a general, large-area image forming effect. This supports the view that the majority of the resolution is generated purely from geometric optics.

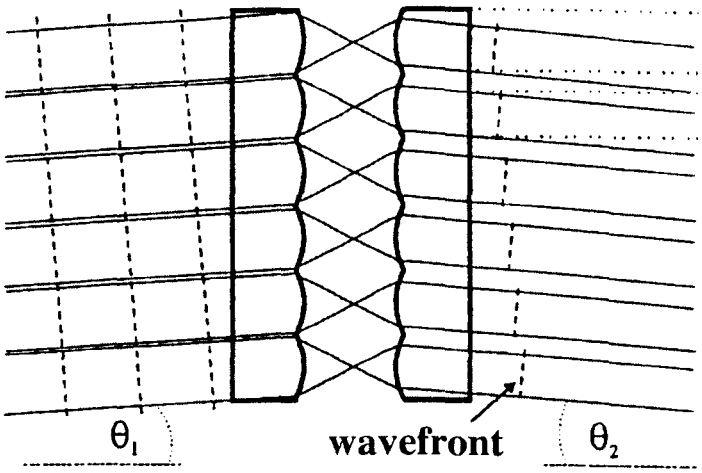

Figure 2-12, Wave-front deconstruction by an optical transmission screen.

While this simple single tier arrangement is capable of transposing the scene to a co-location the depth of focus is limited. This can be overcome by producing a two-tier optical combination.

2.4.2. Two-tier auto-collimation optics

A two-tier network is a combination of macro-lens arrays and micro-lens arrays. The macro-lens array is a regular array of high-quality camera lenses that together synthesis a large, high-speed aperture. The macro-lens arrays are separated by twice their focal lengths and the two micro-lens arrays, are symmetrically located between them. The pair of micro-lens arrays are placed back to back and separated by the sum of their focal lengths. The construction is described as an afocal array. In this combination, the lens arrays form an optical two tier "transmission inversion screen" [figure 2-13].

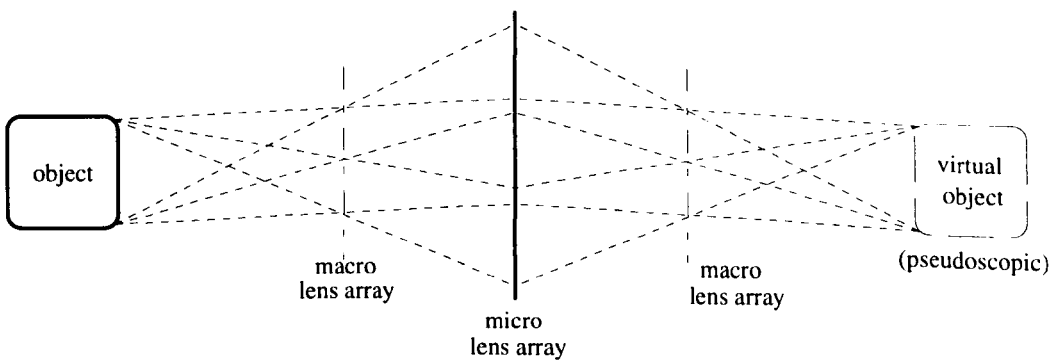

Figure 2-13, Two-tier transmission inversion screen schematic.

The arrangement facilitates the transmission of a three-dimensional optical model having the same size and depth information as the original scene. The benefit of using a macro and micro-lens combination is that it allows the transmission of all the depth planes in the scene, from 300mm (near point) to infinity, to be sharply focused.

The system achieves this incredible depth of focus by using the large-scale lenses to compress all the depth of the scene to within the working distances of the micro-lens screen. This scaled scene has the depth inverted by the back to back micro elements, subsequently creating rays that travel along a conjugate path to a similar large lens which then magnifies the scene back to the correct location at the correct scale (Davies, McCormick and Yang, 1988).

In the system, the large aperture macro-lenses retain the depth of the image, while the smaller micro-lens arrays preserve high lateral resolution. By combining the transmission inversion screen and classical integral photography, a one stage, purely optical photographic system is produced. This is an improvement over a simple single stage transmission screen as the depth of field is improved. In addition, it improves over two stage capture systems as there is reduced image degradation. The largest benefit of two-tier capture is that the scene is both translated and inverted spatially. Additionally, the lens aberrations of the optical paths are cancelled out, as the optical path of the rays through the system is symmetrical. This allows the complex optical train to be constructed from simple, inexpensive, lightweight lenses while still being able to maintain the optical resolution and depth of the image.

The two-stage system can also be produced in a purely reflective mode (Jacobs, 1982; Street, 1983). In this formation, the large scale lenses project the image onto a retro-reflective screen, a device that returns any incident light back in the same direction, e.g. Glass beaded screen, corner cubes or micro-lens mirrors. These image forming rays are sent back to a co-location determined by the relative positioning of a half silvered mirror [figure 2-14].

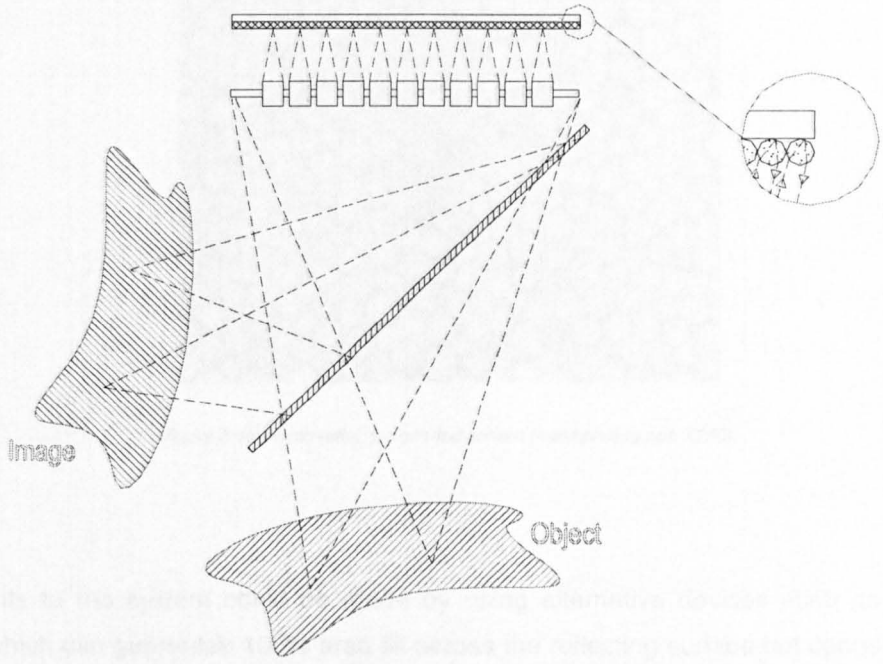

Figure 2-14, Retro-reflective camera schematic.

This arrangement has the benefits of making the camera system lighter, cheaper and smaller as the optical elements for the micro and macro lenses are shared. In addition, this configuration automatically aligns the optical elements of the system so that expensive and complex alignment is eliminated. However, the system has the disadvantages that light can travel directly through the system from certain angles and can bounce within the camera thereby reducing contrast. The image is reduced in overall intensity compared to a transmission system, as only one quarter of the light can theoretically enter the front aperture of the camera to form the final image due to the ray paths reaching the photographic emulsion after passing through a half silvered mirror twice.

Optical loss is also increased as the beaded screens available [figure 2-15] do not have the optical elements uniformly distributed across the surface, and contains obvious dead areas. However, these dead areas are small and randomly distributed across the sheet and therefore do not disrupt the image, although they do contribute to the loss of intensity in the final image. Several macro-lenses contribute to forming a single point in space and thus mask the effect introduced by the dead areas. To further reduce this effect, Street used a diffraction grating to spread the image that was incident on the retro-reflector. This produces an image that has less obvious effects caused by defects in the retro-reflecting material. However, diffraction induced colour fringing effects are introduced.

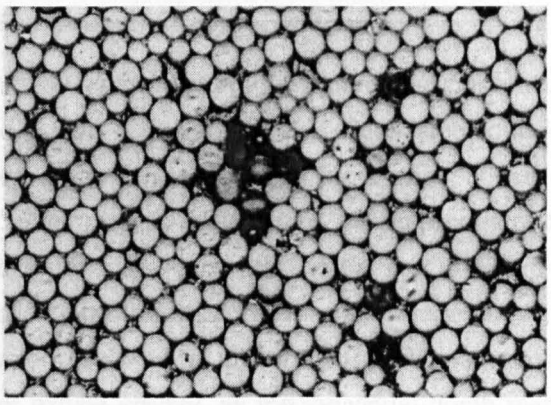

Figure 2-15, Retro-reflective beaded screen (microphotograph X250).

Improvements to the system could be made by using alternative devices such as corner cube reflectors, which can guarantee 100% area fill across the reflecting surface but cannot currently be manufactured with small enough feature sizes. Using large aperture retro-reflective devices reduces the quality of the final image, due to offsets introduced between the incoming and outgoing rays. This effect is shown in figure 2-16.

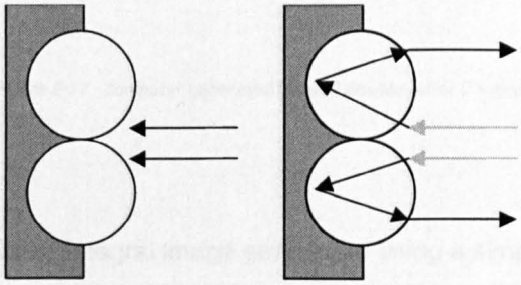

Figure 2-16, Retro-reflective induced ray offsets.

Although advances in physically realising a camera system have been made, to date little interest has been shown in integral imaging as an image capture system. Similarly the computer graphics generation of integral imaging has received little attention.

2.4.3. Early Computer Generation of Integral Images

There have been two previously reported attempts at computer generation of integral images. The first being by Chutjian and Collier (Chutjian, 1968). Their technique involved the generation of discrete computer generated slices of information of the scene. These slices were then subject to multiple exposure onto a photographic plate, from the appropriate distance [figure 2-17 (A)], thereby creating a composite computer generate integral image [figure 2-17 (B)]. The method is complex and to create and capture the resulting images requires using piece-wise generation for the various slices. The system is not at all practical for real-time image generation. Additionally, the image produced cannot exhibit solidity, as the individual depth planes are unable to obscure one another.

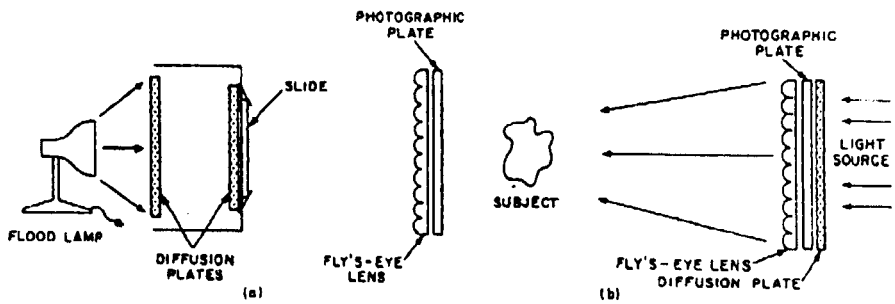

Figure 2-17, Computer generated integral images, after Chutjian.

Igarashi (Igarashi, 1978) studied integral image generation using a simple geometric approximation and succeeded in generation a synthetic integral image. This method allowed a computer to perform the image generating, and to project it from a large CRT onto the back surface of a micro-lens screen. Their method allowed the production of images, but the models used to simulate the lens sheets are very basic approximations and were hampered by the limited resolution of display technology. However, this basic lens model provides a good starting point for an investigation. The next chapter examines the methodology by which the development of a complete system for the production of computer generated integral images can be carried out.

3. COMPUTER GENERATED INTEGRAL IMAGES

The production of integral images relies upon the algorithms developed for computer graphic displays. These imaging fundamentals are introduced, and then the description of how they were extended to form an integral imaging system is given. Finally, a photo-realistic image generation method, based upon ray-tracing is described. Examples of the images produced and comparisons between photographic and synthetic images are used as measures of quality.

3.1. Introduction

Computer generation of "three-dimensional" images has been around for almost thirty years. Essentially, the three-dimensional stored data, held in the form of a three-dimensional vector (x,y,z), is mathematically transformed for orientation and projected onto a two-dimensional plane for display. This provides, as long as the observer remains stationary, the impression that the viewer is looking though a window positioned at the plane of the screen onto the modelled scene. This is achieved through the artificial production of human perception cues, such as perspective, texture gradients, atmospheric effects and obscuration.

Production of early computer images were hampered by the cost of the computational power required to generate the images (immense by the computing standards of the time), the cost of memory and the devices needed to display the generated images. More recently, photo-realistic methods for producing images, along with high quality output devices and hardware accelerators with near photographic display quality have greatly improved the potential for this field of research.

3.2. Generation Methodologies

The methodologies for producing computer representations can be roughly divided into two separate approaches, geometric projection and ray tracing. Geometric projections; where reference points within the scene are used to calculate the position of pixels on a two-dimensional plane. Ray casting/tracing methods; where the pixel positions are used to explore the scene to determine which objects (or sections of objects) are visible at that point.

Both of these methodologies are formed around a simplification of the observers eye location and orientation with respect to the viewing screen. This gives a situation where the viewers eye provides the centre of projection for the world model. These approaches are reported with the goal of producing synthetic integral images.

3.2.1. Planar geometric projections

Geometric projections provide a simple starting point for image production. The mathematics of projection is based upon a pinhole approximation for lenses, which allows the calculations to be reduced to similar triangles. This approach is encapsulated in equation 3-1 and figure 3-1.

$$\frac{P_x}{P_z} = Screen_x \Rightarrow Screen_x = \frac{P_x}{P_z} \times d \tag{3-1}$$

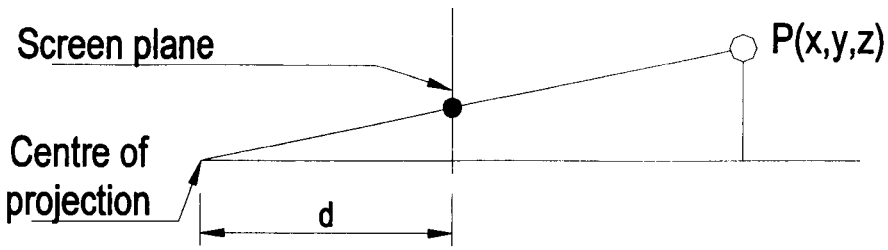

Figure 3-1, Geometric projection of a point (P) onto the screen plane.

Being data oriented, that is the scene generation calculations are performed once per object data entity. Therefore, the technique suffers little overhead for small scenes. This has the advantage that it allows the algorithms to be devised easily and for images to be generated quickly. Disadvantages of this technique are that the images produced are inherently wire-frame and angular due to the surfaces being composed of finite triangular faces. This quickly leads to the situation where complex models produce confusion and loss of information in the image. Therefore, simple structures are best modelled using this method.

The geometric projection algorithms can be extended to allow shading of the objects to provide a facility for basic solid models, a technique known as rendering. The rendering process can become so detailed that the level of realism in the resulting image approaches photo-realism. In fact, many of today's modern commercial image producing software use geometric projection to achieve their results, e.g. 3D Studio Max, AliaslWavefront (Kinetix, 1999; Alias, 1999). The graphics generated with these tools can be seen in many modern cinema films such as Pixars "Toy Story" (Lasseter, 1995). The popularity of geometric projection is due to the visually impressive results that can be achieved for a relatively low computational speed/cost overhead.

Renderer object models have to be constructed primarily from triangular faces. This can cause a form of spatial aliasing called "geometric aliasing" when these straight edge components are visible. The surface details of these faces are "painted" after projection using an approximation to lighting effects or simply by solid filling.

Moving towards a ray-traced model allows the possibility of a more optically correct approximation of lenses, materials and the lighting conditions to be included. Ray tracing, additionally, allows the construction of mathematically correct models and images as the objects in the scene for ray tracers are geometric solids that exist without the inherent need for decomposition into triangular faces.

Ray tracing / Ray Casting

The ray tracing method determines the visibility of surfaces by projecting large numbers of "viewing" rays into a scene. In general, rays are created which emanate from the viewers position through the centre of each of the screen pixels and travel in the direction of viewing as defined by the centre of projection or camera parameters [figure 3-2]. As rays intersect with objects they spawn other rays. These new rays represent the reflection and refraction components of a given surface. These additional rays are also projected into the scene and if found to intersect a solid further rays are spawn to provide extra refinements in the final intensity of the original pixel (Appel, 1968). The rays used in the tracing of the scene and the objects which describe the contents of the scene are specified mathematically, hence ray-object intersections can also be defined mathematically. Equation 3-2 describes a ray starting at position (x_0,y_0,z_0) and extending to position (x_1,y_1,z_1).

$$\begin{aligned} x &= x_0 + t\Delta x \quad y = y_0 + t\Delta y \quad z = z_0 + t\Delta z \\ \Delta x &= x_1 - x_0 \quad \Delta y = y_1 - y_0 \quad \Delta z = z_1 - z_0 \end{aligned} \tag{3-2}$$

Equation 3-3 describes a sphere at position (a,b,c) with diameter (r).

$$(x-a)^2 + (y-b)^2 + (z-c)^2 = r^2 \tag{3-3}$$

Therefore, their intersection can be found by combining these equations, giving equation 3-4.

$$\begin{aligned} &(\Delta x^2 + \Delta y^2 + \Delta z^2)t^2 + 2t\big(\Delta x(x_0 - a) + \Delta y(y_0 - b) + \Delta z(z_0 - c)\big) \\ &+ (x_0 - a)^2 + (y_0 - b)^2 + z_0 - c)^2 - r^2 = 0 \end{aligned} \tag{3-4}$$

To determine the ray/sphere intersections equation 3-4 has to be solved for the variable *t*. If no solutions exist then the ray and the sphere do not intersect. If a single solution exists then the ray only grazes the spheres surface. If two solutions exist then the ray intersects the sphere. The positions of the ray-sphere intersections are calculated by putting the solutions for *t* back into the equation of the ray. Similar calculations are performed to detect intersections for the various other geometric solids from which the scene is built. Complex objects are built using logical operations (union, difference, intersection) on these simple solids.

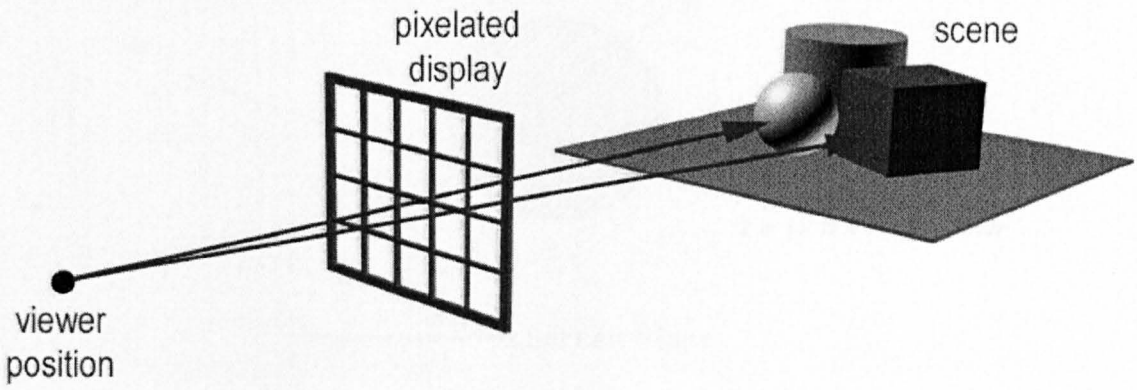

Figure 3-2, Ray tracing into a scene.

The tracing of rays continues until a predefined limiting condition is met. Termination conditions are empirically chosen so that the image has the desired "quality". They are usually based on the conditions such as "the current ray intersects no other objects" or "the ray no longer contributes a large enough colour component to the initial ray". At this point, the sum of the intensities of every ray created by that pixel (modified by constants that are dependent upon the objects materials properties) defines the final pixel intensity.

In the simple case illustrated [figure 3-3], the intensities *I*, *Ic*, *If* and *Ir* represent the pixels intensity, the natural intensity of the object (colour), the intensity of the ray caused through refraction and the intensity of the ray caused by reflection respectively. These are modified by the constants *j*, *k* and *l* which represent various user definable scene and object parameters (the ambient light term for the scene, the transmissibility of the objects and the reflectivity of the object)(Kay and Greenburg, 1979; Whitted, 1980).

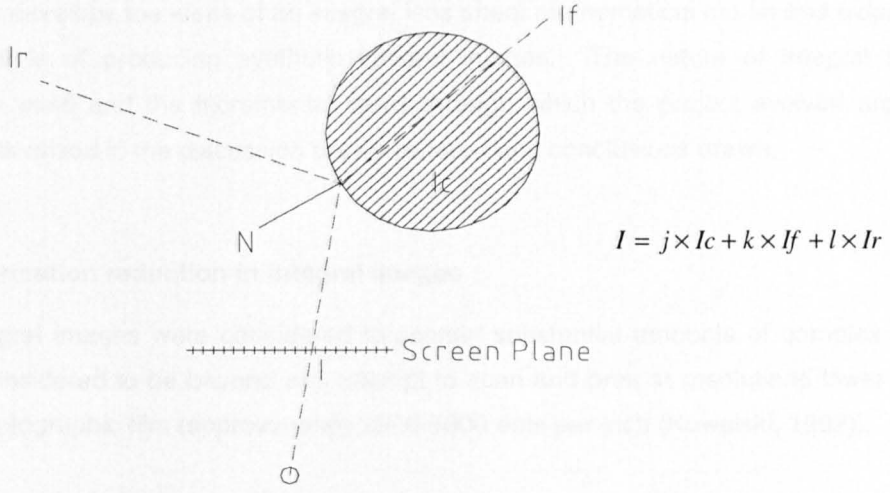

$$I = j \times Ic + k \times If + l \times Ir$$

Figure 3-3, Determining the illumination of a pixel using recursive ray tracing.

Additionally, specular reflections of highly shiny objects can also be produced by adding a term that is dependent upon the angle between the normal, the light source and the impinging ray. As the angle between the normal and the impinging ray approaches the angle between the normal and the light source, the intensity contributed from reflections of the light increases.

Special features such as over-sampling of the two-dimensional image, inter-object diffuse reflection (Radiosity), atmospheric effects and area lights provide greater realism effects but make it necessary to generate a substantial amount of additional rays than one per pixel (Cohen and Wallace, 1993).

3.3. Investigation into the Production of Wire-frame Integral Images

3.3.1. Introduction

Through work undertaken to establish: the feasibility of replaying integral images produced using classical printing techniques (Brewin, 1997), and additionally an investigation to establish if a discrete, blocked pixelated display could be used as a device to replay integral images. It was concluded that a computer could be used to produce the necessary intensity levels to produce a synthetic integral image. Initial work centred on a simple software model using the same simplistic lens approximations as Igarashi. This work was subsequently extended to produce a more correct, practical and realistic model, capable of producing photo-realistic images.

This chapter develops the ideas of an integral lens sheet mathematical model and extends this to a system capable of producing synthetic integral images. The nature of integral images, the assumptions used and the incremental steps through which the project evolved are described. Finally, points raised in the discussion are considered and conclusions drawn.

3.3.2. Information reduction in integral images

Initially, integral images were considered to contain substantial amounts of complex information, and were considered to be beyond any attempt to scan and print at resolutions lower than that of standard photographic film (approximately 3000-5000 dots per inch (Kowalski, 1992)).

The assumptions that integral images require a high resolution stem from figures calculated and published by one of the leading integral imaging authorities Okoshi (Okoshi, 1976). The bandwidth required to transmit a single image was suggested to be as high as 43 Giga-hertz. Perhaps the reason for such high figures for information content is that assumptions were made that the nature of integral imaging was akin to holography. Therefore implying that they are similar in both resolution requirements and the complexity of the distribution of point information.

These bandwidth considerations are impossible to ignore, especially when the micro-image produced behind each lenslet is microscopically examined. From figure 3-4, it can be seen that the micro-lenses have resolved the structure of the camera system optics and have imaged a reasonable amount of information with each aperture. This information relates to the angular intensity information of the objects in the original scene.

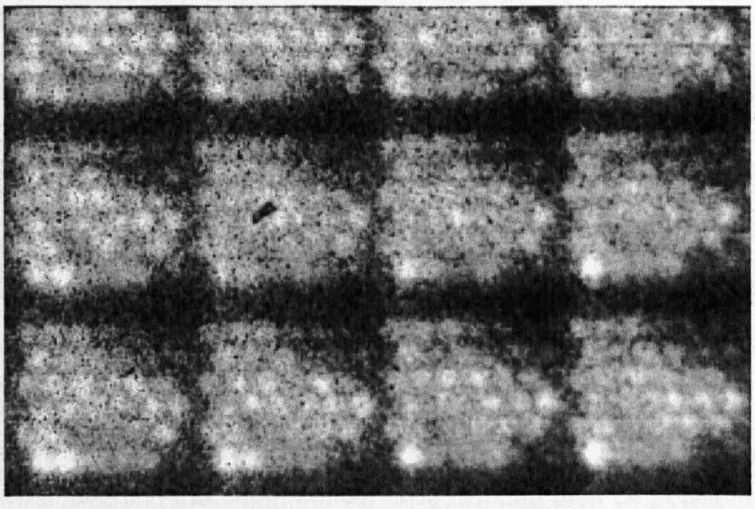

Figure 3-4, Photographic integral micro-images.

The example is of a close imaged scene and it can be seen that the details of the image are unclear, as each micro image only represents a small portion of the object space. However, a high degree of correlation can be observed between neighbouring micro-images.

Practical experiments carried out by Stevens (Stevens, 1991), show that the depth resolution of an aerial image, projected from a two tier integral camera system, is of the order of ±0.075mm using a 0.125mm pitch integral lens array.

A series of experiments were devised using various print techniques at different resolutions to establish if there was a need for a high bandwidth for correct replay of integral images. The results of these experiments showed that the figures previously presented were grossly incorrect and indicated that integral images could be displayed on devices which had replay resolutions significantly lower than one pixel per lens and on systems where complex dot shapes were utilised. Amazingly, the reduced information integral images produced retained their continuous parallax, however they understandably suffered from a loss of resolution and contrast. This basic fact illustrates a fundamental difference between integral and multi-view/stereo images. In stereo multi-camera systems, it is necessary to have an integer number of pixels per view and a minimum of one pixel per view, whereas with integral images continuous parallax can be retained over a huge range of resolutions. This makes the integral imaging technique more flexible even allowing non-integer numbers of pixels per micro-lens to be used without loss of image coherence.

3.4. Optical simplifications

3.4.1. Camera system approximations

The first stage was to develop a computer model of the transmission optics (also referred to as "the camera system"). The nature and the manner of use of the camera system in the production of one stage integral photographs, results in the computer model being a highly simplified version of the original. This simplification is possible as the camera system optically translates a scene from one position in space to another, whilst retaining the correct spatial relationships in all axes (one to one scaling).

The real camera system allows a photographic plate to be positioned at any arbitrary plane in the scene (Davies, 1988). This is achieved by translating object space into another spatial location as a volume image whilst inverting the depth sense. The film can then be positioned as desired. As the resultant space is optically generated, the film plane can be positioned to bisect an object in the scene. However, in the computer model this is not as important, the position of the film plane and objects can easily coexist at the same position in space. Thus, this specific action of the film camera is not a modelling requirement.

The computer model created characterises the actual camera parameters and the positions of all the essential optical elements. This information is used to determine the limiting cases for impinging optical elements. The aperture prevents overfill in the micro images by providing a physical stop that restricts the incident rays projected on the recording screen.

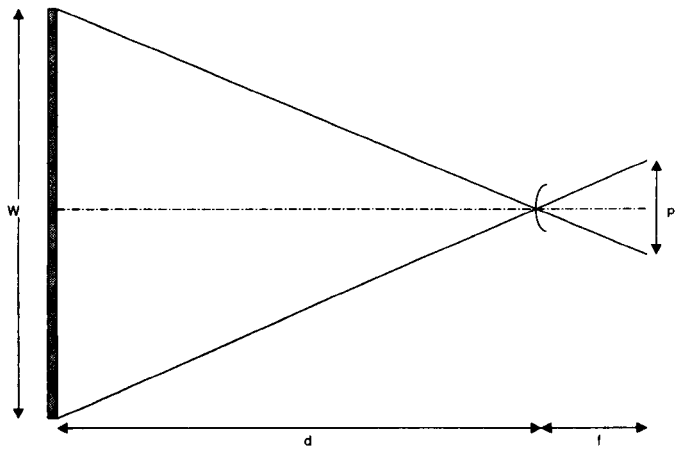

Figure 3-5, Projection of image fields.

The diagram [figure 3-5] shows W as the aperture width, f as the lens focal distance, N as the lens index of refraction and p as the lens pitch. The condition, which correctly limits the maximum angle of impinging rays onto the film plane, is given when equation 3-5 is satisfied.

$$d = W \times \frac{f}{(N \times p)} \tag{3-5}$$

This analysis is essentially a generalisation. It is based only on a simplified pinhole approximation, with adjustments made to allow for refraction of the lens surface, producing a value roughly 1/N times smaller than the figure produced by the pinhole model.

To correctly fill the micro-lens fields it is obviously necessary to control distance d. If the camera aperture is positioned so that the distance from it to the lens sheet is greater than d then the aperture in the micro-lenses will never be overfilled. This is due to the imaged width of the aperture being smaller than the pitch of the lens sheet. When the distance between the lens sheet and the aperture is equal to d then the micro-images are correctly filled. That is there should be no overfilling effects, such as multiple imaging, and no under-filling effects, such as dead areas between the micro-image zones.

If the rays incident on the lens sheet are not limited then the micro-image fields will always be overfilled. This results in data from one image field subsequently being replayed incorrectly through a neighbouring lens [figure 3-6], thereby causing objects in the scene to be visible in both the main image lobe and the side lobes simultaneously, creating multiple instances of the point(s) imaged from that direction. If the micro-lenses are positioned so that under-filling occurs within the micro-lens apertures, then the result is a noticeable blank band when traversing from the main image lobe to the side lobe views. This blank band represents the unused portion of the recording plane (film).

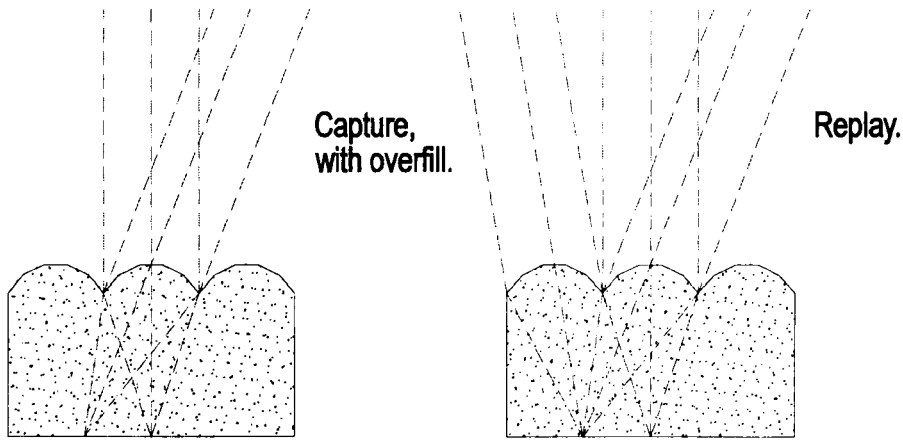

Figure 3-6, Effects of overfill: side lobe replay.

Classical integral imaging as reported by Lippmann is handicapped by the need to use a two-stage process to produce an orthoscopic image in replay. That is, to produce a final orthoscopic image any capture system must perform a spatial inversion. Lippmann achieved this by the replay and subsequent recapture by a similar lens array of the image. This inversion and re-inversion of space to its original orientation is necessary to produce a final image that is orthoscopic.

The transmission camera developed by Davies and McCormick optically performs this important transformation of space while translating the scene from object to image position. This is a major feature of the camera and it allows the integral image capture to be performed as a single stage. This transformation can be performed mathematically by the computer, simply by reversing the sense of the axis which represents the distance from the camera aperture, to enable the objects to be correctly orientated for capture. This spatial inversion can be physically seen and measured, by moving a focusing screen through the various depth planes of the spatial model, and measuring the relative sizes and positions of objects in the scene. If these positions are compared to the original objects, they are identical.

With the camera system model established, the computer based objects are positioned in virtual space and processed so as to appear as if they had been transformed and translated by the physical camera system

The location of points defining the object are transferred to 'film' by projecting rays from their spatial location through the individual micro-lenses onto a virtual film plane. Once the film plane position of the individual rays are calculated the colour and brightness can be recorded. The focus of this research is to investigate methodologies for translating a point in space to a point on the recording plane and recording appropriate colour/brightness.

Computer and photographic experiments have been designed and performed to validate software models, develop methods of approximating system elements and to investigate the visual effects of changing system parameters. The most important things to consider in the system are the cone angle generated by the camera system for any point in space and the final capture micro-lens approximation.

3.4.2. Experimentation framework

The backbone of the application had to be designed to allow an evolving and ever changing, experimental investigation. An initial application framework was established to contain various independent experimental calculation blocks. Within the framework, it was to be possible to maintain a system that provided a constant set of functions from within which the image generation code snippets could be established and tested. Consequently, the framework (shown in Appendix E) is structured in a way that tracked the evolution and development of the software lens models. This structure was established and modified over several iterations and enhancements of the image production code. The effectiveness of this approach demonstrated by the levels of feature enhancements, for example the code progressed from simple processing of single points, to processing of lines and then faces. This early code structure allowed several alternative methods to be quickly prototyped, tested and evaluated.

The code structure allowed the lens modelling function under test to be given the scene data, as a series of three-dimensional points. These processed points were then placed into the frame store and written as a Targa graphics file (Truevision, 1999) by a common function.

3.4.3. Development of micro-lens approximations

As a starting point, to test the assumption that a computer based method could generate integral images, a mathematical geometrical pinhole model was initially chosen as the micro-lens sheet approximation. This model was chosen for two reasons; it provides an extremely simple model by which to transform the object data, and Sokolov (Sokolov, 1911) showed that integral images could be produced using a pinhole plate as a recording device. Igarashi used this model for generating integral images and so it was an obvious starting point as the approximation is both practical and valid. The adoption of a simple mode is self-justifying if effects can be effectively analysed.

3.4.4. Simple pinhole approximation

The principle assumption that allows a pinhole to be treated as a similar image forming device to a refracting lens is that the rays incident closest to the optical axis (paraxial rays) of a lens are the image forming rays in the system. Therefore, only a single calculation is needed to establish the position of the formed point. The diagram produced by a commercial lens analysis tool (ASAP) [figure 3-7] shows that in an uncorrected lens (i.e. a simple plano-convex lens such as a micro-lens), rays incident at the extremes of the lens (marginal rays) focus to a different plane, when compared to the paraxial rays.

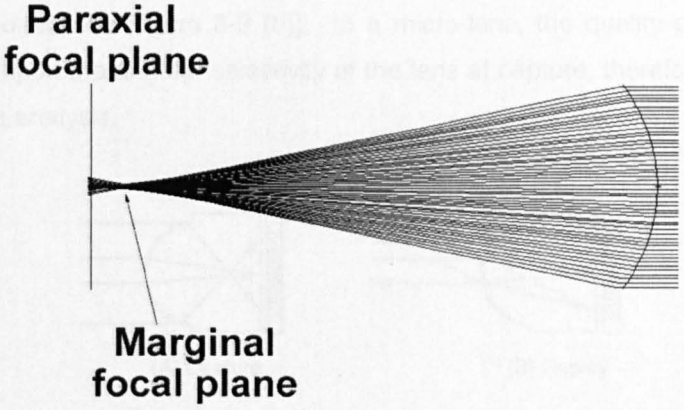

Figure 3-7, Optical ray trace of a plano-convex lens.

This can be seen in the point spread intensity profile [figure 3-8] taken at the paraxial focal plane of the lens, as the spread caused by the out of focus marginal rays is visible but at a far lower level than the paraxial ray focal points.

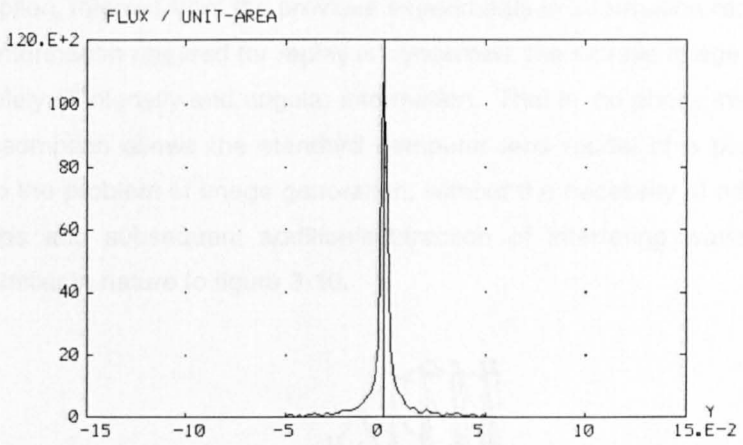

Figure 3-8, Point spread function of a plano-convex lens at paraxial focus.

In a photographic image using an uncorrected lens, these unfocused marginal rays, if recorded at the focal plane lead to reduced contrast and loss of image quality when the image is replayed. This is due, firstly, to the information being out of focus when it is captured and secondly, to the fact that all directional ray information is lost at the time of capture [figure 3-9 (a)]. Therefore, when an image is replayed, the spread, instead of reconstructing a perfect bundle of rays, causes replay in various spurious directions [figure 3-9 (b)]. In a micro-lens, the quality of image formation at replay is dependent upon the angular selectivity of the lens at capture, therefore, marginal rays can be removed from the analysis.

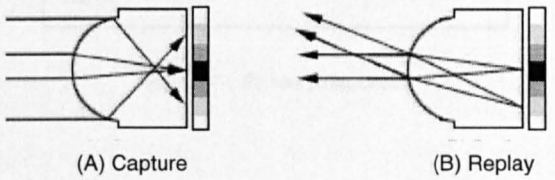

Figure 3-9, (a) Aberrated capture, (b) subsequent replay.

In computer models, which exhibit no spherical aberration or lens distortions, higher resolution images can be created than those that are produce solely by optical means. This is due to there being no defocus of the image points and therefore no confusion of angular information at capture.

A second assumption, inferred from the previous experiments in information reduction and printing, is that as far as information required for replay is concerned, the sample image captured at the film plane consists solely of intensity and angular information. That is, no phase information is present. In effect, this assumption allows the standard computer lens model of a pinhole camera to be directly applied to the problem of image generation, without the necessity of additional optical path length calculations and subsequent addition/subtraction of interfering waves. This produces integral images similar in nature to figure 3-10.

Figure 3-10, Simple pinhole image (close up).

The basic structure of the integral image generation algorithm using a pinhole model as the lens function can be seen in figure 3-11.

```
For every point
    For every micro-lens
        Generate a ray;
        Sum intensity;
    End
End
```

Figure 3-11, Pinhole pseudocode.

Benefits of the simple pinhole model

Since the pinhole is the simplest optical device that can form an image, it has many advantages as a mathematical approximation for a lens. Optical advantages include images that are totally free from distortions, curvature of field and chromatic aberrations. The main advantage for simulation being that calculation can be performed extremely quickly. The projection of a point to a location on the film plane can be simplified to similar triangles, which can be performed relatively fast [figure 3-12].

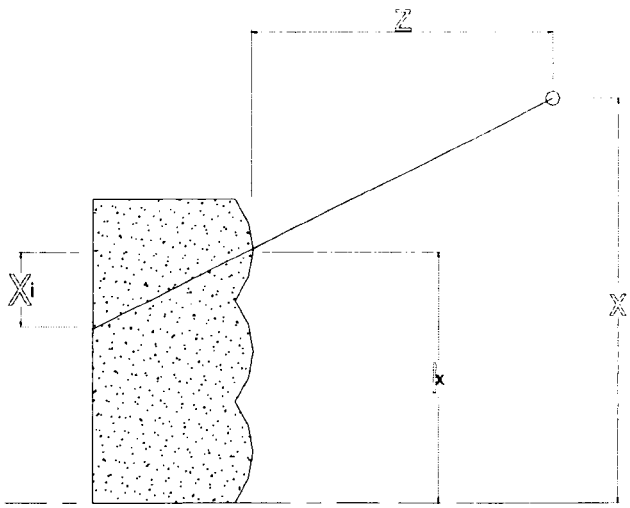

Figure 3-12, Pinhole approximation through similar triangles.

The position of the image point (x_i, y_i) formed through lens (l_x,l_y) of pitch p and focal length f, from object point (x,y,z) can be found by equation 3-6 and equation 3-7 respectively.

$$x_i = (p \times l_x) - \frac{(p \times l_x)}{z} \times f \tag{3-6}$$

$$y_i = (p \times l_y) - \frac{(p \times l_y)}{z} \times f \tag{3-7}$$

In most practical cases computer pinhole models use infinitely small apertures to form the image. This simplifies image formation even further and greatly improves image resolution and depth of focus, as a perfect mathematical pinhole has an infinite depth of focus.

In addition, by using this method the model allows all previously researched computer graphics algorithms, hardware devices and speed-ups to be applied when implementing the system.

3.4.5. Failures of the simple pinhole model

The main negative point of the simple pinhole is that it is only a very basic approximation, and as such ignores more complex lens effects such as diffraction, image point spread and aberration. The model also ignores simple but important lens effects such as refraction, and therefore produces results that are incorrect. This would possibly be acceptable if images for direct viewing (without a lens sheet) were being created and this is the case in conventional computer graphics. However, since the image is going to be replayed on a pixelated device where the pixel size is going to be considerably larger than the effects induced by refraction, such minor alterations to image point position are going to have a very limited effect.

Another negative effect which is apparent when viewing images created with this model, is that any objects which cross the screen plane fade out as the edges of the object approach the screen and then reappear at the other side [See examples in appendix A]. This vanishing of the image at screen plane is caused by the lens aperture size in the approximation used. It is assumed that the aperture of the individual micro-lenses are infinitely small and not, as in the case of the real lenses sheets, an aperture with a physical size. The result is that a definitive cut off zone occurs and points within this area are incorrectly replayed, being only visible at the location of the pinholes. This zone is created by the individual micro-lens field of view and its proximity to neighbouring lenses [figure 3-13].

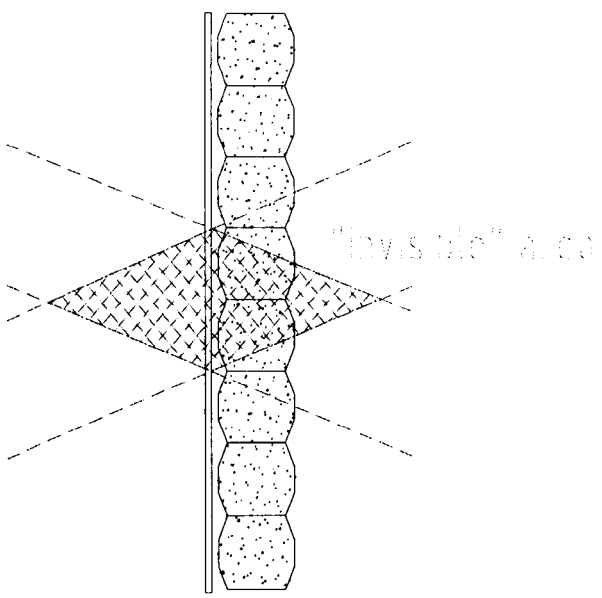

Figure 3-13, "vanished" line segments.

Unfortunately, this effect is not a trivial task to correct in the pinhole method. Correction is dealt with later in this chapter where enhancements to the micro-lens model are described.

The cause of the vanishing of lines segments in the image is due to the fact that as an image point moves to within ±f of the micro-lenses, the image field produced varies from a relatively small point to an area comparable to the lens width. This occurs due to the inability of the lens to focus the object point at these distances. For example, at a position +f (the front focal plane), the image field produced should be as large as the lens diameter due to the light being collimated [figure 3-14 "point 1"]. At distances closer than +f the lens is unable to concentrate the light from the point significantly, resulting in an energy spread which fills more than the lens pitch in area [figure 3-14 "point 2"].

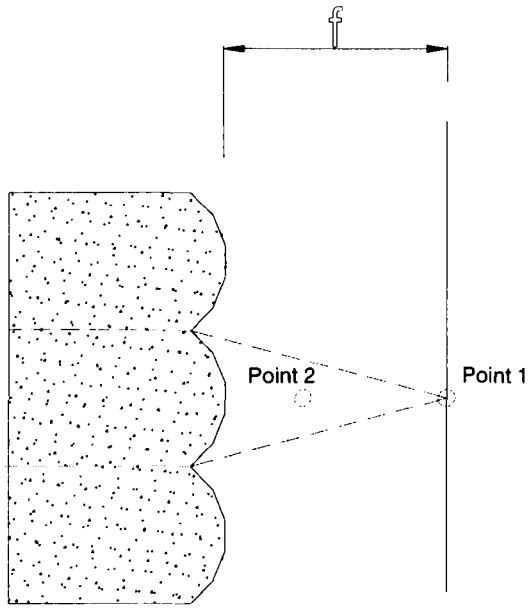

Figure 3-14, Unfocused points.

Of course, this effect does not manifest itself in the simple pinhole model as geometric projection will always map an object to an infinitely small image point.

It was because of this and other inaccuracies of the simple pinhole method that a more correct approach was sought which could model the complex effects associated with spherical refracting surfaces and in addition have the potential for speed and simplicity of the pinhole model. The search started by constructing a complex lens model which contain very few simplifications.

3.4.6. Full optical ray trace

This method has found a following in computer optical analysis tools such as ASAP (Brealt, 1997) [figure 3-8] and should not be confused with the computer graphic generation method also called ray-tracing, with which it shares some similarities.

The method is favoured as an optical analysis tool as it can be made to operate at any level of approximation simply by changing the number of rays that are propagated through a system of lenses. Large numbers of rays are needed to achieve a detailed analysis of the situation. A full optical ray trace is performed by projecting one of a chosen number of rays into the lens space. If this ray intersects the boundary of a lens, the surface normal of that point is calculated and the ray is refracted in accordance with Snells law[1]. This new refracted ray is continued on into the lens space [figure 3-15]. The number of ray hits per unit area of a specified detector gives the intensity of the resultant image at that point. The model can include reflection, can be extended to include optical path lengths and to handle phase information.

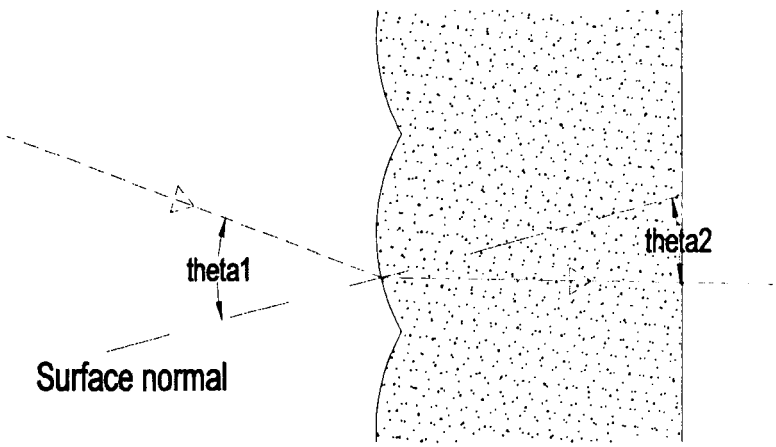

Figure 3-15, Full optical ray trace.

This method of ray-trace was investigated as a possible algorithm to establish if the added optical complexity of the model enhanced image quality.

Essentially, the only physical difference in the production of an integral image using this method when compared to a photographic method is that the modelled light is made non-continuous, discrete and phaseless. No simplifications or approximations were intentionally introduced at this stage, other than for the necessary discretisation of light and the removal of the wave properties.

[1] Snells law being $N_1 \times \sin(\theta_1) = N_2 \times \sin(\theta_2)$; Where θ_1 is the incident angle, θ_2 is the resultant angle and N_1 and N_2 are the indices of refraction of the two materials.

It was found that this method was capable of generating extremely simple integral images. Although practical consideration (mainly speed of the algorithm) showed that it is not as good as a general solution for generating integral images. This judgement is based on the fact that simulation of anything more complex that a single point requires hours of computer time.

The speed issue associated with this algorithm emanates from the fact that there is a necessity for tracing many rays per pixel to ensure that lens effects are correctly exhibited. This vastly increases the complexity. A large number of rays are required, as the intensity profiles produced by the lens model are a summation of the rays per unit area [figure 3-16].

```
For every point
    For every micro-lens
        For N times
            Generate a ray;
            Refract ray;
            Sum intensity;
        End
    End
End
```

Figure 3-16, Full ray-trace pseudocode.

Consequently, a complex and cumbersome method of creating integral images is produced. In addition, as an average computer generated scene can take up to several hours to render, this method would slow it a factor of N (the number of rays per lens) the process. Consequently, the approach is considered inappropriate. In fact, N is required to be reasonably large to sample the details of the lens point spread function.

The full optical ray trace model also includes an extremely accurate lensing approximation which includes spherical aberration and other associated effects and incorporates them into the resultant image. These detrimental effects reduce the information content of the final image by effectively performing a low pass filter by convolution of the imaged scene with the point spread function of the lens. This lowers the highest possible capture resolution but of course produces a more realistic situation. However, when computer generating an image there is no need for such detrimental effects to be included.

Eliminating degradation that is normally present at the capture of an integral image due to the poor quality of the capture optics results in a more idealistic image. Noise is introduced only from the replay process; hence the final viewed image will contain a higher resolution than a classical photographic image displayed at the same resolution.

In the search for a rapid, effective integral image generation system it was decided that the good points of the two pinhole and full optical ray-trace may provide a suitable solution. This hybrid approach is now described.

3.4.7. Hybrid ray trace

The hybrid lens model is developed from the pinhole mode and the full optical ray trace. It is a simple, reduced ray trace model, which includes refraction of the rays at the lens surface and hence, includes lens effects such as aberration and point spread.

The model was based on the following assumptions:

1. Refraction of light is the most important factor in micro-lens image formation;

2. Micro-lenses are simple spherical surfaces;

3. Marginal rays in the micro-lenses are too spherically aberrated to contribute to the formation of an image at the paraxial focal plane;

4. Paraxial rays contain the majority of the energy;

5. Paraxial rays are the principle image forming rays of the system.

The ray trace is carried out for three known points on the lens surface. These points being the pole of the lens (as in the pinhole method) and the extreme limits of the lens. The positions are chosen to capture the main features of the lens with as few possible datum points. Obviously, the system is less general than the full optical ray trace and benefits include speed gain and reduced complexity in mathematics.

The calculations to determine the position and spread of a point behind a single lens is reduced by using the paraxial location to calculate the position of an image point and the two extreme marginal rays to calculate the limits of spread of the point [figure 3-17 & figure 3-18].

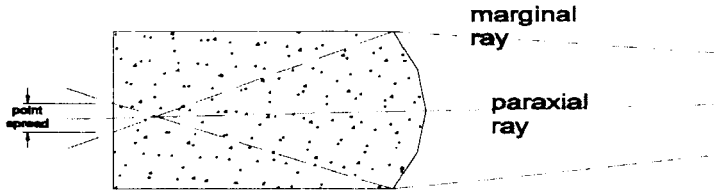

Figure 3-17, Points spread defined by the marginal rays.

```
For every point
    For every micro-lens
        Generate 3 rays;
        Refract rays;
        Calculate intensity profile;
        Sum intensity;
    End
End
```

Figure 3-18, Hybrid ray-trace pseudocode.

Several alternatives are available for the generation of this point-spread function. Simple methods employ the use of a pre-calculated lookup table of results. However, this limits the accuracy to predefined steps. A more practical method is to calculate on the fly using a non-intensive function that is a close match to the correct profile, such as $I = \cos\left(\tan^{-1}(4x)\right)$ [figure 3-19].

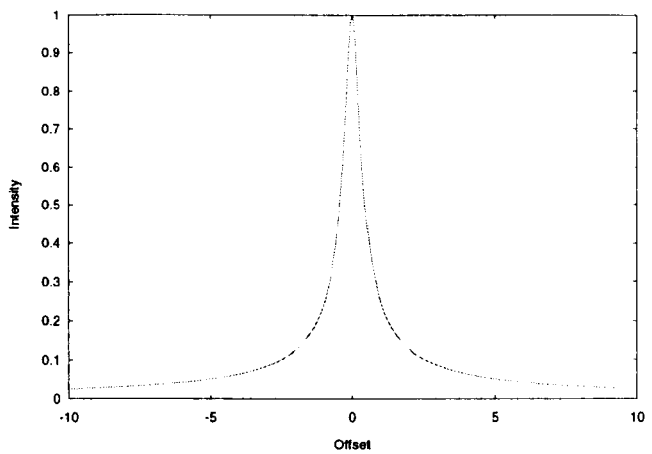

Figure 3-19, Synthetic point spread function.

3.4.8. Benefits of the hybrid model

The model provides a close link to a true lens model as it accurately models the spread of the point from any given lens. This means that the fields are closer to the correct position and are of the correct width when compared to a photographic image. Additionally, this extra accuracy has only a fraction of the calculation overhead of a full optical ray trace. An example section of image is shown in figure 3-20.

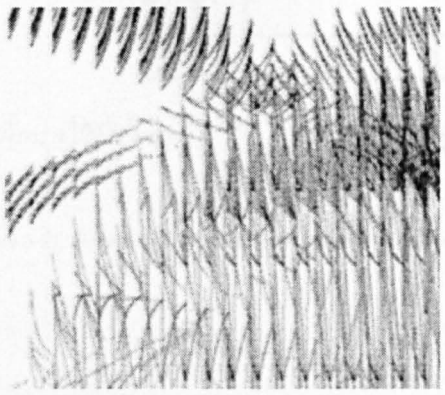

Figure 3-20, Hybrid model integral image (close up).

3.4.9. Failures of the hybrid model

The main failure of this lens model is that it introduces distortions into the imaged scene with a consequent reduction in image clarity over that of a simple one ray pinhole method. This is due to too accurate a model of a very poor imaging lens causing the image of a single infinitely small point in space to be imaged over several pixels.

This spreading of information causes, as in a full ray trace, a lowering of the capture resolution and consequently details in the final scene are lost. Effectively, the system is producing a frequency-limited view of the imaged scene. A method to produce similar results can be achieved through first creating a high-resolution image formed by an imaging device with a perfect modulation transfer function i.e. a pinhole system without diffraction. This image is then post processed using a convolution filter so that an approximation to the lens function is produced on the input signal [figure 3-21].

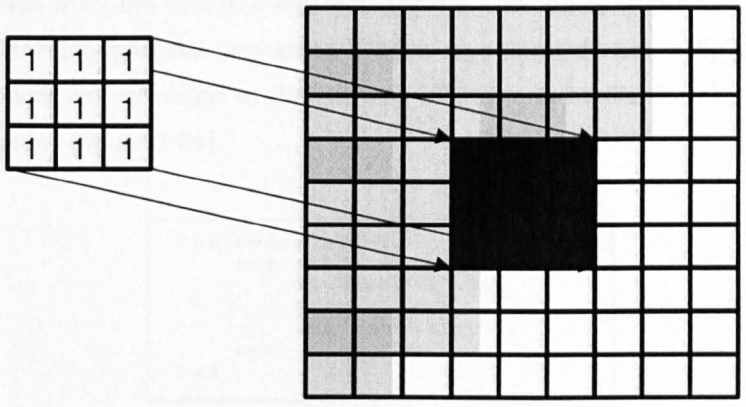

$$c[m,n] = a[m,n] \otimes h[m,n] = \sum_{j=0}^{J-1} \sum_{k=0}^{K-1} h[j,k]a[m-j,n-k]$$

Figure 3-21, Convolution to produce frequency limited images.

By removing more of the lens model refinements, a system can be produced that can generate higher resolution micro-images. Therefore, the model was further simplified.

3.5. Extended pinhole approximation

This approximation brings together the accuracy of the full optical ray trace model and the speed and simplicity of the pinhole model. Spherical refracting surfaces introduce problems when attempting to calculate image positions as the distance from the pole of the lens to the paraxial ray focus is longer that that to the marginal ray focus [figure 3-22]. Paraxial approximation is used to avoid this complication as the rays closest to the optical axis are the main image forming component of the lens.

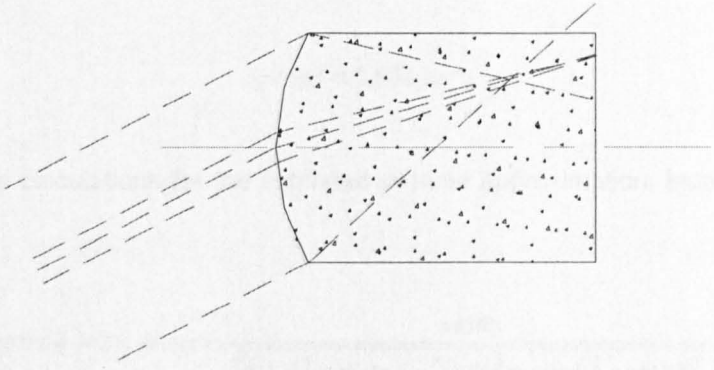

Figure 3-22, Extended pinhole model, refraction of paraxial rays.

The method benefits from the fact that the lens can be reduced to an infinite point (effectively a pinhole again) where only paraxial rays enter. These rays can then be easily processed, applying Snells law to account for refraction at the surface of the lens media thereby giving the pinhole method extra accuracy [figure 3-24].

```
For every point
    For every micro-lens
        Generate a ray;
        Refract ray;
        Sum intensity;
    End
End
```

Figure 3-23, Extended pinhole pseudocode.

3.5.1. Benefits of the extended pinhole model

The method retains its links with the very simplistic pinhole model, making the transformations performed upon any point extremely fast and simple. Unlike the simple pinhole approximation used previously, the model includes refraction effects which not only results in the placement of the image fields at the lens focal plane but does so in correct scale.

This simple change makes a huge amount of difference to the position and spread of the imaged camera aperture. For example, if a camera aperture with a width of 195mm is positioned at a distance of 300mm away from a lens sheet with a refractive index of 1.6 and a focal length of 3.08mm then using the simple pinhole approximation to calculate the extent of the image in the central lens, gives equation 3-8;

$$spread = focus \times \frac{width}{distance} \tag{3-8}$$

$$spread = 2.002mm$$

However, the same calculations for the extended pinhole approximation, incorporating refraction, gives equation 3-9;

$$spread = 2 \times focus \times \frac{width}{\sqrt{4 \times N^2 \times distance^2 + N^2 \times wisth^2 - width^2}} \tag{3-9}$$

$$spread = 1.213mm$$

The calculation shows that even for a simple example, the difference in size of the calculated image fields is relatively large. For the example chosen, a difference of 0.8mm occurs (roughly 1/N times smaller) demonstrating how important refraction is in ensuring the correct formation and positioning of integral images. It is obvious that any analysis which fails to include refraction will be highly inaccurate. Considering that printing devices usually operate at a pixel resolution of 300 dots per inch means that the differences in these two models result in the simple model being nine pixels in error.

Additionally, the artefact previously observed of the disappearance of points close to the lens sheet is accounted for in this model by modifying the model so that points $\leq \pm f$ are treated as a special case. This allows points to cover the lens sheet and still be imaged by pinhole like equations. In these special cases, close points cover the entire lens area. The result is computer generated images which behave naturally.

The model does not incorporate complex negative effects of diffraction and other distortions as these effects are negative and detrimental to the image quality, but the model is now corrected for refracting surfaces. The foregoing allows the synthetically produced images to be as perfect as can be achieved and correctly positioned without distortion caused by optical elements through spherical aberration and diffraction. This is beneficial as the distortions occurring in capture and replay are accumulative. Consequently, a computer generated image should give a higher resolution final image when compared to a photographically produced image taken at a similar resolution. The photographic image contains distortions created at both capture and at replay. As the imaging system is without phase or absolute ray direction at this point these two identical distortions cannot cancel each other out and therefore must compound each other, thereby lowering resolution.

Additionally, a great benefit which comes from the models close association with a simple pinhole projection, is that most standard computer graphics algorithms which rely on the pinhole approximations can be made to work with this model with only slight modifications. The only problem is that the model introduces transformations which are not afine, in that they don't keep parallel lines parallel after the final projection transformation. This is due to the non-linear nature of Snells law and consequently some algorithms cannot be directly applied.

After investigating and developing the hybrid model the alternative approach based on Fourier energy distributions was considered.

3.5.2. Alternatives: Fourier based methods

When a recording plane is positioned behind any lens and the scene in front illuminated an image is formed. If the recording plane is positioned at the focal distance of the lens then the image that is formed is the Fourier transformation of the scene. This occurs because of the partial coherence that exists originating from points in the scene.

During normal production of an integral image the film is located at the focal distance of the micro-lens sheet. This causes the image to be captured as a Fourier transformed version of the original scene. This allows an alternative approach to image formation to be undertaken.

To form an image using Fourier methods requires the transformation of every object in the scene into its frequency representation. Alternatively, every single point in space which lies on the objects surface needs to be transformed [figure 3-24].

```
For every point
    For every micro-lens
        Generate fourier transform;
        Sum intensity;
    End
End
```

Figure 3-24, Fourier based method pseudocode.

This can possibly be simplified as a lookup table of transformed points spread functions from which the image can be built. However, determining every point which lies on the objects surface is not trivial. It was for this reason that this approach was considered inappropriate for practical image formation and was therefore abandoned.

3.5.3. Conclusion

The goal of keeping the approximation as simple as possible to minimise computational overheads for complex scene generation is the main factor in assessing which models are most applicable for integral image generation. The approach of ignoring complex lens effects which are detrimental to the final micro-image resolution, results in a pinhole system which transforms infinitely small object points to the smallest practical image points size (one pixel). This being the best quality that can be achieved in a pixelated system.

To validate this, a simple experiment was conducted to establish if simple mathematical models of micro-lenses, ideally suited to fast computer calculations, could predict the intensity structure of photographic integral images. The experiment involved placing a small physical aperture in front of a diffuse light source and a micro-lens sheet placed a reasonable distance away. The images captured by the micro-lens sheet of the aperture were recorded onto a sheet of photographic film.

After the film was developed, the surface showed small, high contrast details that corresponded to the image of the aperture of the camera system [figure 3-25]. The spacing between these micro-images and the distance across them was measured. These measurements are plotted [figure 3-26] against various distances for a fixed size aperture and constant micro-lens pitch.

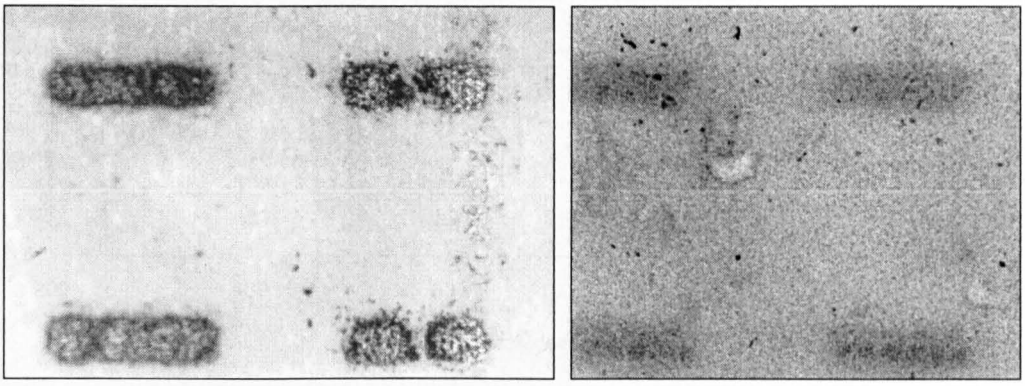

Figure 3-25, Computer and photographically generated image bands (magnification x100).

Comparing the measured image field widths against the two pinhole lens approximations [figure 3-25] gives a good correlation especially between the results and the pinhole plus refraction model. The differences between the two lines includes measurement inaccuracies, the pixelation noise and the inaccuracy resulting from errors in the physical values used for the lens sheet model.

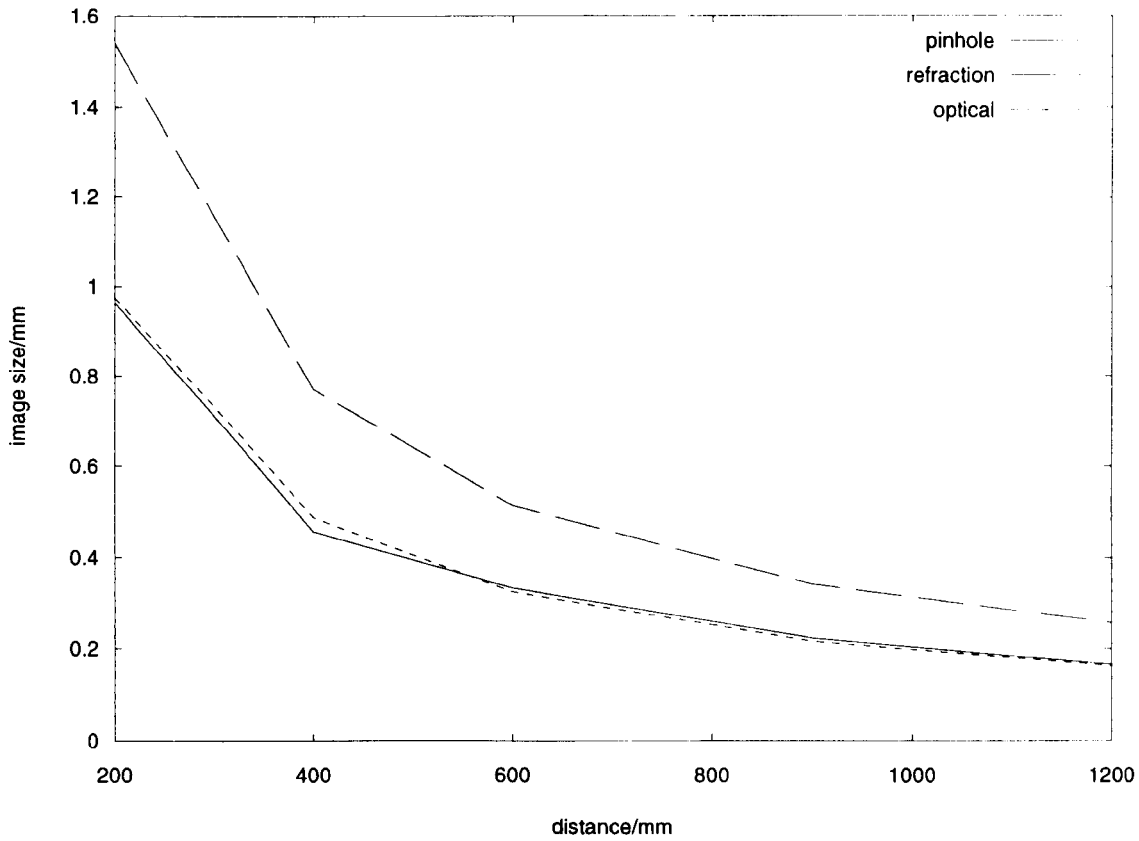

Figure 3-26, Comparison of experimental and theoretical lens sheets.

The graph shows that the straight pinhole approximation is a very rough explanation of the operation and characteristics of an actual micro-lens sheet. On the other hand, the extended pinhole model that incorporates refraction calculations provides a very realistic approximation to the optical performance of an integral lens sheet and matches extremely well with experimental results. This in itself validates the choice of a hybrid model.

3.5.4. Conclusion

The high contrast, low information images replayed surprisingly well considering the brutal nature of the laser printer output. The information survived not only being thresholded to only two values but also inaccurately being placed onto the page. This in itself is impressive.

However, obvious problems were encountered, the clarity of the image being the main problem. This is due to the inability to display details, through lack of greyscale. Therefore, as the printer being used had only two states, each pixel could only represent a hit or a miss. Moving to a different display media based upon dye-sublimation printing techniques which can handle non-dithered colours alleviated this problem.

The extended pinhole method produced results that are comparable to photographically produced images. The method, although simple, allows the production of images that are capable of producing results of higher resolution than those achievable through a purely optical approach. The largest benefit of the extended pinhole method is that the majority of computer graphics production algorithms will work without significant alteration.

The simplicity of image generation through geometric projection allowed various investigations into the effectiveness of several micro-lens models and proved that the method worked. The ray tracing methodology increases scene generation time but allows photo-realistic results to be produced. This includes images generated from solid (non-faceted) models which exhibit surface colours, properties and textures and include complex lighting models to include effects such as specula reflection.

3.6. Development of Photo-realistic Integral Images

Commercial computer generated image engines require the capability to produce and shade models. Basic methods of rendering such as hidden line/surface removal allow wire-frame based objects to be given additional properties and produce images with greater realism. Most modern applications for computer generated images are required to be photo-realistic, that is they must have the ability to model and correctly display the intricacies of the real world, such as inter-object reflections, object surface parameters and complex lighting.

There are, at a basic level, two schools of thought on how to achieve photo-realism in computer graphics. There are the computer rendering packages that use geometrical mathematics to simulate the appearance, of the solid objects and lights. These renderers produce stunning results and are very fast, however their speed is derived from approximations made in the modelling of the lighting, reflection used when drawing the objects.

An alternative approach is to use a pure ray-tracing algorithm. This produces images using a technique similar to the operation of the camera (or more correctly, how the ancient Greeks imagined sight was achieved), casting rays out into the scene (Appel, 1968).

Ray-tracers are on the whole slower at creating images, but have the benefit that the images produced are more mathematically accurate than the approximations created by rendering software. In addition, they are very good at handling specular lighting, reflection and refraction of objects (Kay, 1979). A sphere on a ray tracer is mathematically spherical and the final sphericity is dependent upon the sampling rate chosen by the user. In a renderer the same sphere is made from discrete patches and shaded to give the viewer the impression of a sphere. The final sphericity of the sphere is chosen at the model stage and is independent of the sampling rate chosen by the final user.

The largest benefit in ray tracing is that it is relatively simple to comprehend and to implement. Additionally, the camera models used in ray-tracing are pinhole models. This allows direct application of the previously devised integral imaging generation methodologies to photo-realistic graphic generation.

3.6.1. Development from the wire-frame algorithm

The essential difference between the wire-frame model, using geometric projection, and a photo-realistic ray tracer, is in the direction of flow of scene information. In the wire-frame system, the flow of information is from scene points to pixels. This gives each pixel enough information to form a simple wire-frame image, but not enough information to accurately assign a value to a pixel to include complex lighting, shading and texture terms as the scene is sampled only at the vertices of the scene objects and nowhere else. These vertex points are then used to "paint in" the surface details.

However, with a ray tracer the flow of information is from the pixel into the object space. This difference allows the intensity value of each pixel to be more correctly determined, thereby producing images in which the scene is sampled at various positions, each dependent upon the area and frequency of the initial pixels. Therefore, an image with characteristics close to the one produced by purely optical methods is created.

Classical, ray tracers use a single pinhole as the camera model. This allows the optical camera model to be defined easily and calculation to be effected extremely fast. Given any pixel on the screen plane (akin to the film plane in a camera) the camera description returns the three-dimensional ray direction that directs the ray tracer into the scene. These directions are calculated as functions of the screen position (P_x,P_y) and the view distance (d) [equation 3-10].

$$V_{x,y,z} = (P_x, P_y, d) \tag{3-10}$$

However, it has been shown that the camera model for integral image generation is more complex than the simple, ideal camera system. In the integral image ray tracer there is no one fixed solution for the directions of rays. This is because the micro-lens sheet placed over the screen plane modulates the direction of the rays. The ray determination process requires that a pixels position is checked against all micro-lenses to ascertain which micro-lenses, if any, produce an image of the aperture on any part of the pixel. Once the correct initial path has been established for the pixel it is extended towards the micro-lenses. At the surface of the micro-lens the direction is modified in accordance with a three-dimensional version of Snells law. It is this modified ray which is followed by the ray tracer through the scene objects.

Additional changes have to be made to the standard method of ray tracing as subtle differences are introduced by the nature of the integral image generation process. For example, objects can actually straddle the imaging plane.

In addition, the ray tracer has to cast rays both forwards and backwards along the ray path [figure 3-27]. This is needed to enable scenes that existed in front of, behind and across the screen plane to be correctly represented.

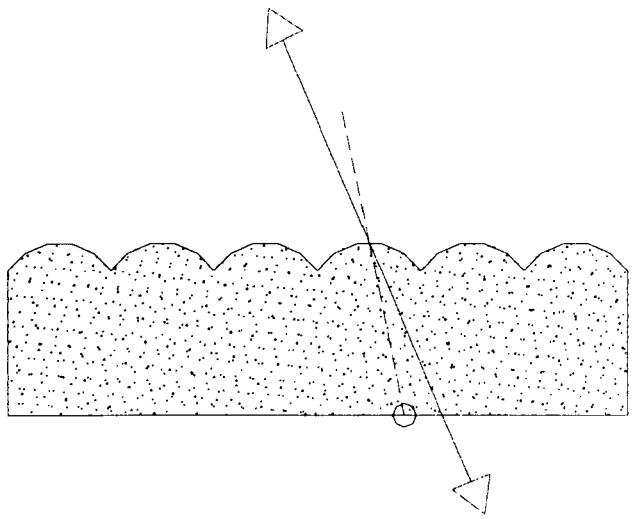

Figure 3-27, Ray tracing with a micro-lens screen.

These changes are necessary as the scene which is to be captured by the integral capture plane exists as a volume encapsulating the plane of capture at the position of interest. Therefore, the standard ray-tracing methodology needs to be extended to allow for objects in front of the lens, crossing the lens and behind the lens. These situations need processing in similar ways to standard image creation and can be extended from the normal ray-tracers operation in the following ways.

The process of capturing objects positioned behind the screen plane is easily extended from classical ray tracer methodology as it simple involves obtaining information about the first surface the ray makes contact with. The process then continues as normal, casting rays to determine reflections/shadows occurring at the point of intersection.

The capturing of information for objects in front of the scene is made more complex by the need to find the furthest object from the screen plane. This is necessary as the viewer is positioned in front of the screen and naturally would see the surfaces closest to themselves. This is additionally complicated by the need to then reverse the direction of travel of the ray at the point of contact and then trace (as normal) back into the scene to find reflection, refraction and lighting information [figure 3-28].

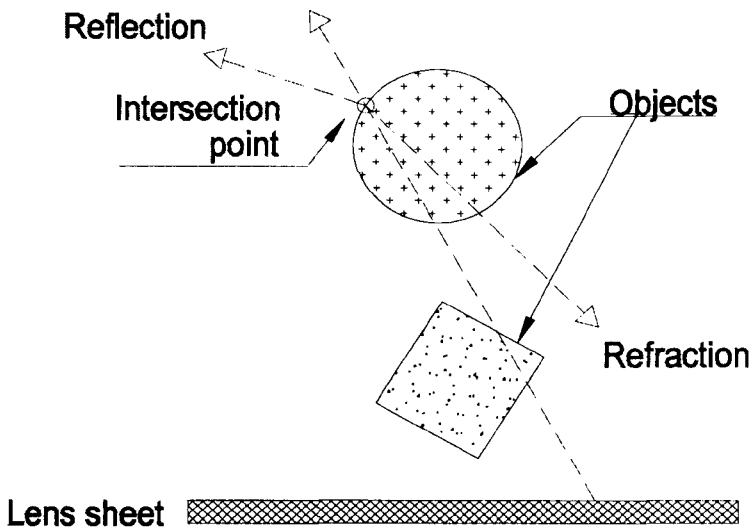

Figure 3-28, Modified reflections/refraction for integral image ray tracing.

This reversal of rays is needed so that the observers perception of the lighting information is correct, it also makes the reflections and refractions operate in the correct direction.

The body of the ray tracer was taken from a package called "POV-Ray V3.00" (Povray, 1999) a publicly available ray tracer, which more importantly is distributed with full source code. This package was chosen as it supported all common ray-tracing fundamentals, as well as the majority of modern advances in ray tracing. In addition, the source code is clearly commented, well managed and clearly laid out, allowing concentration on generating the integral image code, rather than re-implementing well established existing graphics algorithms. The source code is distributed under a licence that allows alteration of the code for educational purposes.

The basic POV-Ray system was extended and modified using the additions and changes developed for the production of integral images previously for use within a geometric projection strategy. However, these changes, were inserted in a way which allowed the primary graphics producing code of POV-Ray to continue working as normal, in this way changes to existing code and user interface were kept at a minimum.

By interfacing the integral imaging code into the POV-Ray source, the generation of images was achieved more quickly than would have been possible if the standard computer ray tracing algorithms were hand coded to fit this project. This made generation of complex ray traced integral images, relatively simple due to having to rewrite a small portion of code to operate in a way expected by a much larger piece of code, rather than the other way around.

This decision allowed the scenes and custom object modellers that support the well-established POV-Ray scene description format to be used as normal for integral scene generation.

3.6.2. Pixel to lens determination

The procedure of tracing rays from locations on the imaging plane through the virtual camera lens into object space introduces further complications above those involved in standard ray tracing and integral geometric projection of points. These complications are involved because given a specific position on the film plane, it is necessary to determine which micro-lens (from thousands), if any, projects the transmission units aperture onto that location. With conventional ray tracing this is extremely simple as there is only one lens involved. However, in integral imaging an array of close packed lenses having a small pitch is the transmission element.

The simplest, but the most computationally expensive solution is a brute force sequential search through all available lenses. This unsophisticated method achieves the desired results, however it can be refined so that only the lenses in the neighbour hood of the pixel position are searched. This greatly improves performance but is still slow relative to the natural simplicity of a single lens camera.

A method of producing a direct mapping from film space onto micro-lens space would allow a simple, computationally non-expensive test (which requires little or no iteration) to be performed. This would allow scenes to be rendered in more acceptable time scales. Two approaches to the problem were explored and tested.

3.6.3. Solution 1: Closest wins

The simplest method of calculating the lens towards which any pixel will be projected is to choose the lens which is closest to the pixel position, rounding towards the centre of the film plane. This simple approximation works for most pixels and can be applied to any arrangement of micro-optical elements. For the lenticular (one-dimensional) case it can be expressed as equation 3-11.

$$lens\_number = ceil\left(\frac{x\_offset}{lens\_pitch} - \frac{1}{2}\right) \qquad (3\text{-}11)$$

However, this produces incorrect results for some cases where pixels are located near the edge of the micro-image. Additionally, this does not take into account the relative size of the camera aperture and fails in cases where the closest pixels to a given lens fall outside the image produced by the lens of the aperture [figure 3-29].

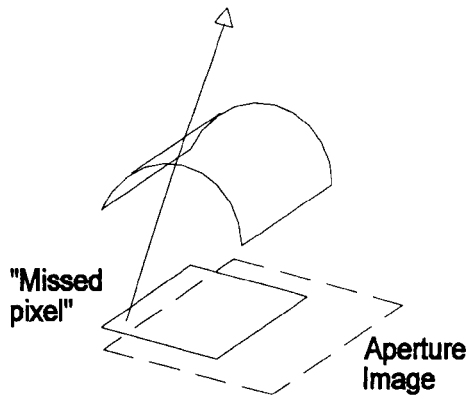

Figure 3-29,"Closest lens" errors.

These missed pixels only occur at the very limits of the micro-image field for lenses which are significantly off the optical axis of the system, therefore allowing the system to function almost correctly. In fact, these misalignments are hardly noticeable when working at the pixel resolution of standard 300 dot per inch print technology and due to the advantages inherent in the lens determination algorithms simplicity. The algorithm operates roughly ten times faster than a limited brute-force search. These misalignments can be reduced whilst keeping the same simple lens determination algorithm. Firstly, calculating the general solution for the projection lens for a certain pixel and subsequently determining whether this combination is capable of imaging any portion of the transmission camera aperture. If this combination is capable of imaging the aperture then ray tracing is allowed to proceed as normal, however pixel/lens combinations that do no image the aperture are ignored and the process is repeated with the next pixel.

Note this algorithm can easily be extended to work for square and hexagonal based micro-lens system.

3.6.4. Solution 2: Accurate method of calculation

To accurately calculate the correct lens a one-to-one mapping function from image pixels to the imaging lenses needs to be generated. However, under certain conditions (overfil) this mapping exhibits many-to-one solutions producing regions of uncertainty where this cannot be resolved. Under these conditions, the micro-images are malformed, however the pixel still requires a lens and a direction to trace. To provide an accurate method of calculation under all circumstances, a combination of several methods is needed. Simple calculations only are required to establish the main bulk of the pixels, as they are close to the optical axis of their imaging lens. The rest of the pixels, near or on the lens boundaries, require an iterative method to establish which, if any, of the neighbouring lenses are imaging in that location.

3.6.5. Conclusion

The fusion of integral capture code in to the POV-Ray structure was completed and photo-realistic scenes were designed and rendered. The images showed all the characteristics of standard photo-realistic computer generated images. They contained realistic shadows, textures, reflection, refraction and lighting effects. Additionally, they contained continuous parallax across the field of view. They also showed considerable similarity with photographic integral images [figure 3-31], the dark bands visible in the photographic image is due to the lens sheet not imaging light at its extremes.

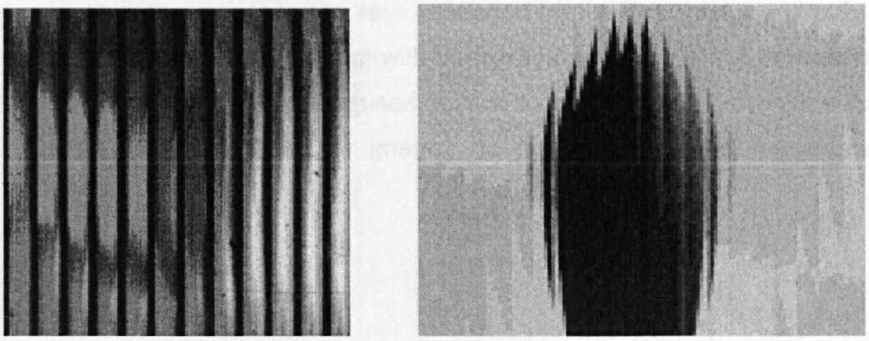

Figure 3-30, Comparison of magnified integral images (photographic and synthetic).

Due to the nature of ray tracing, enhancements such as anti-aliasing of the spatial signal can be achieved. This, as in standard two-dimensional images, achieves a better representation of the area covered by each individual pixel and through smoothing of the high spatial frequencies in the image produces a more visually pleasing effect.

The images still exhibit break up of object points, which is proportional to the depth of the point and are similar to the ones exhibited in the wire-frame images. However, these effects are reduced (visually) when anti-aliasing is used in the production of the image. Conclusions are drawn on the nature of these image break ups in chapter 4.

3.7. Other imaging considerations

When micro-lens images are being produced no additional consideration are necessary, image production takes place as described. However, in the production of lenticular images a lens that images in only one direction is used. This causes the problem that in one direction (usually the horizontal) a large camera aperture is required whilst in the other (usually the vertical) a small aperture is required. The large aperture is necessary to provide a reasonable field of view for the viewer, whereas the narrow aperture in the other plane is required so that the camera limits the amount of diffusion in the image caused by the lack of imaging properties in the vertical. In the real world, the size which the aperture can be reduced to vertically is a trade off between the amount of light which is needed to be received through the system (speed of the camera) and the amount of diffusion that is acceptable (depth of focus). However, in the computer model it is practicable to allow an infinitely small vertical aperture, thus allowing no diffusion of the image vertically and hence producing images that are of higher quality than those achievable by a photographic method.

This produces an interesting point, as the rays produced by the final image will only be correct in the vertical for viewers positioned coincident with the original aperture of the camera system [figure 3-30]. Deviation from this point in space causes objects to appear to distort in the vertical direction, giving rise to the situation that lenticular images do not exhibit natural viewing as micro-lens integrals do.

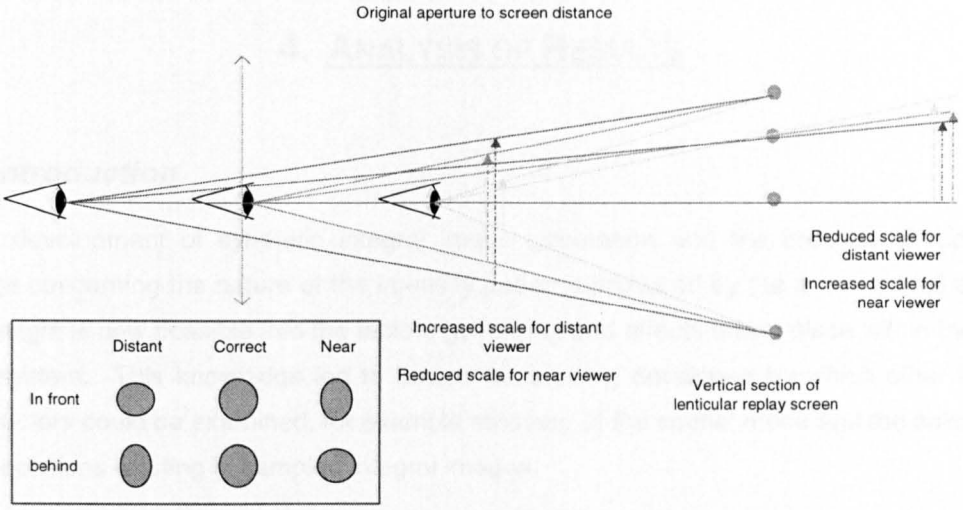

Figure 3-31, Lenticular image distortions.

3.8. Section Conclusion

Computer generated integral images have been produced. They can be generated at different levels of complexity ranging from pure wire-frame models to photo-realistic images. Additionally, from a series of still integral computer generated frames, animations can be produced. These synthetic images exhibit the same characteristics as those generated photographically, and pixelated for display on similar devices. These common characteristics may be specified as; continuous parallax, true colour and objects existing as a real optical model. In addition, they also share; break-up of the image at depth and multiple imaging, the latter due to sampling effects and aliasing.

These characteristics are common to all forms of spatially discrete integral images. Analysis of pixelation effects in integral images are further illustrated and expanded in chapter 4.

An effect which is noticeable in synthetic integral images has been described as “fish tailing”, where the object skews at different rates for points in front of and behind the screen plane. This effect has not yet been identified in photographically produced images and may be an artefact introduced in the sampling procedure.

Examples of computer generated integral images produced using this method are shown in Appendix A.

4. ANALYSIS OF RESULTS

4.1. Introduction

With the development of synthetic integral image generation and the creation of rudimentary knowledge concerning the nature of the intensity patterns produced by the micro-optical elements, greater insight is now possible into the factors governing and effects taking place within the integral imaging system. This knowledge led to further tools being developed by which other important imaging factors could be examined, for example recovery of the spatial mode and the calculation of spatial resolutions existing in sampled integral images.

This chapter examines factors associated with all forms of integral imaging and by examining the features of pixelated images, provides insights into the resolution of pixelated integral images in certain modes of operation.

4.2. Micro-optical image inversion

When integral images are produced using large micro-optical elements (≥1mm) the eye is able to resolve the structure of the lenses and the intensity patterns produced within these elements. For points which lie in front of the capture screen this is hardly apparent, however, for objects which exist behind the screen, sharp edges inclined to the vertical are reduced to a jagged staircase.

Upon close examination of the microstructure of a replayed integral image, it is possible to see that the micro-images of parts of the scene are correctly composed and that for these, the information continues smoothly through neighbouring lenses.

However, for other parts of the scene, the image seems to exhibit an obvious break up of surfaces. In addition, the flow of information across the area of individual micro-lenses are and across the boundaries of adjoining micro-lenses are incorrectly reversed. This results in image disintegration for a sub-section of the image space. The nature of this break up is depicted for the text "abc" [figure 4-1]. The figure shows how two similar objects appear distorted if captured from equidistant positions either side of the capture plane. By careful observation of any of the images shown in appendix A this effect can be seen. It is more apparent in the images produced for replay on large scale lens screens, where the sub-lens structure is readily observable.

Figure 4-1, Lateral inversion of lenticular image fields for text "abc".

This inversion occurs because of the inherent differences between the way that objects positioned in front and behind of a lens are captured, and subsequently how the information is replayed. This transforms the smooth profiles of some of the objects in the scene into a discrete set of steps, giving a jagged or blurred appearance and a non-continuous flow of information. This effect occurs in all forms of integral imaging synthetic and photographic.

4.2.1. Capture and Replay

During capture, objects positioned in front of the micro-lens sheet are recorded inverted [figure 4-2]. A similar process occurs for objects positioned behind the capture plane, except in this case, no inversion occurs.

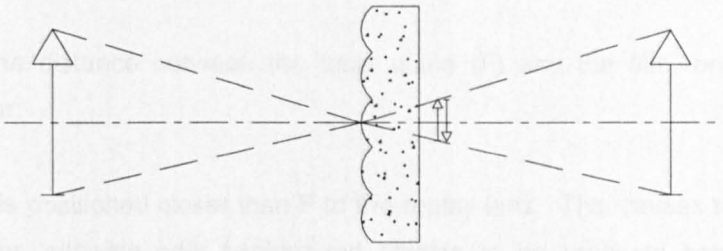

Figure 4-2, Basic principle of lenses object capture.

In addition, the similar locations of the two objects produce similar sized images at the film plane. The primary difference is the orientation of the images with respect to the objects from which they were produced.

However, at replay this subtlety is lost due to the passive nature of film. This is due to the replay lenses being positioned (optimally) at their focal distance from the film plane, therefore the intensities recorded on the film are simply projected with the angular information by the lens [figure 4-3 and figure 4-4].

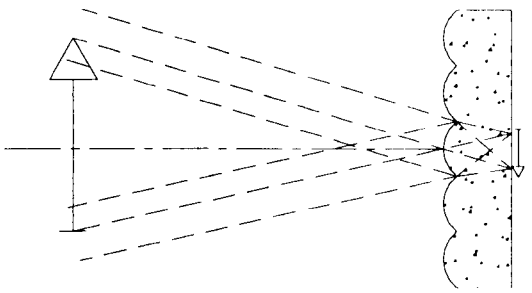

Figure 4-3, Correct angles, correct fill.

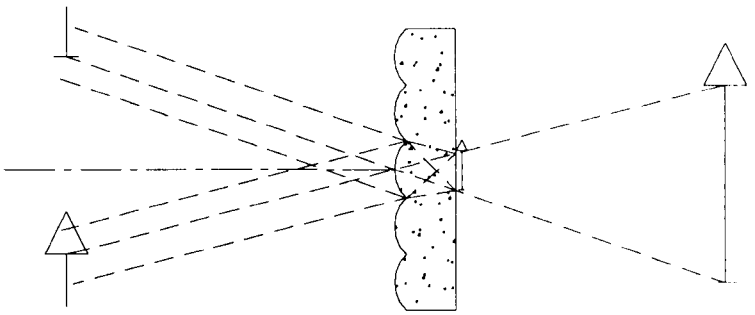

Figure 4-4, Correct angles, incorrect fill.

Depending upon the distance between the focal plane (F) and the film, one of three distinct conditions can occur:

1. The film plane is positioned closer than F to the replay lens. This causes the lens to act as a simple magnifier, allowing only background objects to be replayed correctly (images not inverted) [figure 4-5].

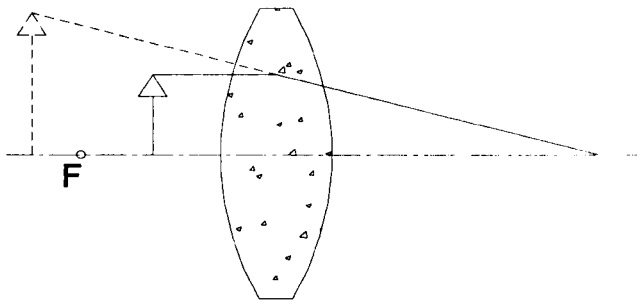

Figure 4-5, Image plane closer that F (simple magnifier).

2. The film plane is positioned further than F from the replay lens. This causes the lens to act as a copy lens, allowing only foreground objects to be replayed correctly (images inverted) [figure 4-6].

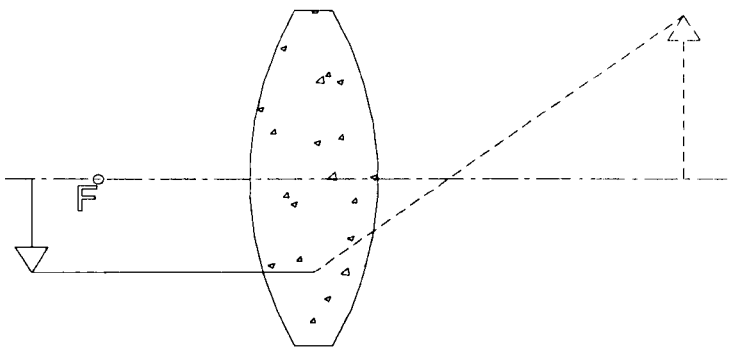

Figure 4-6, Image plane further that F (inversion).

3. The film plane is positioned at F. Images are projected to infinity, only background objects work correctly (no inversion).

Since the information of the two differently orientated film plane images are projected by the micro-lens in exactly the same way and both objects were originally orientated pointing in the same direction, one object must now be incorrectly replayed. The micro-lens can either invert both of the images none.

4.2.2. Results

To test whether these effects indeed manifested themselves in micro-optical images a large scale experimental set-up of the process was created. Large lenses (≈30mm) were used to display from a synthetically produced film plane. The resulting views generated within each lens showed that if the lens is positioned closer than the focal length to the film plane then the micro-images are replayed to a position situated behind the lens plane, remaining non-inverted, relative to the entire object.

For a lens distance larger than the focal length, the image is projected to a position in front of the lens plane. In this case, the action of the lens inverts the micro-image. If the viewers distance coincides with the conjugate image distance then the micro-lens appears totally filled. At a viewing distance closer than this conjugate point, the image appears non-inverted. Additionally, the scale of the image within the lens reduces as the viewer moves away from the image plane. For a distance equal to the focal length of the lens, the image appears virtual and erect.

In summary, this inversion of the images is dependent upon the lens-film distances and the observers viewing distance.

This effect is also visible in micro-lens images, under magnification. Figure 4-7 shows two magnified views of a similar object. The object on the left is positioned behind the lens plane, while the object on the right is positioned in front of the lens plane. The lens pitch in this example is 1.27mm. This shows that micro-optical inversion does occur in lenticular images and is visible.

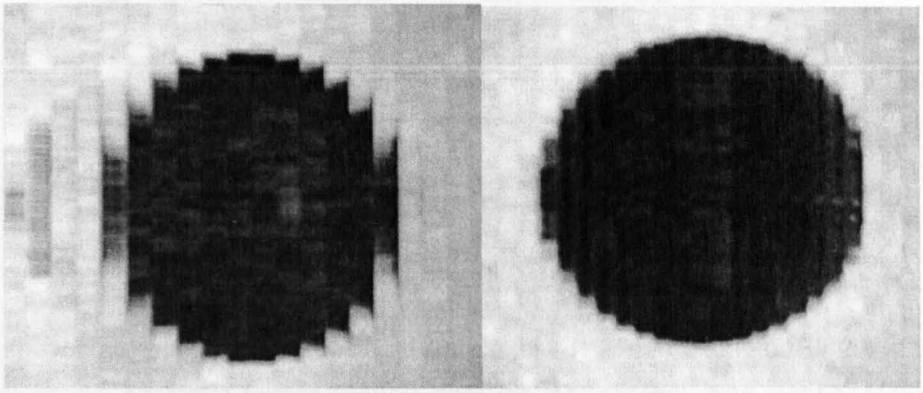

Figure 4-7, Image formed behind (left) and in front (right) of lenticular micro-lens plate.

The majority of combinations of lens focal lengths, observer-lens and film–lens distances showed that detail is visible within one lens aperture, this contradicts existing micro-lens theories produced by Okoshi (Okoshi, 1976). However, this visible inter-optical detail is at a minimum when the observer is positioned at the conjugate distance created by the lens-film separation. In general, as long as the actual lens pitch is above the resolution of the eye it is possible to see this effect in all cases, due to the finite size of the eye aperture.

Additionally, a computer model was devised to predict the number of pixels visible to an observer with an eye of diameter D_{eye} positioned d_{viewer} away from a lens-film combination. The focal distance of which is F_{lens} and having a display resolution of $DPI_{display}$ [equation 4-1].

$$pixels = \frac{DPI_{display}}{25.4} \times F_{lens} \times \frac{D_{eye}}{d_{viewer}} \qquad (4\text{-}1)$$

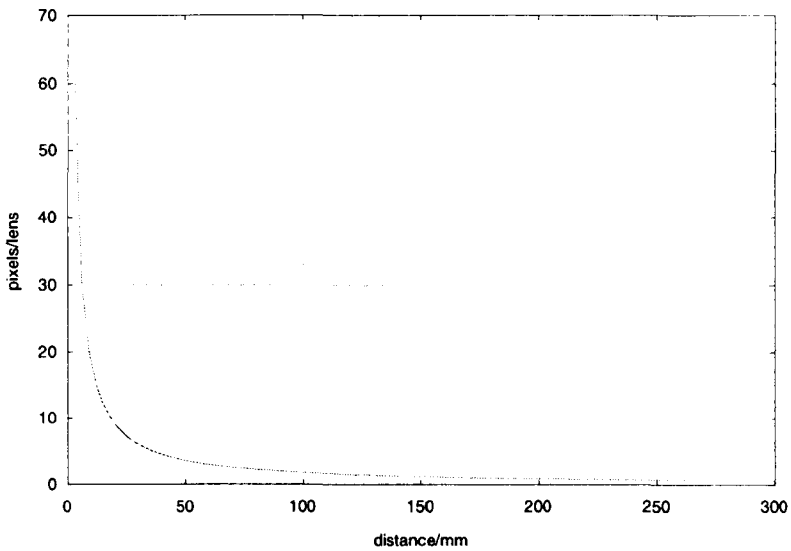

Figure 4-8, 300 dpi pixels visible per lens at a given viewing distance.

Figure 4-8 shows the results for the computer model of a 1.27mm diameter F# 2.4 lens with 300 dots per inch pixels, against a human viewers distance (D_{eye}=5mm). The number of pixels visible per lens quickly tends towards zero as the viewer distance increases. This means that the main factor in image quality for images viewed from a reasonable distance is the lens pitch.

However, the image inversion still occurs as pixel boundaries are visible no matter what size the neighbouring pixels are magnified to.

4.2.3. Conclusions

Within any scene, objects exist on each side of the sampling plane. In this case, the lens is expected to perform two distinct and mutually exclusive operations. This conflict of interests leads to the situation where one set of objects must be replayed incorrectly. If images are recorded so that objects only exist on one side of the lens plate, then this effect can be eliminated by choosing a lens thickness appropriate for the situation.

This reversal of lens information will occur in all forms of micro-lens imaging, where object locations straddle the lens sheet. This is caused by the differing ways in which points situated in front and behind the lens plane are required to behave. These two situations are mutually exclusive and require the lenses to perform tasks at replay, which cannot simultaneously be carried out.

There are a number of possible solutions to overcoming this micro-image reversal problem, neither solution being ideal:

1. Reduce the size of the lens sheet so that the effects are below visual perception (≈1 minute of arc);

2. Limit the composition of images so that they have foreground or background but not both;

3. Lenses can be made to fill completely, but this is limited to one specific viewing distance. Any slight deviance from this position leads to inversion of part of the image space. Depending upon the viewers distance either the foreground or the background micro-images are inverted.

4.3. Sampling Theorem Considerations

4.3.1. Alaising effects in two-dimensional images

A two-dimensional image can be considered as a signal that is a function of space. This information is sampled when the image is digitally captured. When sampling an image so that a continuous function is transformed into a discrete function, which only exists at predetermined sample points, it is necessary to take into account that each sample point must in some way represent an area and aliasing effects are possible. In two-dimensional images [figure 4-9 (A)], aliasing is apparent as objects smaller than the sampling mesh are reduced in size or at worst completely disappear. This is also apparent on details such as edges at a slight angle to the regular sampling grid. In this case, the smooth edge disappears and is replaced by a jagged staircase and as the level of sampling is further reduced features are lost [figure 4-9 (B)].

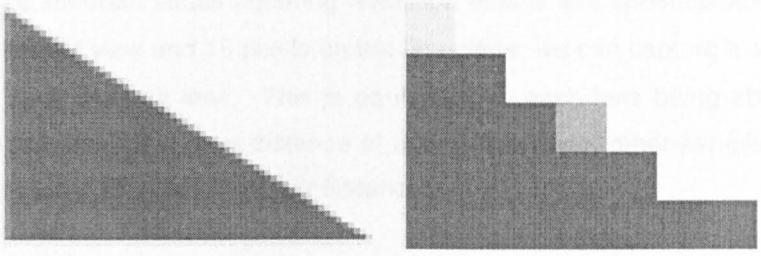

Figure 4-9, Aliasing effects due to levels of pixelation.

Nyquist, in 1924, devised his sampling theorem that predicts the minimum sampling rate required to capture any signal (spatial or temporal) without losing detail. Unfortunately, with only a finite number of equally spaced sample points it is always possible to position any given signal so that it is misrepresented by the samples. An example of an image requiring an infinite number of samples would be a triangle, as each corner will eventually become so small as to evade detection by any finite set of samples.

Producing an infinite number of samples is not a practical solution for any discrete device. Therefore several alternatives may be employed, the main and the easiest to apply, is that of over-sampling.

Over-sampling the signal is achieved by sampling the spatial signal at a much higher rate than that at which the final output is to be displayed. These extra samples improve the representation of the area that a single pixel represents. The multiple values, which represent an area, are then averaged together, sometimes weighted to provide relevance, to obtain the final value for the pixel.

No enhancement can ever make up for a lack of sampling points in an image. However, by using an increased number of over-samples and including stochastic noise into the regular spacing of the samples points a more visually pleasing result for a human observer can be achieved.

4.3.2. Aliasing effects in integral images

Aliasing effects are present in all discreetly samples computer generated images, integral or not. These effects are caused by the sampling errors on the two-dimensional representation of three-dimensional space which is encoded onto the back face of the virtual lens sheet.

However, since this is not the final viewed information, unlike two-dimensional images, and the image information for a single points is located at several places across the film plane, the aliasing effects cannot be removed at this stage.

The Nyquist sampling theorem states (ignoring refraction effects and spherical aberration) that for a micro-lens a 30° field of view and 15 pixels on the film plane, we can capture a spatial resolution of period 30/(15*0.5)=4° in each lens. This is equivalent to each lens being able to produce a spatial signal of period 4cm for a point distance of 30cm. However, other sampling effects occur dependent upon the lens pitch and the viewer distance.

These effects are not limited to synthetic integral images, aliasing effects are evident and over-sampling is needed when taking integral images to commercial print resolutions. For example, better results were gained in the final image if the original integral photographic image is initially scanned at a much higher rate that the display resolution.

Several experiments were carried out to evaluate the effect of sampling on an integral image. A virtual object is positioned in space and captured using the discrete ray tracing algorithm. The nature of the effects produced by aliasing in the integral image determines the usable depth for positioning the objects in the scene. This depth alters as the sampling rate is varied.

In these experiments a single, simple object was chosen, in this case a solid blue sphere. This sphere was imaged at a known fixed distance from the recording plane. By keeping the scene positions constant and varying the resolution, aliasing effects were introduced into the resulting image. The final display was produced on a 300 dot per inch resolution dye-sublimation printer and the fractional sampling rates were created by grouping neighbouring pixels (2 or 4 pixels) to create lower resolutions. The results are given in the table below [table 4-1]. The corresponding images can be seen in appendix A.

Resolution	Depth	Apparent problems
300 dpi anti-aliasing	–50mm	smooth profile
300 dpi no anti-aliasing	-50mm	slightly jagged profile
150 dpi no anti-aliasing	-50mm	more jagged profile
75 dpi no anti-aliasing	-50mm	very jagged profile and severe break up of image

Table 4-1, Effects of aliasing.

In previous experiments, using a pinhole model and two tone, black and white laser prints it was evident that a break up occurred when the objects in a scene reached a certain distance from the recording plane, the source of this error being unknown. The series of experiments gave a possible explanation for the observed effects. The experiments showed that as the sampling rate decreased and the angular resolvability of the system is reduced, the image break up increased. The angular resolvability is linearly magnified with depth, therefore this results in reduced depth resolution with decreased sampling rates. This can explain the effects apparent in computer generated images, aliasing increases as the objects move further from the screen plane. However, this effect cannot only be associated with computer generated integral images. Any image which is of high contrast and heavily pixelated will also clearly show these effects, in accordance with Nyquists sampling theorem.

These results suggest that the necessary sampling rate for any object is dependent upon the depth of capture. This supports the idea that a pixel represents an area, which when projected through its corresponding lens represents angular information [figure 4-10].

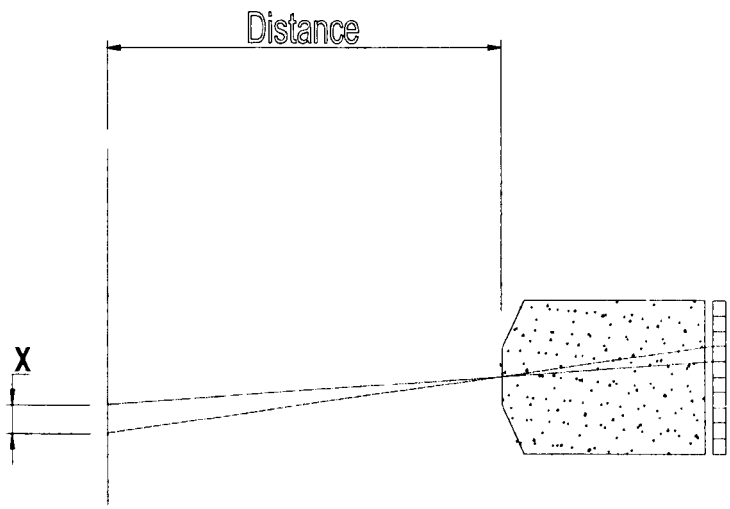

Figure 4-10, Pixel spread with respect to distance, linear magnification.

The diagram shows that as the objects move further from the recording plane, the area a pixel represents increases, in effect the sampling rate is inversely proportional to the depth being recorded. Thereby, implying that there should be a physically usable space in which the image is maintained for any given sampling ray defined by:

$$Freq_{samples} = \frac{F_{pixel}}{F_{lens}} \times d \qquad (4\text{-}2)$$

Where F_{pixel} is the pixel pitch, F_{lens} is the focal length and d is the distance away from the lens plane.

Alternatively, for a lens sheet with a thickness of 3.08mm and index of refraction of 1.6 and with a 300 dpi printer, this being a commonly available specification.

The printer pixel size is given as:

$$pixel\_size = \frac{25.4mm}{300dpi} = 0.085mm \tag{4-3}$$

Therefore, one pixel taking into account refraction represents an angle given by:

$$angle = \sin^{-1}\left(IOR \times \sin\left(\tan^{-1}\left(\frac{pixel\_size}{lens\_thick} \right) \right) \right) \tag{4-4}$$

This results in a pixel representing an angle of 2.52°, corresponding to a spatial coverage at 300mm from the screen plane given by:

$$spread = distance \times \tan(angle) \tag{4-5}$$

Consequently, a single pixel represents a spread of 13.197mm at 300mm. The effect is represented graphically as shown in figure 4-11.

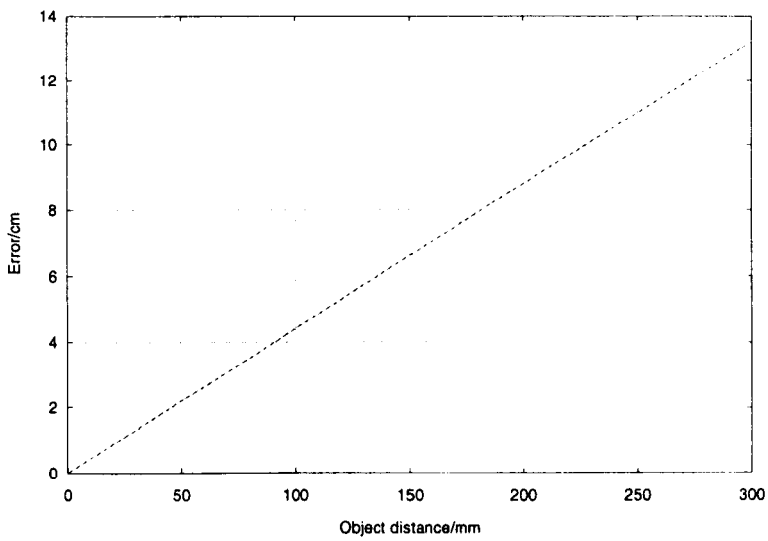

Figure 4-11, Sampling error at 300 dpi with respect to object distance.

This means that the smallest resolvable spatial point size increases linearly as the distance from the screen plane increases and at a point distance of 300mm it is 13mm. The situation can possibly be improved by the effect of multiple micro-lenses reconstructing a single point in space. In this case, overlaying of the fundamental point spreads will result in a complex intensity spread being reconstructed. However, this process, using incoherent light, cannot reduced the physical size of this spread only the point size perception, as all wave-front combinations are additive.

4.3.3. Spatial resolution of pixelated integral images

Given that the pixelated information is increasingly spread as light travels away from the lenticular plate, spatial accuracy conveyed by each pixel is also similarly reduced. Consequently, the spatial resolution of an integral imaging system should correspondingly decrease as the inverse of the objects distance from the plane (*1/d*). The result is that there is a maximum depth associated with a minimum spatial resolution for a pixelated device with a specific screen plane resolution.

Integral images exist in space as full optical models, independent of the observer. Thus, the resolution of the system is derived from the accuracy of the display media modified by the optical properties of the micro-lens sheet.

4.3.4. Analysis of point resolution in object space

To simplify the analysis of point resolution in object space, only a single lens is taken into consideration and the increased resolution obtained by the action of multiple lenses on a point in space is ignored. This results in the resolution (measured in lines per inch) being given by:

$$resolution(d) = \frac{1}{2 \times d} \times \frac{lpi}{N} \times \sqrt{4 \times f^2 + pitch^2 - N^2 \times pitch^2} \qquad (4\text{-}6)$$

In equation 4-6, *d* is the distance of the measurement, *lpi* the screen resolution, *f* the micro-lens focal length, *pitch* the micro-lens aperture size and *N* the lens media index of refraction.

Taking a standard printer operating at 150 lines per inch (300 dpi) and assuming the micro-lens has the following parameters 1.27mm pitch, 3.08mm focal length with an IOR of 1.6, then the resolution variation with is as shown in figure 4-12. The reduction in resolution is seen to be proportional to *1/d*.

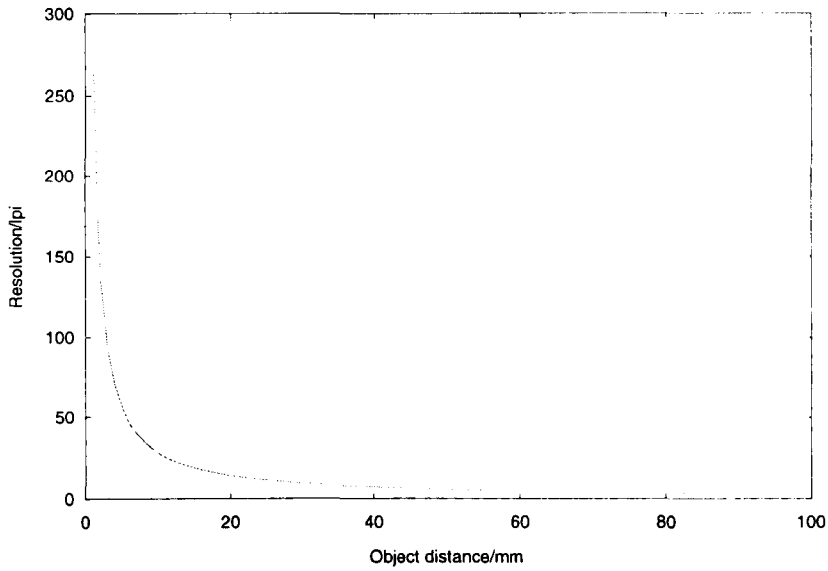

Figure 4-12, Resolution with respect to depth.

When reconstructed, the spatial acuity of a point is improved due to the action of multiple micro-lenses. The resulting overlaying of projected pixel information in space effects the final intensity profile of a spatial point [figure 4-13].

However, the majority of the information representing a single point in space can only be recovered when interrogated, as an optical model, by retrieving the information onto a flat diffusing screen located co-incident with the location of the spatial point. Projecting this intensity information onto a diffusing screen concentrates the information about every point onto the screen irrespective of the rays original direction. The whole integral image information is recovered rather than the subset of information that has the correct angular component to enter the pupil of an observer.

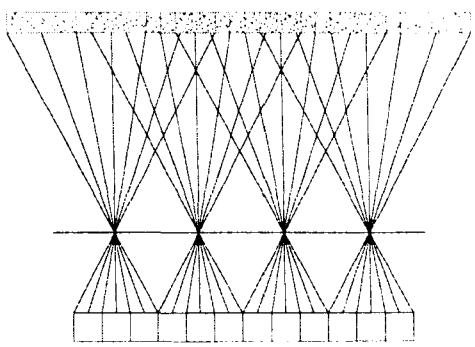

Figure 4-13, Reconstructed Aerial point resolution.

The resolution of the integral replay system can also be measured in a viewer dependent situation. Spatial acuity of points is a valid analysis of the imaging system, however the actual resolution that is observable is equally important.

4.3.5. Analysis of viewing resolution

Viewing resolution is the accuracy of the image captured on the retina of the observer's eye and as such cannot take into account any of the global point information as the pupil is, by nature, highly directionally selective.

Consider a stationary observer at a viewing distance from the lens plane from which distance they perceive no greater resolution than one pixel per lens. The observer only sees the lens pitch as the resolution due to each micro-lens projecting a single magnified view of a pixel. This then implies that the lens pitch is one factor that has a great influence over the resolution of the image.

It is the relationship between the object-screen distance, the viewer-screen distance and the screen resolution that creates the final viewing resolution. If an object is positioned a distance away from the integral lens sheet, the sampling rate across that object is effectively greater due to the object filling a larger angle to the eye and subsequently covering a larger number of lenses on the image plane [figure 4-14]. Objects further away from the screen plane are sampled more than objects closer to the screen plane, therefore resolution improves as objects approach the viewer.

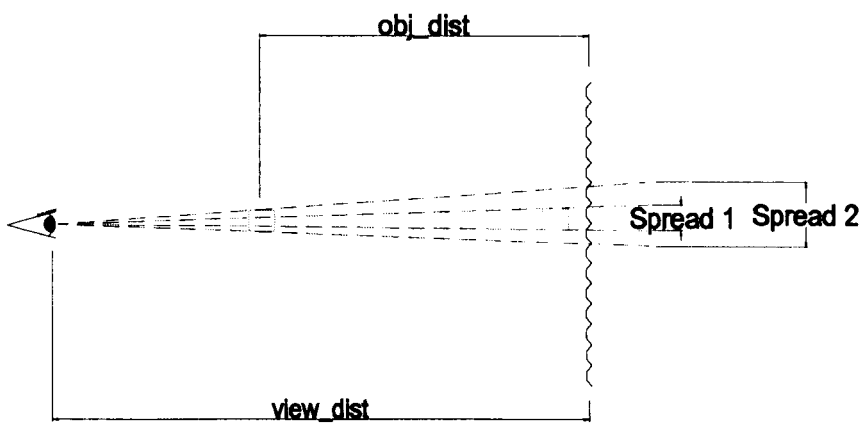

Figure 4-14, Lens sampling as an effect of distance.

It can be seen that an object further from the screen plane, subtends a greater angle to the eye and therefore, a viewer would receive information about that object from several lenses (spread 2). More lenses than would be required to replay the same object if that object was closer to the lens sheet (spread 1). However, this only holds true for images that are considerably larger than the pitch of the micro-lens sheet. When dealing with features smaller than the lens sheet pitch sub-lens sampling effects (aliasing) is more influential.

Ignoring negative lens effects such as aberration and diffraction, it is possible to produce a mathematical relationship, based solely on geometric optics, between the observers position (*view_dist*), the objects distance (*obj_dist*) and the pitch of the lens sheet, equation 4-7.

$$lpi = \frac{12.7}{(view\_dist - obj\_dist) \times \left(\frac{pitch}{view\_dist} \right)} \tag{4-7}$$

The function plotted for a 1.27mm lens sheet with an observer positioned 500mm away from the lens plane is shown in figure 4-15.

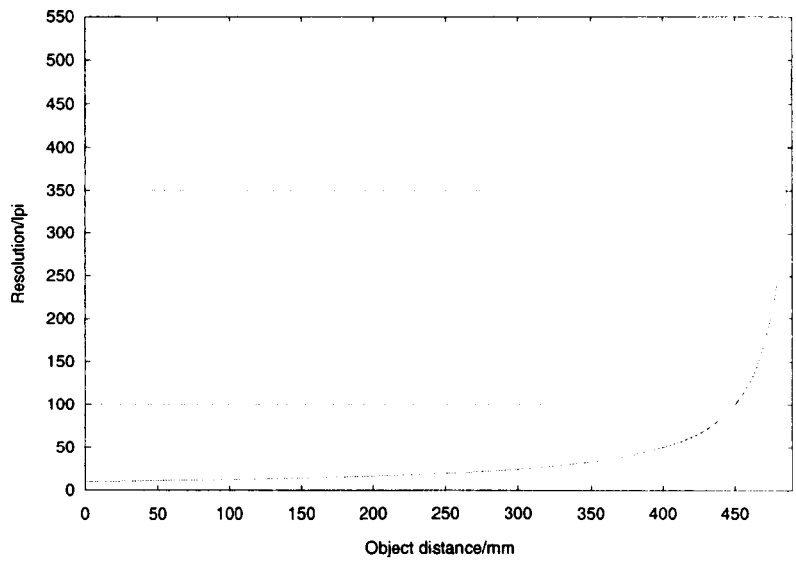

Figure 4-15, Lens sheet resolution (LPI) with respect to object distance (mm) and fixed observer.

4.3.6. Conclusion

The observable resolution of an integral image is controlled by the pitch of the micro-lenses, the objects position and the observers distance. However, this is not the complete answer as the micro-lenses used in integral displays have their own resolution characteristics and thus, it must be a combination of the two effects which gives the correct description of integral image resolution.

Photographic, non-pixelated images have a much larger volume of resolvable depth, which results in images with higher perceived quality. This is simply due to photographic emulsion having a pixel resolution of 3000-5000 dots per inch (Kowlaski, 1992), considerably higher than the 300 dots per inch of standard print techniques. Additionally, photographic emulsion "pixels" are arranged randomly over the substrate, no structure is apparent. Therefore, aliasing effects are further reduced.

To date no work has been reported relating to the resolution of integral pixelated images. This is discussed in the next section.

4.3.7. Resolution predictions for pixelated integral image displays

An experiment was conducted to measure the resolvable spatial resolution with respect to object depth. Integral image synthesis code was used to produce various square wave patterns at differing frequencies at various locations in space. The spatial frequencies used were 0.5, 0.66, 1.0, 2.0, 5.0 and 10 lines per mm. The pattern depths chosen were from 0mm to 35mm in steps of 5mm, all forward of the lens sheet. The nature of the experiment was to determine whether two points were resolvable to 50% modulation. It was predicted that resolution would diminish with distance from the micro-lens array plane. The experiment was carried out for micro-lens pitches of 1.27mm and 0.6mm. The pixel size in both cases was 300dpi, since the images were produced using an available dye-sublimation printer.

A selection of the generated integral images are shown in figure 4-16. They consist of 6 vertical patterns each of a different spatial frequency (10,5,2,1,0.666 and 0.5 lines/mm) positioned a constant distance away from the capture plane (0,5,10,15,25,30 and 35 mm). The charts for 5,15 and 30mm are shown.

The assessment was made by direct and magnified (x2.5) observation and by use of densiometer with the aim of finding the 3db point.

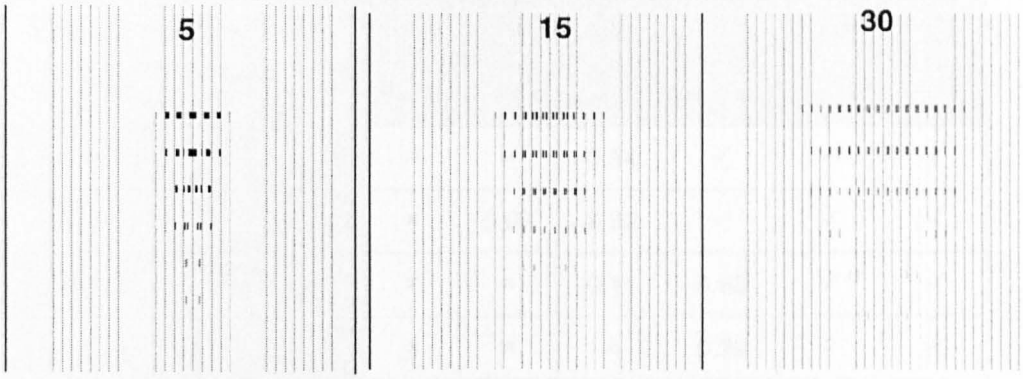

Figure 4-16, Integral image for resolution depth experiment.

The results in table 4-2, and table 4-3 show the approximate modulation ratios for the 1.27mm and 0.6mm lens sheets. However, the full pick up area of the densiometer was too large to be accurate for spatial frequencies above 2 lines per mm.

Spatial Frequency / mm^{-1} / Depth / mm	10	5	2	1	0.666	0.5
0	×	×	×	0.71	✓	✓
5	×	×	×	×	0.64	✓
10	×	×	×	×	0.43	✓
15	×	×	×	×	0.21	✓
25	×	×	×	×	×	0.43
30	×	×	×	×	×	0.18
35	×	×	×	×	×	×

Table 4-2 , 1.27mm pixelated resolution results.

Spatial Frequency / mm^{-1}	10	5	2	1	0.666	0.5
Depth / mm						
0	×	×	0.54	✓	✓	✓
5	×	0.07	0.32	✓	✓	✓
10	×	×	0.11	0.68	✓	✓
15	×	×	×	0.39	✓	✓
25	×	×	×	×	0.65	✓
30	×	×	×	×	0.42	✓
35	×	×	×	×	×	0.47

Table 4-3 , 0.6mm pixelated resolution results.

The results show that lenticular arrays operating with limited numbers of discrete pixels behind each lens hold resolutions equivalent to their own pitch for small distances from the front of the lens plane, regardless of that distance. At increased distances (more than 10f), resolution quickly diminishes. The results show that it is the lens pitch, and to an extent the pixel pitch, that is the determining factor in image resolution.

4.3.8. Conclusions

Sampling of integral images results in aliasing effects in the optical model. These sampling effects manifest themselves as a three-dimensional break-up of space. Two-dimensional anti-aliasing techniques can reduce the noticeable effect of under-sampling in standard images, and possibly perform a similar task in the computer generation of integral images. However, direct application of two-dimensional anti-aliasing techniques only temporarily solves the problem. Due to their nature, these techniques only treat the situation as being two-dimensional and have no knowledge of the spatial problem that they are being asked to solve.

In addition, it can be shown that there are essentially two modes of operation simultaneously existing simultaneously within an integral image. The first is the reconstruction of the global optical model that exists in space independent to any observer. This mode of operation, relies on intersecting beams to form the spatial acuity of the model independently of the observer. The defining resolution of this optical model is dictated by the linear magnification of the individual display pixels.

The second mode of operation is the interrogation of the directional image rays of the model by and independent observer. This resolution is dependent on the relationship of the observers distance to and the pitch of the micro-lens screen.

Therefore, it is suggested that an anti-aliasing solution for integral image generation is required that operates in the two domains:

1. A sub-lens anti-aliasing that performs low-pass filtering on adjacent pixels.

2. An inter-lens anti-aliasing that performs low-pass filtering across adjacent lenses.

The overall effect of forming an integral image with pixelated displays is that the spatial information of the image, which corresponds to angular information in the final image, is given a finite area. This blocking of information causes angular ambiguity in the image. Specific image points in the scene will be given location error, due to information from which they are formed being projected by micro-lenses with a certain spread.

4.4. Section conclusion

Effects that manifest themselves from too low a sampling rate can be overcome, as with any sampling problem, by increasing the sampling rate so that it is within acceptable limits for points at a given distance. Alternatively, anti-aliasing techniques need to be devised to reduce and/or mask the effects manifested by aliasing. Any such technique needs to be based on an understanding of the integral image rather than using a standard two-dimensional image construction approach. For example, an anti-aliasing system could be used to mask the integral imaging effects, such as double imaging and moiré.

A key factor in relation to pixelated integral images is that depth resolution is determined fundamentally by the pixel sampling rate and that the break-up of images with respect to depth is a form of aliasing. Therefore, for a specific pixel resolution a certain depth of focus must be tolerated. Anti-aliasing can make this appear more appealing to viewers but cannot improve on the fundamental negative effects of a low sampling rate.

On a more general level, considering a lens operating at the focal plane as an optical Fourier transform device, which the micro-lenses in integral image capture are, produces an interesting question. The Fourier transform of a square wave in the spatial domain is a *sin(x)/x* pulse in the frequency domain, additionally the transform of a square wave in the frequency domain is a *sin(x)/x* pulse in the spatial domain. This means that if images are forced into being represented at the Fourier plane as square blocks of information (i.e. a pixel) then this is going to be transformed and projected into the spatial domain as a *sin(x)/x* pulse. This has the effect of reducing the resolution of the final image as the multi-peaked waveform of *sin(x)/x* would blur the resulting image. Even worse is that a finite pulse in the frequency domain will result in an infinite pulse in the spatial domain, meaning that this effect is non-local.

5. INTEGRAL IMAGE PROCESSING

5.1. Introduction

It has been shown that computer generation has allowed the production of artificial integral images. Additionally, the knowledge utilised in the production of the image can be used for the analysis and processing of existing photographic integral images. Integral image processing knowledge would allow the use of standard image processing techniques in the integral image field. For example, feature extraction, edge detection and various cut and paste processes.

5.2. Comparison of pixelated integral images and multi-view stereo images

Generally, there are two methods of generating a pixelated multi-view image. The simplest method is to interleave a fixed integer number of pixels behind each micro-lens, and to cycle through each view in turn [figure 5-1]. This results in an image that contains alternate bands of each view.

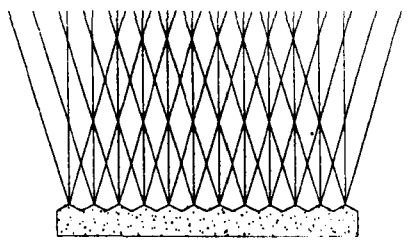

Figure 5-1, Multi-view (1).

The problem associated with doing this is that the images on the display are projected back to infinity. This causes the image to be viewed uncorrupted only from a distance that subtends a small enough angle to the display, to avoid viewing any neighbouring pixel boundaries. A situation which occurs, at around 1.8m from a 125mm x 100mm plate.

The second method involves a carefully constructed micro-lens array display area screen in which the pitch varies so that the rays produced by a pixel converge to a fixed point in space [figure 5-2]. This situation dictates a fixed viewing position for an observer, and outside of this zone negative effects occur.

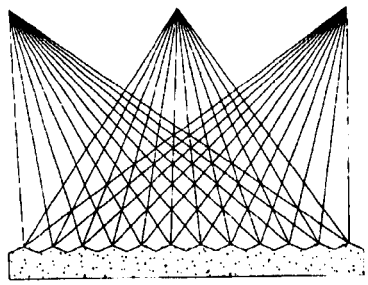

Figure 5-2, Multi-view (2).

However, when producing an integral image photographically, no discrete viewing positions or directions are formed, as the information captured behind each micro-lens is continuous. There is a similar consideration needed to be understood when pixelating integral images. The number of pixels per lens directly effects the number of accurate rays reconstructing a point in space and therefore this effects the resolution with varying depth.

5.3. Dissection of an Integral Image

A photographic integral image contains continuous scene information within its angle of view. A situation was modelled to extract part of the information contained within an integral image under very specific conditions and display it as a two-dimensional image. The views extracted correspond to the theoretical case of a viewer positioned an infinite distance away from the screen (as in some forms multi-view construction), of which each micro-lens contains an exact constant integer number of pixels. This position was chosen as it allows the mathematics of the analysis to be greatly simplified, as all infinity rays emerging from any lens on the image plane are parallel to every other lens. In addition, all rays from across the plane are visible to the viewer [figure 5-3], i.e. there is no vignetting.

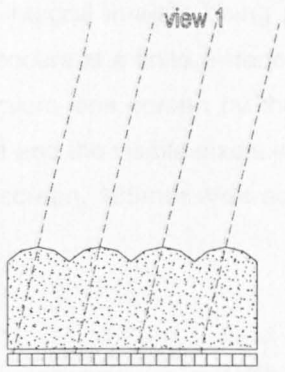

Figure 5-3, Parallel projection to extract views.

The two-dimensional image extraction process was initially tried on computer generated images, as the number of pixels per view can be guaranteed to be constant, and subsequently on an accurately scanned original integral image. The images where produced using a 1.27mm micro-lens screen and scanned at 300 dots per inch, thus giving 15 pixels per micro-lens. From this fifteen two-dimensional images were extracted corresponding to one view per micro-image pixel [figure 5-4], where view '0' is composed of the first pixel of every micro-lens image, view '1' is composed of the second and so on.

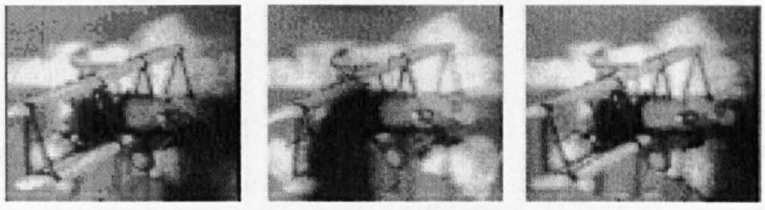

Figure 5-4, Pixelated integral image infinity views [frames 0,7,14] of "biplane" image.

The image frames show a subset of the image views. Most importantly, these portions of integral image actually look like a low-resolution version of the original photographic image. In a sequence of several of the images it is possible to see a black band progress across as the virtual observer moves from on view to the next. This is because no attempt was made to start the processing at the first pixel of an image band. Additionally, when replayed in the form of an animation, it is possible for this to be done to the rotation of the images, and the relative motion of the objects in the scene.

Due to the pixelated nature of the integral images being processed, it can be shown that this special case of projection to infinity occurs at a finite distance. That is, when the angle subtended to the most extreme edges of the micro-lens screen by the viewers eye is not large enough to extend into a neighbouring pixel area and the visible pixels in an image are all in the same position in every lens. For a 1.27mm pitch screen, 125mm wide scanned at 300dpi resolution this effect occurs at;

$$distance = width \times \frac{focal}{0.085} \tag{5-1}$$

$$distance = 4.53m$$

This shows that the artefact should not be normally noticeable in real world (i.e. finite) viewing situations, at this distance the pixels and even the lens pitch is below the level of human visibility. However, the overall visibility of this production of discrete numbers of the viewing positions in the integral aperture in practical situations is reduced. This is due to images commonly having non-integer numbers of display pixels behind each micro-lens.

Having non-integer numbers of pixels behind each micro-lens produces a spatial moiré that manifests itself in the pattern of pixels switching in the integral image. This introduces a flipping pattern that occurs at differing positions across the lens plane, removing the more noticeable global flipping apparent in multi-view.

5.3.1. Conclusion

The effect of visible flipping between the pixels of an integral sub-image only occurs for certain specific viewing situations. The main criteria for this effect is that the image has been pixelated into a constant integer number of pixels per micro-lens and that the viewer is at least a certain distance away.

As a viewer progresses through the angle of view of the image, a zone will occur where only the first pixel of the sub-image of every micro-lens can be seen through the lens apertures. Further progression in a direction to cross a pixel boundary will result in the viewer seeing only pixels adjacent to the original in the micro-image.

Generally, integral images exhibit a continuous nature in their angle of view. However, with pixelation of these images the micro-sub images are sampled to discrete positions and levels. Most arrangements of pixel pitch and lens pitch will produce a spatial moiré pattern that exhibits itself in the order of the pattern in which the micro-lenses on the replay sheet change from one pixel to the next.

However, under very specific conditions when there is a constant integer relationship between the pixel and the lens pitch, these pixel changes occur simultaneously across the plate as a whole.

Using this special case to simplify the calculations, several views (the number of views correspond to the number of pixels per micro-lens) can be extracted from an integral image. Once these two-dimensional images have been extracted, standard stereo depth-reconstruction algorithms, which utilise two of more stereo pairs, can be applied with minimum alteration so that they operate with integral images.

Possible applications of this technique are shown in the next section.

5.4. Integral Depth Information Extraction

Integral images store the depth map of the scene encoded optically in the intensity profiles of the many micro-images on the photographic plate. A detailed understanding of the nature of integral images makes it possible to extract this information by reversing the generation technique, to produce three-dimensional spatial location data from an integral photograph.

5.4.1. Stereo depth reconstruction

Currently, it is possible to produce three-dimensional depth information from a set of classical stereo images. Analysis of the image information stored within a stereo pair allows the determination of individual depth values for features in the scene. Depth values associated with points are inferred by locating the same feature in both images and then using the disparity between these two positions to calculate a possible point location $P_{(x,y,z)}$ [figure 5-5] (Olivias, Salembier and Garrido, 1997; Beß, Paulus and Harbeck, 1997).

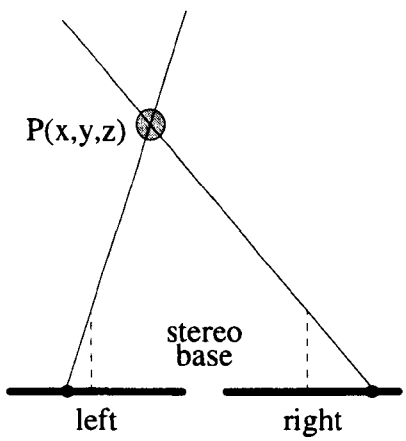

Figure 5-5, Stereo pair depth reconstruction.

The accuracy of the depth information extracted using this method can be significantly increase by using multiple stereo views of the same scene. This allows the triangulation of the point to be greatly improved by increasing the image base size, and an increase in general accuracy due to the removal of false hits from repeating patterns.

5.4.2. Integral depth reconstruction

Depth reconstruction through integral images has several benefits over conventional stereo depth recovery. Integral images require only a single image to be taken and therefore require no processing to be applied in the alignment of the images. Additionally, integral images are captured using a large number of small spatially separated lenses, this means that correlation used to extract depth of features can work on a large number of small, highly similar micro-images. Figure 5-6 shows the level of similarity between neighbouring sub-image bands in an integral image, having a large number of image pairs and having a short baseline between these pairs makes extraction, matching or tracking of features easy.

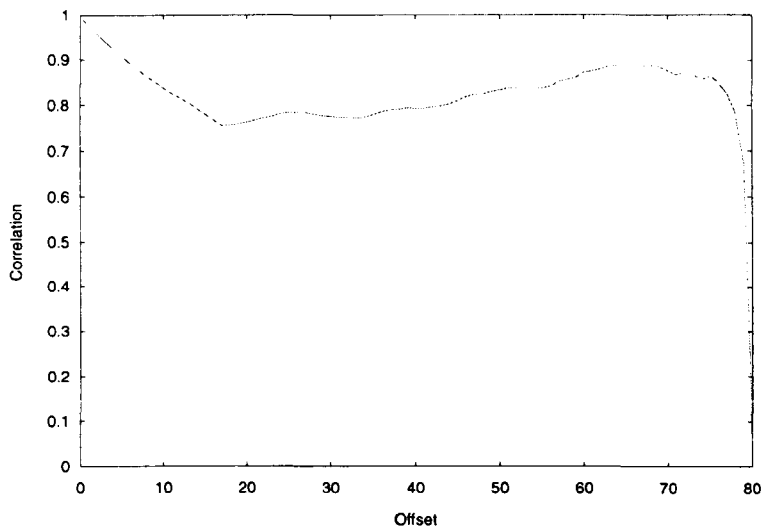

Figure 5-6, Extent of correlation between neighbouring micro-lenses.

There are many problems associated with these methods when applied to digitised media. For example, statistical errors are introduced by the pixelation of the image at generation/capture, caused either by scanning of an original photographic image or by discretisation of an electronically generated image where infinitely small areas convert to finite elements. However, as more information can be gained using the distributed information contained in more than one sub-image, the overall reconstructed error can be reduced.

A simplistic attempt was made at depth reconstruction using a modified ray-tracing algorithm that applied the standard methodology in reverse.

5.4.3. Method A – Reversed ray trace

Experimenting with a simple system using a revered ray tracing method [figure 5-7] to reconstruct the data locations showed that the placing of image points to any accuracy is not a trivial task. This is mainly hampered by the nature of the lens sheet.

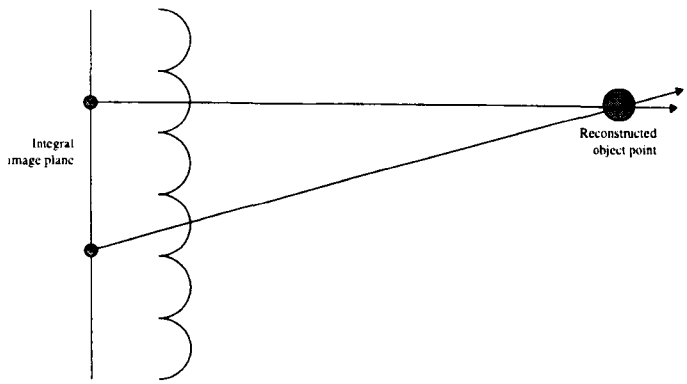

Figure 5-7, Tracing of rays to located image points.

With stereo depth reconstruction, the two views are physically separated, typically by the inter-ocular distance (60mm). With an integral image, the separation between sources of information is the lens pitch, usually chosen to be small (≈1mm). The closeness of the micro-lenses induces large amounts of "ghost" points to occur in the reconstructed volume. These ghost points are formed by the incorrect, intersections of neighbouring lens ray bundles at or close to the screen plane [figure 5-8].

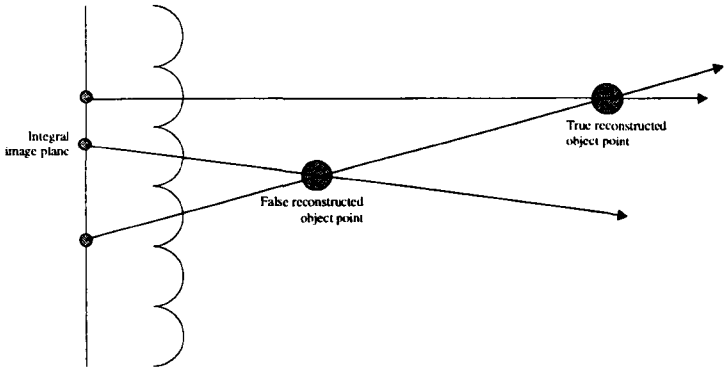

Figure 5-8, Creation of "ghost" points.

This problem of "ghost" points could not be fully resolved. Accuracy in locating the points was extremely poor, as the true point locations where washed out by adjacent false hits.

Consequently, an alternative technique using multiple baselines was considered.

5.4.4. Method B – Multiple baseline correlation

In this alternative method, a similar technique to that described in section 5.3 is used with several "views" being extracted from an integral image. These images are processed as a set of multiple baseline stereo pairs to provide the reconstructed depth information using a conventional stereo method, with additional accuracy due to the synthesis of multiple viewing positions. The stereo reconstruction method used was a windowing correlation algorithm (Okutomi, 1993), which performs calculations based on the intensity values of the image and requires no additional stage of feature recognition or segmentation.

This algorithm simplifies the reconstruction process, as it is purely numerical using only correlation to find the "best fit". Therefore, it does not need complicated independent intelligent detection strategies. The combination of several disparate views into the processing, removes the problems of "false hits" caused by image projection points being spaced close together.

The multiple baseline correlation method produced results that indicated a degree of depth extraction [figure 5-9], the image shows a monochrome image where the intensity values corresponds to the relative depth of the point. From these relative depth values and knowledge about the locations of the derived views the true depth value can be attained.

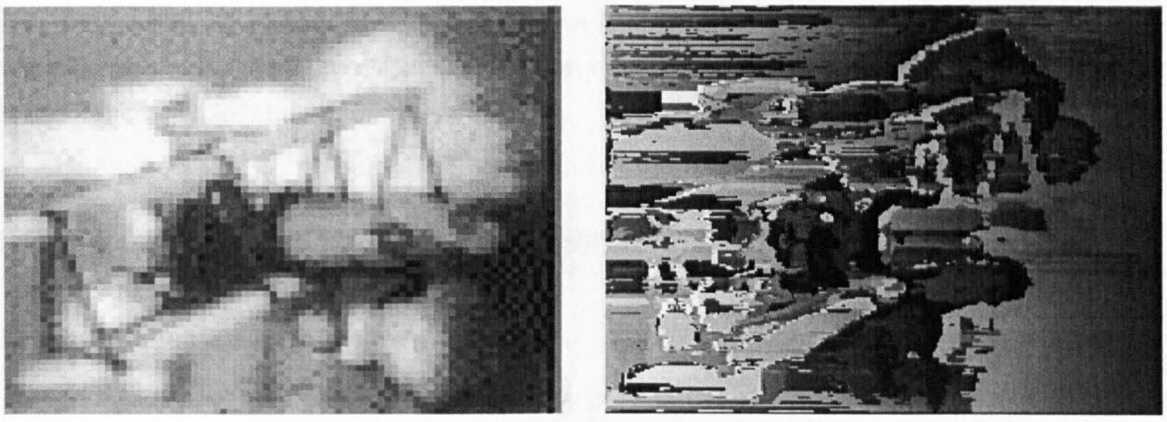

Figure 5-9, "Biplane" image and depth map.

However, the results produced were not ideal. They were noisy and prone to errors introduced by artefacts in the integral image. One such artefact is visible on the right side of figure [5-9], this is caused by the location of the dead space between micro-image fields.

5.4.5. Conclusion

Two approaches to depth reconstruction are reported. The simplest method proved to have too many problems associated with it to be considered as successful. However, by extracting multiple two-dimensional images from an integral image, standard multiple-baseline stereo reconstruction methods were applied without significant alteration to the algorithm. An approach based on this method should provide a profitable approach in the solution to this problem.

The methods attempted were not specifically designed for an integral image and hence problems were encountered due to the fundamental nature of this type of image. However, the multiple baseline method showed promise and achieved sufficient accuracy to produce a partial depth map for an integral image. Therefore, a method specifically designed to operate on integral images utilising the individual sub-images, the high correlation between them and allowing for the negative effects produced by integral images (black bands) should perform well. Either producing a model defined from the depth map or a pixel by pixel depth map would allow digital manipulations of integral images to be performed.

A more detailed investigation would provide a working solution and using information encoded by the integral imaging process could increase the effectiveness of data set extraction. As integral images already effectively contain multiple baselines and have a high degree of correlation between sub-images.

Post processing of integral images has shown that image manipulation is possible in three-dimensional images. Pre-processing a computer modelled scene allows other displaying methods of integral images to be utilised.

5.5. Integral Image Projection System

5.5.1. Introduction

Image projection systems are beneficial as they provide ways of displaying large area images to the viewer(s). Three-dimensional projection systems allow the cost of large area micro-lens arrays to be compensated by the flexibility of displaying many individual still images onto one single piece of screen.

The projection system proposed is designed around half of an integral transmission camera [figure 5-10]. Several volume images are created around the micro-lens array, these images are translated and transformed through a macro-lens array and recombined as a magnified aerial image. This is image can be viewed directly or can be re-integrated using an afocal combination of micro-lenses. The magnification caused by the system allows the micro-lenses to image well within their acceptable range whilst still allowing the display of large amounts of depth.

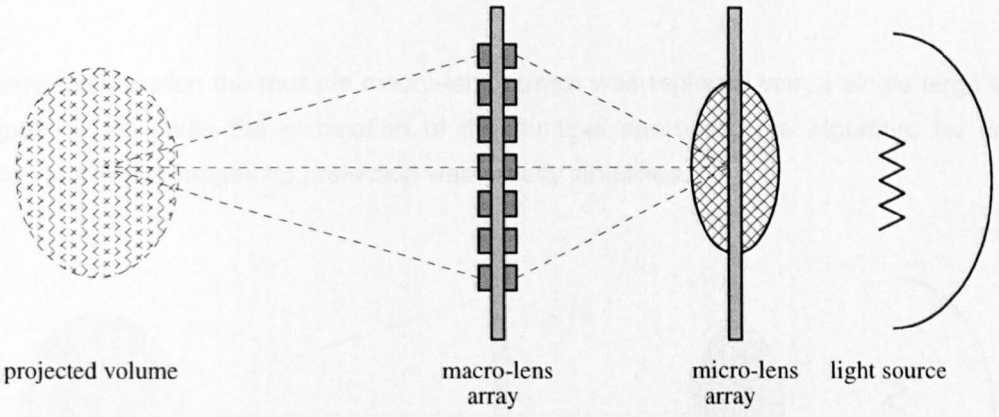

Figure 5-10, Complete projection system.

Another modification that can be made to this system overcomes the effects of sub-image reversal apparent for points behind micro-lens sheet. By biasing the micro-images to be in front of the micro-lens screen, correct replay is ensured [figure 5-11].

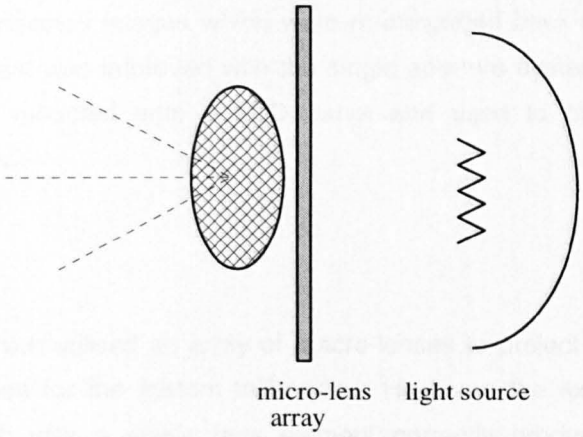

Figure 5-11, Alternative first stage of projection system.

5.5.2. Initial investigation

A computer simulation was produced to establish if the principles of the device were correct. These simulations required the modification of the integral image generation code to allow the capture of several reduced scale macro-lens images. The computer generated integral image was then replayed using a physical version of the projection system. This initial attempt produced projected images that had poor detail and low contrast. This caused the images to produce no significant depth cues.

To improve the situation the multiple macro-lens design was replaced with a single large aperture lens [figure 5-12]. With the elimination of the multiple apertures, the algorithm for computer production of integral images for projection was greatly simplified.

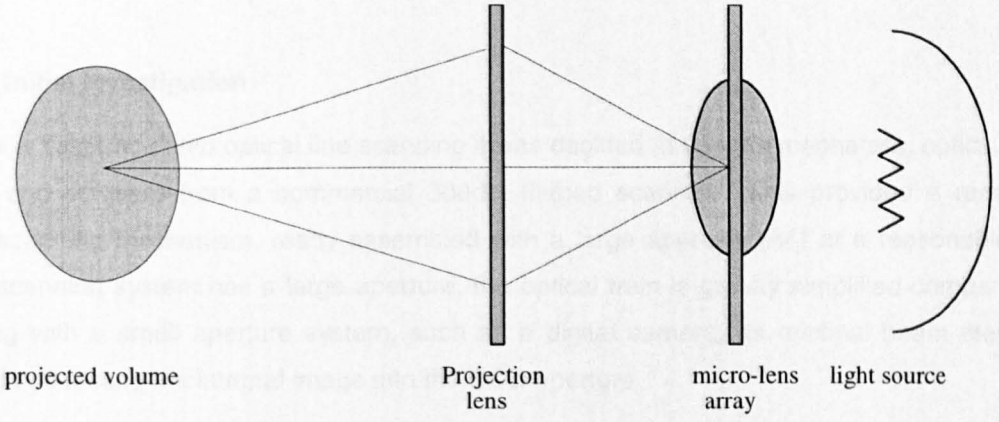

Figure 5-12, Simplified projection system.

This system produced projected images which were re-integrated back to their original size and position in space. Contrast was improved with the single aperture system. The micro-lens array has subsequently been mounted onto a LCD panel and used to project integral computer generated moving images.

5.5.3. Conclusion

The proposed system which utilised an array of macro-lenses to project the image produced too much geometric aberration for the system to handle. However, the experimental set-up which performed the same job with a single lens element correctly produced a projected image. Unfortunately, large aperture lenses tend to be expensive, heavy and be uncorrected. The benefits of using multiple smaller scale apertures is that the lenses are cheaper, easily available and lighter.

5.6. Electronic Capture of Integral Images

5.6.1. Introduction

Electronic capture of integral images had never been attempted at the start of these experiments. As with computer generation, electronic replay and transmission of integral image data, current established theories showed that this is not possible with the ranges of capture resolution available. Earlier print experiments and subsequent LCD panel display of integral images showed that these theories did not hold. Therefore, electronic image capture was considered feasible.

The final goal of these experiments was to achieve a real-time, electronically captured integral image, however, as a first step towards that goal it was decided to capture the images using a single pass, large aperture colour line-scan imaging system.

5.6.2. Initial Investigation

To allow a "fast track" into optical line scanning it was decided to use the mechanics, optics, control system and software from a commercial 300dpi flatbed scanner. This provided a reasonable quality scanning mechanism, ready assembled with a large aperture (A4) at a reasonable price. As the scanning system has a large aperture, the optical train is greatly simplified compared with capturing with a small aperture system, such as a digital camera, as minimal beam steering is required in directing the integral image into the CCD aperture.

In a flatbed scanner, the document to be scanned is placed onto a glass table. Illumination occurs from the underneath surface and the image is captured using the light reflected from the objects surface. This method of image capture was not fully appropriate for the task of integral image capture, and several additions needed to be made to force the scanner to operate for this application.

5.6.3. Design of Experiment

Primarily, the scanner produced light to illuminate an opaque object. This xenon strip light source was also used to detect the linear CCD current position, via an optical feedback loop. To achieve integral image capture the scanner was modified such that the xenon strip light source was disabled. This was required so that only the light emanating from the image scene was captured and not reflected illumination from the scanner. With the xenon light source removed a substitute electro-mechanical feedback system was implemented to allow the scanner to reset itself to its predefined start location.

Secondly, the front glass plate of the scanner was replaced so that the scan head travelled across the back surface of a lenticular screen (1.124mm) [figure 5-13]. This modification allowed the CCD head to capture the micro-optical images formed by the lenticular sheet.

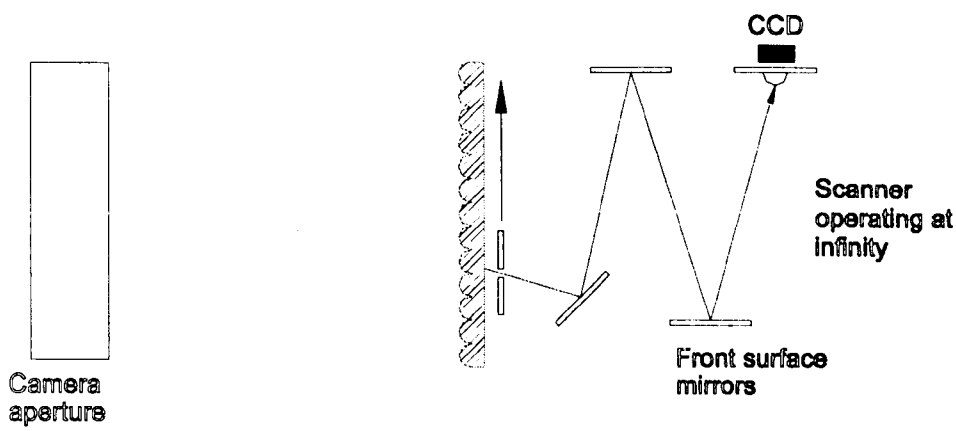

Figure 5-13, Line-scan capture system.

5.6.4. Results

Initial results showed promise, but lacked a large imaging area due to the directional nature of the light information. This small image area was caused by the functioning of the scan head. It was constructed not from a large area strip CCD but from a small area CCD to which the image of the object was focused onto from (effectively) infinity. This set-up causes obvious problems and results in a scanned integral image being severely vignetted [figure 5-14], because image fields created by the micro-lenses at the extremes of the sheet are directional, therefore, most of the intensity information missed the CCD aperture.

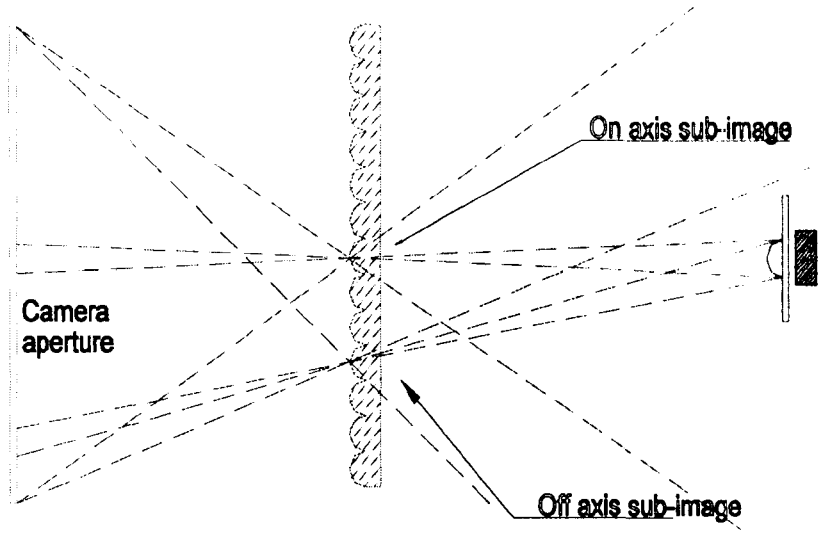

Figure 5-14, Vignetting caused by directionality of rays.

5.6.5. Redesign of Experiment

To overcome this, the rays from across the entire area of the lenticular plate need to be steered into the scanner aperture. The complex nature of the integral sub-images complicates this task, and requires complex micro-optical paths to achieve a satisfactory solution. As a temporary solution, an optical diffuser was placed in direct contact with the back surface of the capturing lenticular sheet. This reduced the directionality of the rays in the micro-images by an amount large enough to produce a captured image [figure 5-15].

This is not a practical solution to the problem of direct capture as introducing the diffuser sheet alters not only the directionality but reduces the intensity and corrupts the image with the diffuser structure. The use of diffuser sheet in the capture of integral images is an attempt to mimic the performance of photographic film, but in a real-time, transmissive manner. The job of the diffuser sheet is to allow all the rays hitting any area to be captured by the CCD so that they are imaged. This is achieved, in the case of a simple diffuser sheet, by destroying the directionality of the light rays and scattering them in random directions. This however, is a poor way of achieving such a complex task, the diffuser sheet operates in an *ad hoc* manner and scatters as much light away from the CCD as is sends towards it. Additionally, the diffusers available are not perfect and rays are still directional to an extent. Intensities reaching the CCD are therefore, still not representative of the intensity that would be captured photographically.

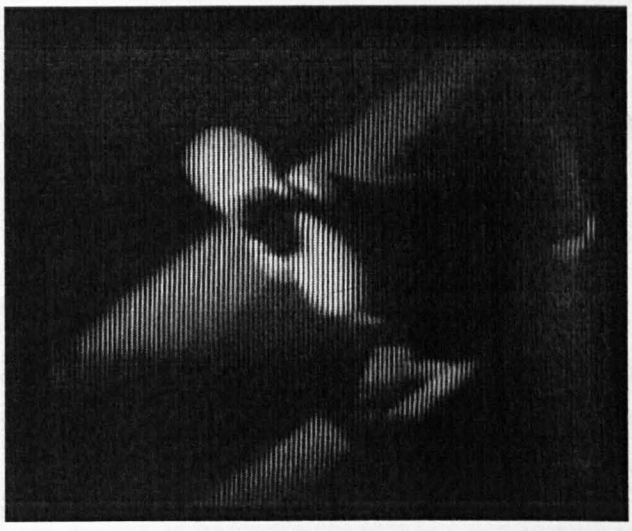

Figure 5-15, Line scanned integral image.

The efficiency of the capture path in this attempt at direct integral image capture was extremely low, a 1500 Watt light source was required to illuminate scene to a satisfactory level for capture by the scanner. This was caused by the design of the scanner, which incorporates a very bright light source extremely close to the imaging surface and the use of diffuser. However, this loss was mainly caused by using a retro-reflective camera design to optically translate the imaged scene, thus reducing the scene instantly to one quarter of its original intensity. This was alleviated by utilising a single lens to perform a similar process. However, this produced pseudoscopic images that needed re-projection through a similar lens arrangement to re-invert the spatial orientation and could not be directly viewed.

5.6.6. Conclusion

These experiments produced encouraging results quickly and simply. The results exhibited all the characteristics of photographic integral images, apart from depth of focus and an obvious drop in resolution, as the images could be captured at 300dpi at the most. Additionally, the simple set-up without diffuser showed the dramatic effects caused by the directionality of the sub-images. However, the impressive results achieved through the introduction of a simple passive device as a diffuser sheet, provided hope that a more complex system of light steering would produce even better intensity results.

The simple *ad hoc* solution of using a commercial scanner introduced some problems that can be overcome. The major one being that the scanner/scanner software was calibrated for the scanners light source, a xenon tube. This caused the images scanned as integrals to be heavily biased towards the red/orange end of the spectrum. This problem can be solved by either using lights that emit the same wavelengths as the original scanner to illuminate the image or using photographic filters to reduce the amount of red/orange that is received by the scanner.

Post processing of the image is a possibility but achieves only a partial solution as colour information that is lost cannot be fully re-created by the imaging software.

5.7. Section Conclusion

Integral images have shown that they are robust in nature, can be captured electronically and can be processed to extract information. Post-processing has shown that depth extraction from an existing integral image is possible. However, the nature of the images means that the extraction process will have to incorporate the integral structure into its strategy. Fortunately, the main algorithm body can be derived from existing stereo extraction algorithms, such as the one reported by Okutomi.

Electronic capture has shown that integral images, previously thought to contain huge amounts of information, can actually be captured using a discrete CCD device. Admittedly, in this experiment the CCD was a linear array and produced a slow scan image of the scene, despite this the resulting images still replay, showing depth and continuous parallax.

The projection of integral images, although initially showing disappointing results is another promising activity. Projection of images allow small area integral displays to produce large area images, which contain objects with massive depth. This leads to images being replayed as real size (1 to 1 scaling) with correct orientation and depth retained. Currently, this has been achieved photographically and through the use of computer generated images displayed on LCD displays. This technique has achieved the projection of both still and moving integral images.

Both integral image projection and depth extraction have since been investigated separately by other individuals in the 3D Imaging Group as PhD projects.

6. Conclusions

Before the start of this project the nature and structure of photographic integral images was largely unknown. Previous attempts at describing the nature and structure of integral images had produced several contradicting conclusions. This project set out to rectify this situation and achieve computer generation of integral images through the analysis of photographic integral images, geometric optics and through practical computer based experiments. The experiments were designed to validate theoretical findings and illustrate the essential characteristics of the integral image forming process have been found and understood.

A comprehensive review of integral imaging highlighted the fact that integral imaging as a modality had largely been forgotten due to the difficulty involved in producing micro-lens arrays and the predicted resolution requirements. However, recent interest in micro-lens arrays, stimulated by the optical systems revolution and the need for optical interconnects, optical computing and light intensification elements has stimulated new interest. It can be expected that as micro-lens arrays are improved, integral imaging will be a natural benefactor. The literature review considered the many technical aspects involved in the development of integral imaging as a photographic technique plus dealing with issues involved in the computer generation of images.

In the initial work the structure of integral images was established and subsequently modelled. It was found that the field size and position of the sub images behind each micro-lens varies slightly and non-linearly for micro-lenses progressively displaced from the centre of the aperture. The variation is small enough not to be detected by the naked eye but can be measured using a travelling microscope. The variation of the field size and location relative to the micro-lenses is an important factor when attempting to display an integral image on a regular matrix of pixels. This variation of size and location of the micro-image fields is essential to the accurate replay of computer generated integral images.

This discovery led to the development and refinement of a computer based method for generating synthetic integral images. Several "camera models" were examined in which this artefact was incorporated and these models have allowed the chief aim of computer generation of photo-realistic integral images to be realised. The initial mode examined was the pinhole approximation. This model had several benefits as a starting point. The main point being that the optical calculations required are trivial thus making global understanding of the problem possible. From this model enhancements were made, resulting in models that emphasised different characteristics. Finally, a model that incorporates the calculation simplicity of the pinhole model and the optical accuracy of a full optical approach was chosen as this gave the best balance of features with which to produce images quickly and accurately.

The outcome was three software models capable of producing integral images.

In photographic images the grain size of the emulsion is approximately 5 microns, producing an effective "pixel pitch" in this medium of 5 microns. Of course, when displaying images on a liquid crystal display (LCD), there is a significant reduction in information density. In the display used (NEC 10 inch diagonal colour) the pixel pitch is 207 microns. This reduction in resolution and the pixelation of the image produces a situation where, when a 1.27mm unidirectional replay screen is used there are roughly 6 pixel behind every micro-lens. The main effect introduced by this discretisation of the integral information is the reduction of resolution at extended depths, this is understandable and can be explained by considering the image magnification and effective area a given pixel is chosen to represent at a certain depth.

Computer generation of images is computationally expensive. Hence, practical solutions to the problem of generating real-time computer generated images, for example hardware accelerated graphic cards are necessary. Computer generation of integral images may be assumed to be taking this problem and compounding it by introducing many different angular variations from which each point is seen. A number of speed-up techniques have been considered these include utilising the extremely high degree of correlation between neighbouring lenses (as many as the 8 neighbouring lenses in an integral image has extremely high correlation). This plus other data and calculation re-use which is inherent in the production of integral images may increase the feasibility of producing a system to generate integral images at high speeds. This plus other techniques, such as embedding the algorithms in hardware and generating whole images from parallel partial subsets would possibly allow these images to be generated in or near real-time.

This work led to the production of various synthetic three-dimensional images. The artificial images shared similar properties to those generated using a photographic method for integral image production. Additionally, the development of this method has produced knowledge that has led towards explaining effects apparent in the photographic integral images, and has produced a better understanding of the effects of pixelation upon integral images than previous attempts. It has been shown that integral images are extremely robust, not only can they be formed using an approximation to a lens as the computer model but can be rendered onto various output mediums and still exhibit key features such as continuous parallax and continuous depth. Obviously, as with any image, reducing the output resolution of an integral images does have an effect on image quality but in general integral images are extremely robust to image degradation with respect to data sampling or reduction.

A practical achievement of the project is the discovery that integral images can be seen to replay correctly if output as traditional laser printer reproductions (300dpi or 600dpi normally) and that computer generated images perform equally well at these low spatial resolutions. Given that laser printers can only output on or off points with limited spatial precision, images produced using this method have extremely poor intensity resolution. However, with this output medium it was evident that the images still maintained continuous parallax and exhibited depth. The key factor when reproducing images using general purpose printing devices is that unless the device can be controlled it produces grey level intensity values by outputting dither patterns. This dither trades the effective resolution of the device for intensity resolution. However, when magnified by the integral image micro-lens this effect can destroy the image almost completely.

Various other discrete imaging formats all with differing properties have been used to display integral images and with each format integral images were seen to maintain their continuous nature.

During the project computer generated integral images exhibiting horizontal parallax only were displayed electronically for the first time using LCD flat panel displays in conjunction with a decoding micro-lens arrays. The electronically displayed integral images were judged to contain continuous parallax and hold sufficient depth resolution of greater than 200mm to be achieved on the 210mm diagonal direct view, back lit LCD panel.

An objective was to produce a simple computer model of the integral process to facilitate the practical production of visibly impressive scenes. It has been shown that a 100% mathematical description of the form of a given integral scene is impractical and unnecessary even for general photo-realistic image generation. In particular the images produce will be encumbered with the optical inaccuracies of the capture lenses. Additionally, a 100% accurate description would require large amounts of computation to achieve the production of even simple images, the challenge of rendering such a schema in real time is extremely daunting and even with today's computer speeds impossible. Therefore, to achieve a practical integral image generation method the negative side effects of the simple optical elements used for capture where removed and the imaging process stripped to its fundamentals. Using a simple computer model eliminates effects such as spherical aberration and other distortions that require complex mathematical models to synthesise without reducing the accuracy of the pixel images produced. The accuracy of the pixelated images produced is unimpaired by adopting this approach thereby, allowing the generation of images using minimal amounts of computing time.

To achieve an understanding of the effects active in the generation of integral images several experiments were initially carried out. These involved capturing simple high contrast scenes using an integral camera. These easily analysable situations were then used to establish an understanding of the situation. Later, to provide an actual comparison between computer generated and photographic integral images several controlled experiments were carried out Through these experiments the accuracy of the position and structure of the computer generated integral images could be ratified.

The development of an integral image generation method is described and the various stages of its evolution have been documented. Finally, its output accuracy is measured and compared to similar measurements of images produced using physical lens arrangements As an empirical proof, actual images produced using the described methods are shown and comparisons show that their characteristics are identical.

Images generated produced using this method are theoretically capable of producing results with a higher final resolution higher than is possible photographically. This increased resolution is due to producing computer generated images with perfect, albeit virtual lenses, and therefore eliminating the negative effects apparent in the optical images due to vignetting, spherical aberration and coma. These detrimental effects are responsible for reducing optical throughput of the physical system in the frequency domain causing blurring in the spatial domain

The methods developed have been shown to be equally applicable for the generation of complex scene images, with complex lighting calculations through the blending of image ray-tracing software and the integral generation method. Producing images through the geometric projection of every point in the scene was found to be computationally expensive Not only did all the scene points need to be transformed, they had to be transformed per lens This resulted in a situation which had a complexity of N*L (where N is the number of scene points and L is the number of lenses). To generate higher detailed scenes the number of points needed to be increased, causing obvious problems). By shifting the generation methodology to the tracing of rays the image generation was made largely complexity independent Additionally, the lighting calculations used within the ray-tracing methodology gave the opportunity to produce images with per-pixel lighting calculations, thus improving realism.

The knowledge produced has allowed the expansion of the understanding in the field of integral images through the analysis and processing of image data Notably, in explaining optical distortions that occur in all three-dimensional lensed imaging processes and in the analysis of the maximum spatial resolutions possible within a pixelated integral image

The ability to produce images to essentially custom specifications has allowed progression and development of techniques such as the projection of full-scale integral images The image generation technique adopted based upon a pinhole model which allowed for refraction of the imaged light, allowed for the production of images which had been positioned and distorted to counter act the distortion and transposition produced by the physical projection lens system Therefore, in the final viewed image the scaling throughout the scene is returned to unity

In summary this investigation has produced key results in the following areas:

- The nature of pixelated integral images can be understood by applying geometric optic theories. Simple geometric formulas can be applied to the operation of integral imaging processes and can be extended to complete methods for generating the complex micro-views required for integral imaging.

  A relatively computation inexpensive approach has been produced and demonstrated The method of generation created removed most of the complex optical effects introduced by simple spherical lenses. As these effects are detrimental to the final result, this allows the generated integral images to have a higher possible capture resolution than images produced optically

  The main objective of keeping the micro-lens approximation as simple as possible to minimise computational overheads for complex scene generation, and complex lighting, was realised in a modified pinhole model of the micro-lenses. This allowed general computer graphics approaches to be easily applied to the generation of integral images Additionally, this maintained the imaging accuracy that came from including accurate refraction in the micro-lens model.

  Not only can the generation of pixelated integral images be understood through geometric optics but the knowledge gained can also be applied equally validly to the photographic integral process.

- The nature of general micro-lensed imaging produces micro-image inversions in the scene when viewed. This effect was first noticed in computer generated integral images, but was subsequently shown to be in photographic images

The effect occurs in all three-dimensional imaging processes that use micro-lenses to capture a scene that exists on both sides of the capture plane. These micro-image inversions cannot be removed by modifying the arrangement or by post-processing as they are produced because of the fundamental differences in the operation of lenses when they are imaging objects both from in front *and* behind of them. However, they can be removed by limiting the viewers position or by positioning all the objects in the scene on the same side of the display screen. Both of these solutions are unacceptable for general viewing.

- Integral images can be and have been produced without phase information and consequently suffer no significant deterioration. Therefore, phase can be ignored as an important imaging factor.

Without phase information in integral images there can be no globally organised addition/subtraction of waves improving resolution through construction/deconstruction. Without phase, the question of resolution is based on geometric considerations. This means that each micro-lens view is a two dimensional representation of the angular information visible from that lenses individual perspective. These angular views are interrogated at replay by the position of the viewer's eye and it is the integration of these separate sub-image components that form the final image.

- Post-processing of the micro-images is possible. Treating the intensity values of the micro-images as two-dimensional information allows the data to be modified/analysed. This creates the facility to extract features, extract depth maps or perform colour correction to integral images.

- Electronic capture and display of integral images is possible. Images can be electronically captured at resolutions considerably lower than photographic resolution. Integral images captured in this way or computer generated can then be displayed using discrete display devices such as LCD or conventional print methods. These images can be captured as small-scale images and re-projected so that the final image is displayed with correct scale.

Reviewing the initial aims of the project it can be seen that;

- The nature of the lens decoding elements has been investigated and determined through the use of theoretical work and practical experiments;

- A complete mathematical analysis of integral image generation has been produced.

- Simple computer generated integral images have been generated.

- More complex full computer generated images have been achieved and highly detailed photo-realistic computer generated images have been created as proof of principle

6.1. *Suggestions for Further Work*

Currently, images are produced in a serial manner. Calculations are performed on a pixel-by-pixel basis. The downside of this is that the calculations for a single pixel must wait until the previous pixels calculations have finished. However, using ray-tracing as the image creation procedure allows for several improvements of the execution of the code. Fundamentally, these can be used to increase computation speed.

- Parallel computation can be utilised by sub-dividing the image plane into work units. This allows several process units to independently work on the production of a single frame, thus significantly reducing the time for a it to be generated

- Custom designed DSP processors could be utilised as the parallel processing units to perform either a sub-section or all of the generation calculations. Producing the possibility of a hardware solution to the problem of generating these images at or near real-time speeds

The knowledge gained from the integral image generation process can be applied to the processing of depth extraction from integral images. This has been shown at its most simple level. However, furthering this technique would allow image manipulations to be performed on captured three-dimensional digital images. Currently, image manipulations of digital images are necessary in the production and editing of two-dimensional television. Therefore, it would be reasonable to assume that three-dimensional versions of these basic manipulation tools would be required to process three-dimensional television.

Two-dimensional manipulation of digital images is a relatively simple task. The data is typically stored as an non-encoded two-dimensional array of numeric intensity values. However, the nature of integral images means that three-dimensional information is encoded into a two-dimensional image. Processing of this three-dimensional data set is therefore made more complex. Image processing techniques that work solely upon the colour palette of the image, such as colour balancing and normalisation, can be applied to integral images in a non-involved way. Complex tasks require a much higher degree of computation to achieve.

Finally, by imposing a definite, fixed number of pixels per micro-image, either by dynamically changing the micro-lens pitch or the pixel pitch, would reduce integral imaging to a multi-view system under viewing situations where the observer is viewing the image from a particular distance from the display screen. Although the images would mix more smoothly from one view to the next as the views are comprised of continuous information spread across the entire angle that each pixel represents, that is the information is not from a single discrete viewing angle. However, at a certain angle, defined by the pixel size, an observer would only see the first pixel from an image block and if the observer then moved, the whole plate would snap to the second pixel at the same instant as the viewer crosses the pixel boundary.

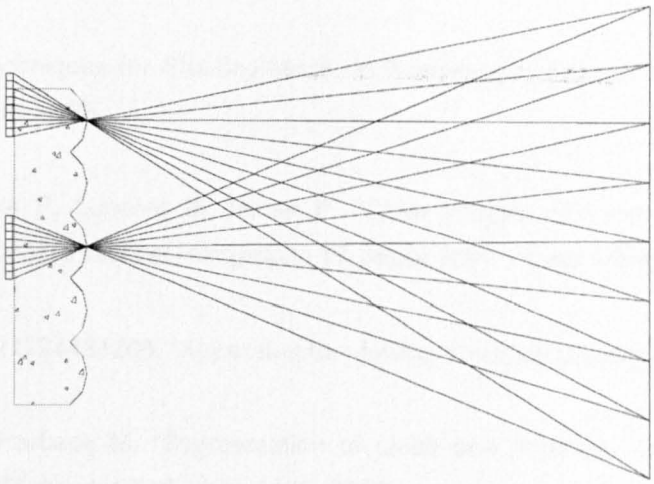

Figure 6-1, Degradation of integral to multi-view.

In effect, the viewer would only see one view at a time and these views would switch to the next view at the same point, producing an image which is closer in behaviour to multi-view than integral imaging.

As pixelated integral images stand, this flipping from image pixel to the next occurs at differing places across the plate, allowing a single pixel to contribute angular information to more than a single viewing position. This effectively destroys the hard pixel flipping effect as seen in multi-view images and maintains the impression of continuous parallax using a pixels display. The rate of this flipping can be calculated through establishing the pitch of the moiré pattern generated by the interference of the pixel and lenticular pitches. Experimentation is needed to establish what moiré pitch is desirable to produce the most natural viewing conditions, without detracting from the image.

REFERENCES

Abrash M, Doctor Dobbs Journal, Internet Based Graphics Forum, "http://www.ddj.com/", Jan.1991-Dec.1992.

AliasIWavefront corporation, "http://www.aw.sgi.com/", 1999.

Alves J (Director), "Jaws 3D", Universal Studio Films, 1983.

Appel A, "Some Techniques for Shading Machine Renderings of Solids", Spring Joint Computer Conference, pp *37-45,* 1968.

Benton S, St.-Hilaire P, Lucente M, Hubel P, "Color images with the MIT holographic video display", SPIE Vol. 1667, *Practical Holography VI,* paper 1667-73, pp. 73-84, 1992.

Benton S, US Patent US4431265, "Apparatus for viewing stereoscopic images", 1980.

Beß R, Paulus D, Harbeck M, "Segmentation of Lines and Arcs and its Application for Depth Recovery", ICASSP97, paper 2525, page 3165, 1997.

Bogusz A, "Optical Holoscopy", Optics and Laser Technology, Vol.21, No.2, pp 123-124,1989.

Brewin M, Forman M, Davies N, "Electronic Capture and Display of Full Parallax 3D Images", Stereoscopic Displays and Virtual Reality Systems II, SPIE 2409, pp 118-124 (1995).

Brewin M, Davies N, "Electronic Capture and Display of Full Parallax 3D Images", SPIE Vol.2409, pp 118-124,1996.

Burckhardt C, "Optimum Parameters and Resolution Limitation of Integral Photography", Journal of Opt. Soc. Am, Vol.58 No.1, pp 71-76, January 1968.

Burckhardt C, Collier R, Doherty E, "Formation and Inversion of Pseudoscopic Images", Appl. Opt., Vol.7 No.3, pp 627-630, April 1968.

Burckhardt C, Doherty E, "Beaded Plate Recording of Integral Photographs", Appl. Opt., Vol.8 No. 11, pp 2329-2331,1976.

Chutjian A, Collier R, "Recording and Reconstructing Three-Dimensional Images of Computer Generated Subjects by Lippmann Integral Photography", Appl. Opt. 7, No 1, pp 99-101, (1968).

Cohen M, Wallace J, "Radiosity and Realisitic Image Synthesis", Academic Press Professional, Inc., first edition, 1993.

Davies N, McCormick M, "Three Dimensional Optical Transmission and Micro Optical Elements", SPIE '93 Int. Symposium on Optics, Imaging & Instrumentation, San Diego, USA. Vol.1992, 247-252,1993.

Davies N, McCormick M, Brewin M, "Design and Analysis of an Image Transfer System using Micro-lens Arrays", Opt. Eng., Vol.33 no.11, pp 3624-3633,1995.

Davies N, McCormick M, Yang L, "Three Dimensional Imaging Systems: A New Development", Appl. Opt. 27, No. 21, pp 4529A534, 1988.

DeMontebello R, "Wide Angle Integral Photography - The Integram Technique", Proc. SPIE 120 pp 73-91,1970.

Foley J, van Dam A, Feiner S, Hughes J, "Computer Graphics: Principles and Practice", second edition, Addison-Wesley publishing, 1991.

Gabor D, "A new microscopic principle", Nature, no.161, pp 777-779,1948.

Gabor D, "Microscopy by reconstructed wavefronts", Proc. Phys. Soc., no. A194, pp 454-487, 1949.

Gabor D, UK Patent 541-753, 1940.

Glassner A, "An Introduction to Ray Tracing", Academic Press, London, 1991.

Gordon N, Jones C, Purdy D, "Applications of Microlenses to infrared Detector Arrays", Infrared Physics, Vol.3, pp 559-604,1991.

Grebennikov O, Tr. LIKI No.17, 104, 1971.

Herman G, Liu H, "Three dimensional display of human organs from computed tomographs", Jour. Computer Assisted Tomography, pp 155-160, 1977.

Horou I, Minoru Y, "50-inch Autostereoscopic Full Color 3DTV Display System", SPIE 1669 pp176-179, 1992.

Igarashi Y, Murata H, Ueda M, "3D Display System Using a Computer Generated Integral Photograph", Japan. J. Appl. Phys. Vol.17, No.9, 1978.

Ishihara Y, Tanigaki T, "A High Photosensitivity IL. CCD Image Sensor with Monolithic Resin Lens Array", Proc. International Electron Devices Meeting, Washington D.C., pp 497-500,1983.

Ives H E, "Optical Properties of a Lippmann Lenticulated Sheet", J. Opt. Soc. Amer., vol.21, pp 171-176, 1931.

Jacobs S, "Experiments with Retro-Directive Arrays", Opt. Eng 21, No. 2, pp 281-283,1982.

Kay D, Greenburg D, "Transparency for Computer Synthesised Images", SIGGRAPH 79, pp158-164, August 1979

Kinetix corporation, "http://www.kinetix.com/", 1999.

Kowalski P, "Applied Photographic Theory", Wiley, 1992.

Kratomi S, US Patent US3737567, "Stereoscopic Apparatus Having Liquid Crystal Filter Viewer", 1972.

Lasseter J (Director), "Toy Story", Pixar Animation Studios, 1995.

Leith E N, Upatnieks J, "Reconstructed wavefronts and communication theory", J. Opt. Soc. Amer. vol.52, no.10, pp 1123-1130,1962.

Leith E N, Upatnieks J, '-Wavefront reconstruction with continuos-tone objects", J. Opt. Soc. Amer. vol.53, no.12, pp 1377-1381,1963.

Leith E N, Upatnieks J, -Wavefront reconstruction with diffused illumination and three dimensional objects", J. Opt. Soc. Amer. vol.54, no.11, pp 1295-1301,1964.

Ignatev N, "Two Modes of Operation of a Lens Array for Obtaining Integral Photography", Sov. J. Opt. Technol. 50 1 pp 6-8, 1983.

Lippmann G, "Eppeuves Reversibles Donnant La Sensation Du Relief", J. Phys. Paris 821, 1908.

McCollum, US Patent 2388170, 1943.

Merritt J, "Common Problems in the Evaluation of 3D Displays", SID 83 Digest, pp 192-193,1983.

Moore J, Travis A, Lang S, Castle 0, "The Implementation of a Multi-View Autostereoscopic display", IEE Colloq. "Stereoscopic television" No.1992/173 pp4IS-4/16, Oct.1992.

Newman W, Sproull R, "Principles of Interactive Computer Graphics", McGraw-Hill, second edition, 1979.

Nims J, Lo A, "The Nimslo system", Brit. J. Photogr. 1979.

Nims J, Lo A, 'Three dimensional pictures", US patent no.3852787, 1974.

Okoshi T, 'Three Dimensional Imaging Techniques", London, UK: Academic Press, 1976.

Okutomi M, Kanade T, "A Multiple-Baseline Stereo", IEEE Transaction on pattern analysis and machine vision, Vol.15, No.4, pp 353-363, April 1993.

Oliveras A, Salembier P, Garrido L, "Stereo Image Analysis using Connected Operators", ICASSP97, pages 3169 – 3172, 1997.

Pedrofti F, Pedrotti L, "Introduction to Optics", second edition, Prentice Hall, 1993.

Popovic Z, Spague R, Neville Connell G, "Techniques for Monolithic Fabrication of Microlens Arrays", Applied Optics Vol.27, pp 1281-1284,1988.

Rodgers D, Alan Adams J, "Mathematical Elements for Computer Graphics", McGraw-Hill, 1990.

Schwartz A, "Head Tracking Stereoscopic Display", IEEE Trans. Electron. Devices ED-33(8), pp 1123-1127, August 1986.

Sokolov A, "Autostereoscopy and Integral Photography by Professor Lippmann's Method", Izd. MGU, Moscow State Univ. Press, 1911.

Sony Company Information, IMax projection system http://www.imax.com/, 1997.

Sproull R, Sutherland W, Ullnev M, "Device Independent Graphics", McGraw-Hill, 1985.

Stevens R, Davies N, "Lens arrays and photography", J. Photo. Sci. 39, pp 1-9, 1991.

Stevens R, Hutley M, Hembd-Solner, "The imaging properties of the Gabor superlens", NPL Report CLM 5, 1998.

Street G, International Patent No. WO 83/03686, "Method and apparatus for use in producing autostereoscopic images", 1983.

Street G, International Patent No. WO 94/20875, "Method and apparatus for image alignment", 1994.

Tetsutani N, Omura K, Kishino F, "Wide-Screen Autostereoscopic Display System Employing Head-Position Tracking", Optical Eng. 33(11), pp 3690-3697, November 1994.

Travis A, "3D Autostereo Display, - are 16 views enough", 4th European workshop on 3D Television, Rome, Oct 20-21,1993.

Truevision Inc., Targa file format, http://www.truevision.com/, 1999.

Usher M J, "Information Theory for Information Technologists", Macmillan Publishing, 1984.

Valyus N, "Stereoscopy", Focal Press, London, 1966.

Virtuality Plc, "http://www.virtuality.com", 1997.

Watkins C, Coy S, Finlay M, "Photorealism and Ray Tracing in C", M and T Publishing, New York, USA, 1992.

Watt A, "Fundamentals of Three Dimensional Computer Graphics", Addison-Wesley, 1989.

Watt A, Waft M, "Advanced Animation and Rendering Techniques", ACM Press, 1992.

Whitted T, "An Improved Illumination Model for Shaded Display", Communications of the ACM, 23(6), pp343-349, June 1980.

Xenotech WWW site, "http://weblynx.com.au/xeno.htm", 1996.

Yamazaki T, Kamijo K, Fukuzumi S, "Quantitative Evaluation of Visual Fatigue", Proc. Japan Display '89, pp 606-609,1989.

GLOSSARY

Afine transformation	A geometric transformation which maintains the orientations and the scale of the objects.
Afocal lens combination	A situation where a series of two lenses are separated by their joint focal lengths.
Greyscale image	An image which has one channel. This channel defines the intensity of the image at certain positions.
Pitch (of a lens)	The distance between two similar points on a repeating structure, such as the distance between to lens centres on a lens sheet.

APPENDIX A: COMPUTER GENERATED RESULTS

Page Number(s)	Description
111	Early black/white integral image.
111	Wire-frame example
112	Photo-realistic examples (1.124 lens sheet)

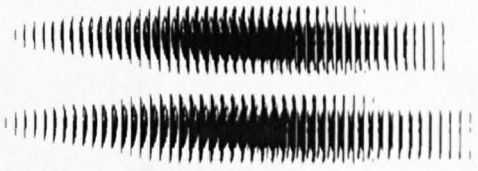

Figure A-6-1, Early Black/White Lenticular image (1.27mm)

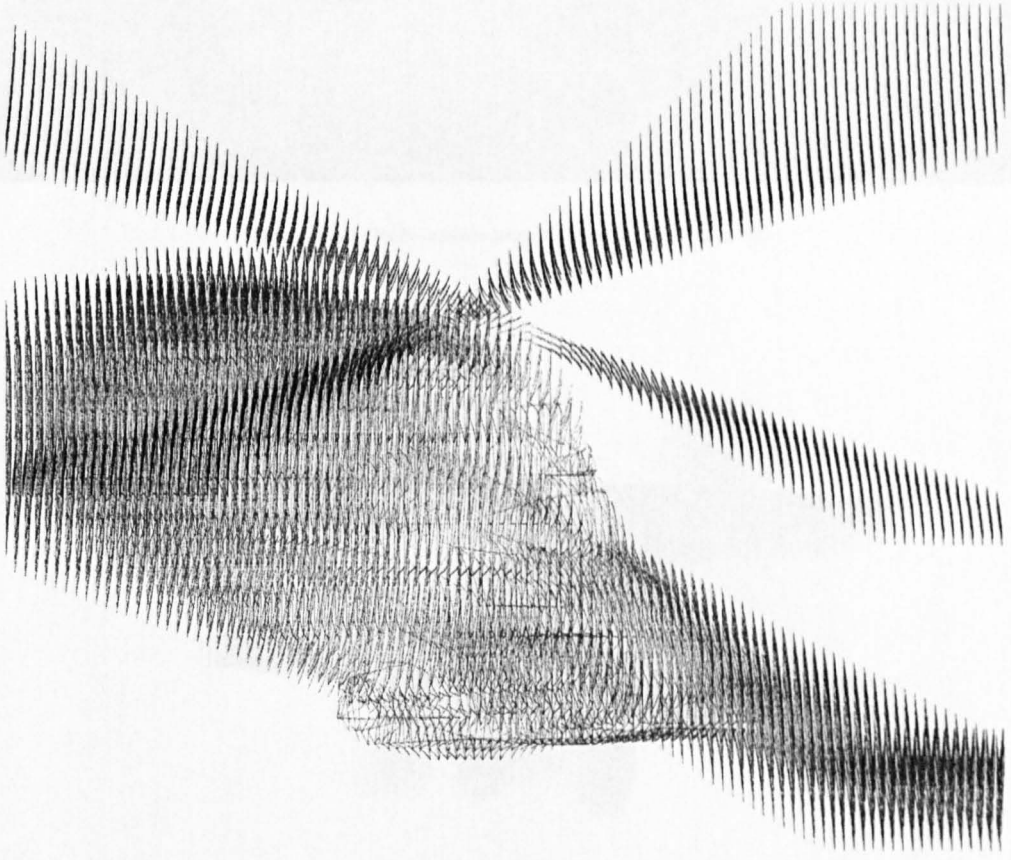

Figure A-1-2, Lenticular wire-frame image with colour attributes.

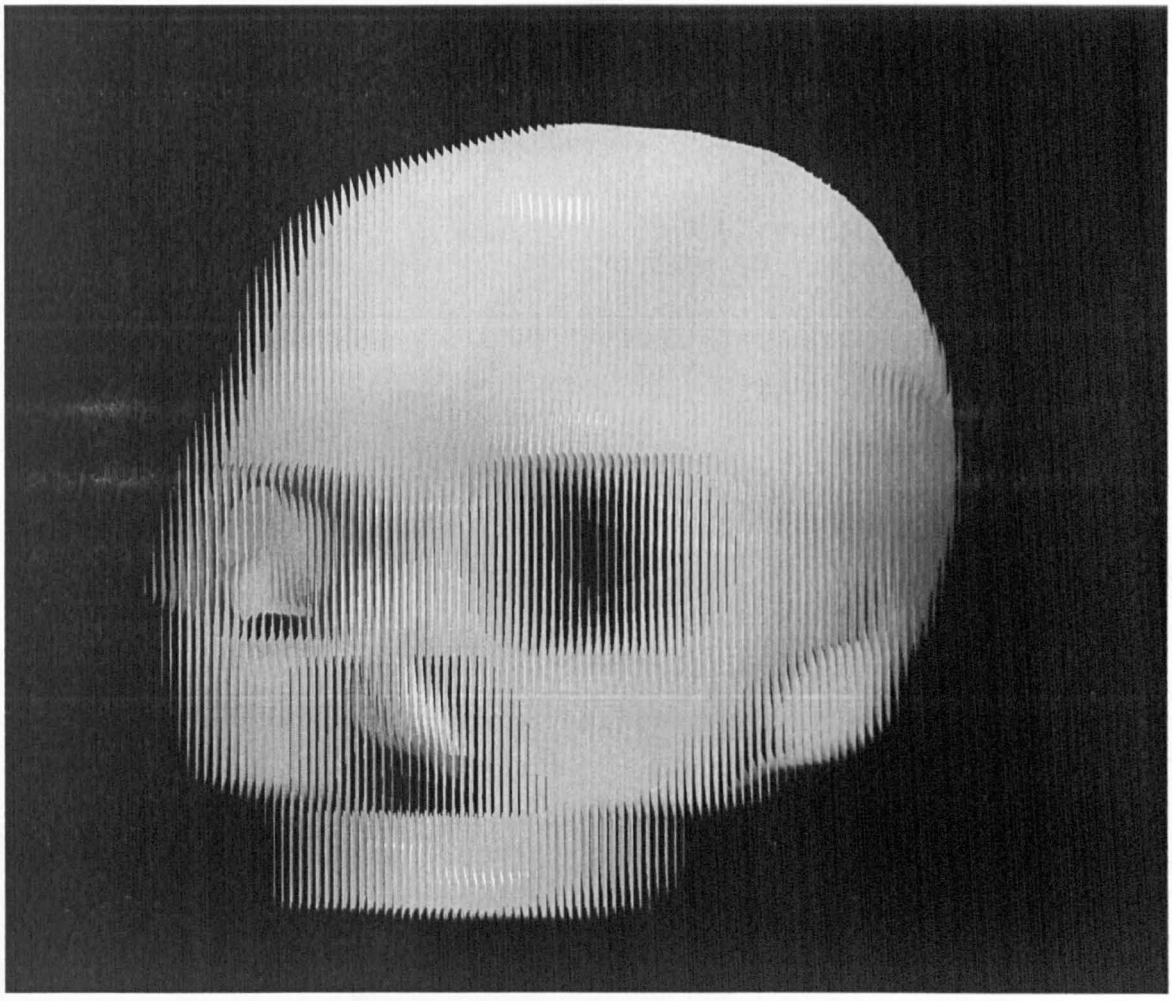

Figure A-1-3, Photo-realistic integral image "skull" (1.124mm)

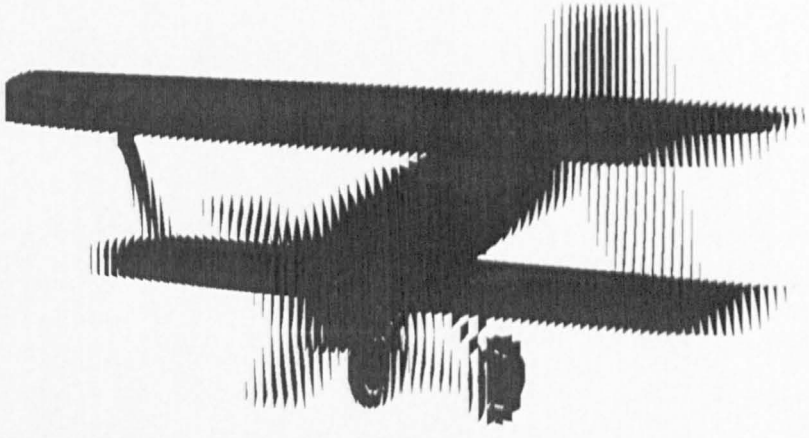

Figure 1-4, Photo-realistic integral image "biplane" (1.124mm)

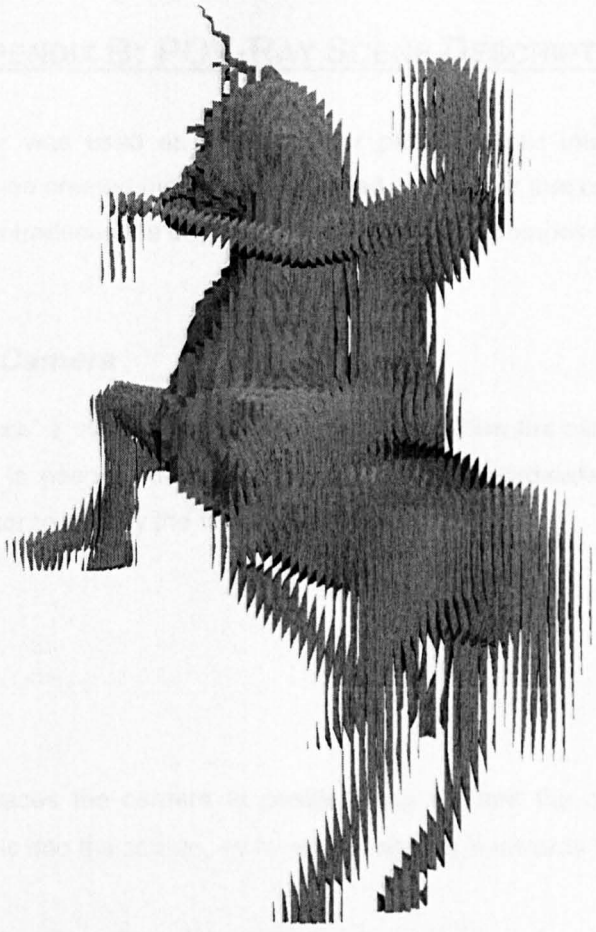

Figure 1-5, Photo-realistic integral image "horse" (1.124mm)

APPENDIX B: POV-RAY SCENE DESCRIPTION

The POV-Ray ray-tracer was used as the basis for photo-realistic integral image generation. Therefore, the images to be created need to be specified in a format that can be understood by the ray-tracer. This section introduces the common file elements and composition of a scene file.

6.2. Defining the Camera

The **camera{** XE "**camera**" **}** statement describes where and how the camera is positioned in the object space. A vector is needed to specify the x, y and z co-ordinates of the position of the camera and another vector to specify the direction of view.

```
camera {
  location <x, y, z>
  look_at  <a, b, c>
}
```

location <x,y,z> places the camera at position <x,y,z> from the centre of the ray-tracing universe. By default, +z is into the screen, +y is vertical and +x is towards the right.

look_at <a,b,c> rotates the camera to point at the co-ordinate <a,b,c>.

6.3. Defining Simple Objects

```
sphere {
    <x, y, z>, r   // <position>, radius
}
```

Vector <x,y,z> defines the position of the sphere and r the radius of the sphere.

```
box {
    <x1, y1, z1>,  // Near lower left corner
    <x2, y2, z2>   // Far upper right corner
}
```

A box is defined by specifying the 3D co-ordinates of its opposite corners.

```
cone {
    <x1, y1, z1>, r1     // Center and radius of one end
    <x2, y2, z2>, r2     // Center and radius of other end
}
```

The cone shape is defined by the centre position and radius of each end.

```
cylinder {
    <x1, y1, z1>,      // Center of one end
    <x2, y2, z2>,      // Center of other end
    r                  // Radius
}
```

The cylinder is defined by the centre position of each end and a single radius.

```
plane { <x, y, z>, offset
}
```

The plane object defines an infinite plane. The vector <x,y,z> is the surface normal of the plane. The offset is the distance that the plane is displaced along the normal from the origin.

6.4. Defining a Light Source

```
light_source { <2, 4, -3> color White}
```

The vector in the **light_source{** XE "**light_source**" **}** statement specifies the location of the light.

6.5. Constructive Solid Geometry (CSG) Objects

6.5.1. CSG Union

This creates a single CSG union out of the two objects.

```
  union{
    sphere { <0, 0, 0>, 1
      pigment { Blue }
      translate -0.5*x
    }
    sphere { <0, 0, 0>, 1
      pigment { Red }
      translate 0.5*x
    }
  }
```

6.5.2. CSG Intersection

This creates a single CSG intersection out of the two objects, producing an object that is formed by the common elements of both objects.

```
intersection {
    sphere { <0, 0, 0>, 1
      translate -0.5*x
    }
    sphere { <0, 0, 0>, 1
      translate 0.5*x
```

```
    }
    pigment { Red }
  }
```

6.5.3. CSG Difference

This creates a single CSG difference out of the two objects, producing an object that is formed by the un-common elements of both objects. This is the inverse of an intersection.

```
intersection{
    sphere { <0, 0, 0>, 1
      translate -0.5*x
    }
    sphere { <0, 0, 0>, 1
      translate 0.5*x
    }
    pigment { Red }
    rotate 90*y
  }
```

6.5.4. CSG Merge

This creates a single CSG object out of the two objects. The produced object is similar to an union except that internal details inside the created object are ignored.

```
merge {
    object { Lens_With_Hole translate <-.65, .65, 0> }
    object { Lens_With_Hole translate <.65, .65, 0> }
    object { Lens_With_Hole translate <-.65, -.65, 0> }
    object { Lens_With_Hole translate <.65, -.65, 0> }
    pigment { Red filter .5 }
  }
```

APPENDIX C: MICRO-LENS FABRICATION : PHOTO-SCULPTING

To produce full fill micro-optical arrays where the lens characteristics are accurately controlled a simple and cheap manufacturing method was devised.

Introduction

The enabling technology for modern integral imaging has been the development and production of large areas of micro-lens sheet (Davies and McCormick, 1993). These advances have not only allowed the investigation and extension of current imaging techniques but also the development of new optical components such as, super lenses and optical beam steering devices (Stevens, Hutley and Hembd-Solner, 1998).

The production of micro-lens arrays using a resist reflow technique has been extensively reported (Ishihara and Tenigaki, 1983; Popovnic, Spague and Nevile-Connel, 1988). This method is based around four simple stages. First the substrate, usually an optically clear material (such as glass), is coated with a thick layer of photo-resist (a substance which chemically changes depending the amount of ultra-violet radiation (UV) it has been exposed to). This photo-resist layer is then exposed to UV radiation using a chrome mask to block off desired areas [figure 5-10].

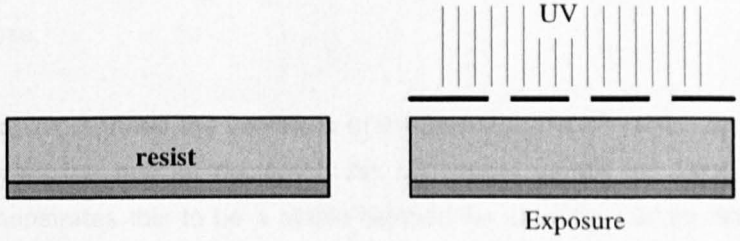

Figure C-1-6, Reflow method [stages 1 & 2].

The sample is developed and the softened photo-resist washed away. If a circular chrome mask is used at the exposure stage then the structure that is left on the plate consists of cylinders on material. The plate containing photo-resist cylinders is then placed into an oven and heated until melting point. When this occurs, the surface tension on the photo-resist exerts a force that pulls the form from a cylinder into a hemisphere [figure 5-11]. Once cooled, these can be used as optical elements or can be used as a master in a moulding process to produce several copies in better optical materials.

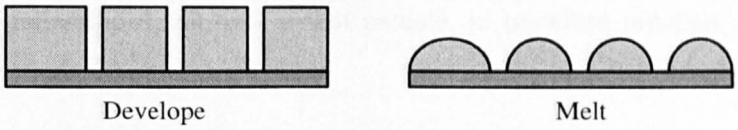

Figure C-1-7,Reflow method [stages 3 & 4].

Arrays produced by this method have fill factors approaching 75% as there is a need for a separation gap between each cylinder at the melting stage to stop the photo-resist elements flowing together. In optical systems, the un-lensed light, introduced by fill factors being less than 100%, introduce noise into the resultant image. N T Gordon (Gordon, Jones and Purdy, 1991) reported a sophisticated technique able to create full fill using direct photo-resist etching using ion beams. However, this approach is expensive.

Initial investigation

The method for producing full-fill micro-lens arrays, proposed by Davies and McCormick, relies upon the production of a single, large greyscale mask. This mask image is scaled and duplicated across the entire area of photo-resist by an optical projection system comprising a series of optical elements. The essential element of this series being a micro-lens plate, which performs the scaling and multiplication of the mask image. A micro-lens plate with less than a 100% fill factor can be used for this purpose.

Davies and McCormick reported the versatility of the technique in an earlier paper (Davies, 1993). This paper discusses the task of designing the necessary masks for three-dimensional photo sculpting and demonstrates this to be a viable method for creating custom designed lenses with virtually any surface profile.

The method discussed uses photographically produced greyscale masks which allow direct in house control of mask generation and thereby reduced cost. The first stage is to determine the opacity of the exposed photographic emulsion to UV radiation. To simplify this task the several steps in the process and their corresponding responses to intensity were grouped together and treated as a whole.

The following method was applied:

1. Assume a linear response of the system to intensity;

2. Create a mask for a surface profile which descends from the highest point to the lowest point in a straight line;

3. Expose the generated mask over a test sample, to generate reaction of the system to the mask;

4. Measure the resulting profile, using a Talystep machine.

5. Use these measurements to correct the assumed system response to intensity. The difference between the produced photo-sculpted surface and the desired linear one, gives a correlation between the straight line system response model and the actual system response;

6. Return to step two and repeat until the generated profile matches the desired profile.

By using the actual response of the system as an input stimulus, a response function for the entire system can be produced. This can then be used to correct the original mask generation process, allowing any surface profile to be correctly rendered.

Using this approach to create the lens mask removes several problems that are encountered with many other methods. Specifically the need for a commercial printing device capable of producing output with high numbers of discrete intensity levels was removed. On the other hand, this method introduces several new stages into the process which each transformed the resists response to UV radiation:

- The response of the monitors (Sony Trinitron, 19-inch diagonal, 256-colour screen) phosphor to computer generated intensity values.

- The intensity response of the film (Kodak technical pan 25-ASA, high-resolution film).

This process allowed the creation of images which have relatively high spatial resolution (sub-micron when scaled onto the final resist) and a high greylevel resolution (256 levels). Compared with the method described by Gordon, the resolution of the system, both greylevel and spatially, is not extremely high. This is because Gordon directly creates a mask with feature sizes of 1μm using an ion beam, while this method uses photographic film to achieve a similar result. Admittedly, Gordon has absolute control over his entire process and his use of large number of greylevels (1000's) allows sculpting in resist materials with very steep response curves to linear intensity inputs. However, the method developed does allow the development and in-expensive production of microstructures in house.

Computer mask production

The creation of a greyscale mask for photo sculpting, is a relatively simple procedure. Two things need to be known the desired lens profile and the response of the photo-resist materiel to ultra-violet radiation. The profile of the lens determines the exposure for each point on the lens, which when cross-referenced with the resist exposure function gives the energy required to sculpt to the required depth. Additionally, minimum and maximum depth values need to be calculated for the lens profile as these determine the high and low depths of the mask and this combined with the number of grey levels gives the vertical resolution of the process for any given profile.

In practice, the production of greyscale masks for this process requires an understanding of:

- The relationship between depth of etch and intensity.
- The relationship between the greyscale resolution of the output device and the tendency for step formation in the resulting microstructures.
- The output device response to intensity (gamma value).

Practical experiments in photo-sculpting

Once an etch mask has been produced, there are several ways in which this image can be exposed onto the resist surface. One method [figure 5-12], uses a single stage to copy the mask image onto the resist.

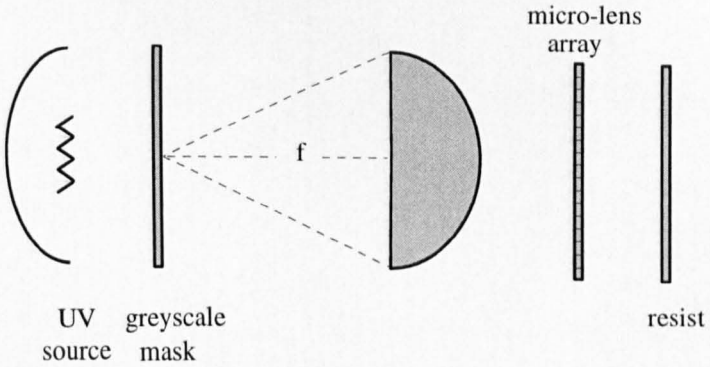

Figure C-1-8, One stage mask multiplication and exposure.

A second method uses the same equipment, except the photo-resist is replaced by a sheet of photographic film. Exposing this film produces a scaled and replicated image of the original mask. The film sheet can now be used as a master to produce sculpted lenses requiring only an UV source.

Conclusion

Lack of grey scale resolution is the greatest drawback of using this method. A high number of greylevels is required, not for the sculpting of the design, but for the calibration cycle, as a high number of samples (greylevels) are needed to effectively control and use a resist with a steep response to UV radiation.

The mask generation program can easily be altered to produce output in the form of illuminated physical shapes. This method was reported by the National Physical Laboratory (NPL) but has been used previously. Basically, a spinning shape is illuminated and casts a predetermined shadow consequently the intensity at any given distance from the centre is controlled.. Obviously, the result is that a variable amount of light throughput is projected onto the photo-resist over a fixed time. The accuracy depends upon the spinning speed and the accuracy of the shape. However, this technique only is applicable to symmetrical features such as micro-lenses.

The method explored and developed for greyscale masks has a possible use not only in micro optics generation as described here but also as a technique for general micro engineering.

APPENDIX D: EQUIPMENT USED

3D Studio Max version 1.0, Kinetix, http://www.ktx.com/ - Commercial 3D modeller and render.

Adobe Photoshop version 4.0, Abobe systems inc., http://www.adobe.coml - Commercial image manipulation package.

ASAP http://www.breault.com/ - Commercial optical design ray tracer.

GCC GNU C compiler version 2.7.3 - Publicly available Unix compiler

Imagemagick version 3.7, http://www.wizards.dupont.com/cristy - Image manipulation toolkit.

MathCAD Version 7 - Commercial mathematics calculation tool

NetPBM – ftp://wuarchive.wustl.edu/graphics/graphics/packages/NetPBM

GNUPlot, http://www.cs.dartmouth.edu/gnuplot_info.html

Parallel Virtual Machine (PVM), http://www.epm.ornl.gov/pvm/

POV-Ray Version 3.00, http://www.povray.org/ - Persistence of vision ray tracer.

Sun Microsystems Sparc Ultra 1, http://www.sun.com/ - Unix workstation.

DEC Alpha, http://www.digital.com/ - Unix workstation

XV version 3 – shareware image display package.

APPENDIX E: LENS SHEET SPECIFICATIONS

Pitch	IOR	Thickness	300 DPI pixels/lenslet
1.27mm	1.xxx (polystyrene)	3.08mm-3.30mm	15
0.600mm	1.52	2.65mm	7.087
1.124mm	1.675	3.23	13.276
0.845mm	1.6	2.37	9.981
0.625mm	1.6	1.24mm	7.382

APPENDIX F: EXPERIMENTAL FRAMEWORK